

Earthquakes and offshore wind turbine installation; A review and analysis of mitigation measures for cranes on jack-ups

N.D. van Engelen

Technische Universiteit Delft



Earthquakes and offshore wind turbine installation;

A review and analysis of mitigation measures for cranes on jack-ups

by

N.D. van Engelen

to obtain the degree of Master of Science

in Offshore & Dredging Engineering at the Delft University of Technology,

to be defended publicly on Wednesday June 23, 2021 at 13:00 AM.

Student number: 4383826
Project duration: September 1, 2020 – June 1, 2021
Thesis committee: Prof. dr. ir. A. Metrikine, TU Delft, chairman
Dr. J. S. Hoving, TU Delft, supervisor
Ir. E. Krol, GustoMSC, daily supervisor
Ir. D. Schimmel, GustoMSC, daily supervisor
Ir. A. Hofman, GustoMSC, supervisor

This thesis is confidential and cannot be made public until June 23, 2022.

An electronic version of this thesis is available at <http://repository.tudelft.nl/>

Preface

Dear reader,

I, Niels van Engelen, have written this thesis as a part of the Master of Science in Offshore & Dredging Engineering at the Delft University of Technology. GustoMSC, a world market leader in offshore engineering solutions, has initiated the research objectives of my research. Under the supervision of professors from the TU Delft and employees of GustoMSC, we contributed by means of this thesis to innovations necessary in the offshore wind industry to counter tomorrow's climate change.

I would like to sincerely thank my graduation committee for their guidance, support and supervision throughout my research: A. Metrikine, J.S. Hoving, A. Hofman and in special my daily supervisors, E. Krol and D. Schimmel. Additionally, I would like to thank all other employees of GustoMSC who have broadened my knowledge at such a fast pace. In particular, T. Blankenstein, as he is always open for discussions and is very competent in the research area of my thesis.

Besides these great engineering minds, I am very grateful to my family and friends that supported and encouraged me during my research. Special thanks go to my brother Thijs van Engelen, who provided very helpful assistance during the process of writing my thesis.

And last but certainly not least, I would like to share how blessed I am to have such an wonderful girlfriend. She has been by my side through all the ups and downs that came across last year, and our nine years before. Since we started my graduation as an engaged couple and she is still by my side, I am looking forward to our wedding in about a month time.

Yours sincerely,

*N.D. van Engelen
Rotterdam, June 2021*

Abstract

Due to a high demand for offshore wind energy the industry is expanding to evermore challenging locations such as seismic prone areas. The corresponding seismic shocks and vibrations can be transmitted to jack-up vessels and their cranes used for the installation of these offshore wind turbines. Since a potential collapse due to seismic activity carries large human and financial risks, the main objective of this thesis is:

”To determine the best solution to mitigate the dynamic response of cranes for offshore wind turbine installation in seismic prone areas.”

Therefore, we study existing mitigation measures and find that the dynamic absorber and base isolation systems are promising solutions. However, we only find the dynamic absorber to be feasible for implementation.

Subsequently, we investigate the influence of the dynamic absorber on the dynamic response of the crane by performing seismic time history analyses. We find a mitigating influence for the vast majority of simulated cases. More specifically, the dynamic response in the out-of-plane direction is reduced by 10 percent on average. Furthermore, the dynamic absorber is highly effective in the mitigation of harmonic vibrations such as those that are induced by Rayleigh waves that occur near the end of earthquakes. This finding suggests that a dynamic absorbers might also be suitable for mitigating wave and wind loads in the crane as these loads prescribe a rather harmonic signal.

The conclusions of this thesis give the offshore wind industry a clear indication that a dynamic absorber is an effective measure to mitigate the dynamic response of a crane that is based on a jack-up.

Contents

1	Introduction to the seismic analysis of cranes for offshore wind turbine installation	1
1.1	Problem definition of the dynamic response of cranes for offshore wind turbine installation	2
1.2	Objectives of this thesis	3
1.3	Methodology for the investigation in this thesis	4
1.4	Structure of this thesis	5
1.5	Nomenclature of crane parts	6
2	The state-of-the-art of the seismic analysis of jack-up vessels and their cranes	7
2.1	General history of jack-up vessels	7
2.2	Design requirements for jack-up vessels	8
2.3	GustoMSC: The seismic analyses of jack-up vessels	9
2.4	Literature on important considerations in the seismic analysis models of GustoMSC	10
2.5	Existing measures to limit earthquake damage	11
2.5.1	Ductility through structural configuration	11
2.5.2	Direct Damping Apparatus	12
2.5.3	Base Isolation Systems	12
2.5.4	Dynamic Absorbers	13
2.5.5	Active control device	13
2.5.6	Discussion on mitigation measures	13
2.6	A more detailed elaboration on the Base Isolation systems & Dynamic absorbers	13
2.6.1	Base Isolation Systems	13
2.6.2	Dynamic Absorber	15
3	Simulation model for the seismic analysis of a jack-up with a crane	19
3.1	Structural dynamics and finite element analysis	19
3.2	Opensees as solver for the governing system of equations	20
3.2.1	Opensees - Model builder	20
3.2.2	Opensees - Analysis	20
3.2.3	Opensees - Recorder	20
3.3	Model design considerations for solving the governing system of equations	20
3.3.1	Model design of the current jack-up model	21
3.3.2	model design of the current crane model	22
3.4	Corrections to the crane model	23
3.4.1	Correction of the boom hinge stiffness	23
3.4.2	Correction of the boom hinge orientation	24
3.4.3	Correction of the Rayleigh damping	25
3.5	Verification of the crane model	26
3.6	Adjustments of the hull mass distribution of the jack-up model	27
3.6.1	Adjustment to counter a duplicate crane mass	27
3.6.2	Adjustment to represent the crane model in the hull mass distribution	28

4	Influence of the dynamic response of the crane on the motion of the jack-up	29
4.1	Methodology: Measuring the influence of dynamic modelling of the crane	29
4.1.1	Variation of the Monte Carlo simulation	30
4.2	Data collection and processing	32
4.3	Analysis of the displacement differences of the jack-up	34
4.3.1	Displacement difference	34
4.3.2	Displacement ratio	35
4.3.3	Displacement difference vs displacement ratio	36
4.3.4	Influence of the variables on the distributions.	37
4.4	Conclusion: Influence of the crane on the motion of the jack-up.	40
5	Review of Mitigation measures and their implementation	41
5.1	Review of mitigation measures	41
5.1.1	Ductility through structural configuration	41
5.1.2	Direct Damping Apparatus	41
5.1.3	Base Isolation Systems	42
5.1.4	Dynamic Absorbers	42
5.1.5	Active control device	42
5.1.6	Conclusion: Promising mitigation measures	42
5.2	Implementation of a base isolation system	42
5.2.1	Location of the base isolator in the crane model	43
5.2.2	Parametric description of the base isolation system	43
5.2.3	Change of iteration algorithm	44
5.2.4	Confirmation of the slip behavior of an implemented base isolation system.	45
5.2.5	Accounting for the overturning moment that is present in the crane	45
5.2.6	Check the Base isolation system for a lower friction coefficient	52
5.2.7	Conclusion: Implementation of the base isolation system	53
5.3	Implementation of dynamic absorber	54
5.3.1	Location of the dynamic absorber	54
5.3.2	Parametric description of the dynamic absorber	55
5.3.3	Confirmation of the mitigation of dynamic response of the crane	57
5.3.4	Implementation of the dynamic absorber in multiple configuration cases	59
5.3.5	Conclusion: Implementation of the dynamic absorber	59
5.4	Conclusion: Implementation of mitigation measures	60
6	Influence of the dynamic absorber on the response of the crane	63
6.1	Methodology: Measuring the influence of the dynamic absorber	63
6.2	Data collection and processing	64
6.3	Analysis of the force differences in the boom hinge	66
6.3.1	Force difference	66
6.3.2	Force ratio	66
6.3.3	Force difference vs force ratio	67
6.3.4	Force ratio vs maximum absolute force of the benchmark model	68
6.4	Analysis of the case with the highest force difference in out-of-plane direction	69
6.4.1	Earthquake input signal	70
6.4.2	Acceleration of the base of the pedestal	71

6.4.3	Forces in the boom hinge	72
6.4.4	Displacement of the jib vs the pedestal	72
6.4.5	Displacement of the jib vs the dynamic absorber	72
6.5	Conclusion: Implementation of the dynamic absorber in the crane	74
7	Conclusions and recommendations	75
7.1	Conclusions	75
7.2	Recommendations	77
	Bibliography	79
A	Close-up maps	81
B	Variable distributions	83
C	How the OpenSees model is build:	91

Introduction to the seismic analysis of cranes for offshore wind turbine installation

Due to rapid climate change, the demand for renewable offshore wind energy is growing fast. In order to harvest more and more energy from the wind, offshore wind turbines are growing in both size and mass. At the same time, these large wind turbines are installed on ever more challenging locations to meet the future demand for renewable energy.

The Taiwan Strait and locations close to the Japanese shore are such challenging locations for which the construction of bottom founded offshore wind turbines is currently considered. As shown in the maps of Figure 1.1, these areas have an acceptable water depth for bottom founded offshore structures and have a high average wind speed due to strong ocean currents. At the same time, they are challenging construction locations since they are heavily affected by earthquakes and tremors.

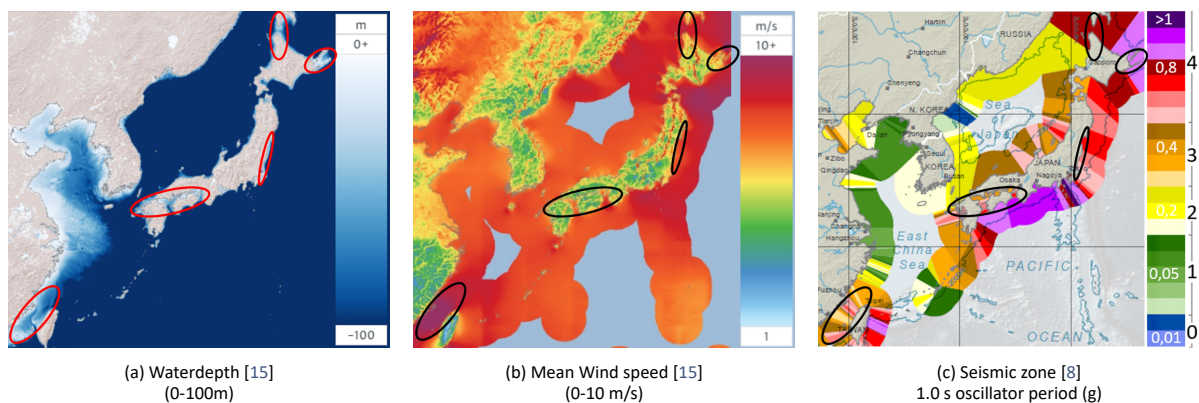


Figure 1.1: Potential locations for wind turbine installation.
(Close-up maps can be found in appendix A)

The shocks and vibrations from seismic activity can be transmitted to offshore platforms used for the installation of offshore wind turbines. This causes stress on these structures which may lead to serious problems, such as (but not limited to; the pivots supporting the platforms may break or slip away, the crane boom may break off and payloads may be lost.

Next to the obvious danger such events cause for the crew inboard, breakdowns like these can lead to lengthy damage repair activities which put a break on offshore installation operations. This may result in a large eco-

conomic burden for the stakeholders involved, but also in a delay in the expansion of the wind energy generation which is needed rapidly to counter the climate change mentioned earlier. This indicates that there is a need for solutions which can offset or absorb the energy of tremors and earthquakes and thereby prevent resulting breakdowns.

Jack-up vessels, as shown in Figure 1.2, are the most common structures used for wind turbine installation. New engineering challenges arise as wind turbines grow and the wind industry expands rapidly across the globe. The dynamic behavior of the crane on a jack-up vessel becomes more important as the length of the boom is increasing and operations are executed in more seismic prone areas. In collaboration with GustoMSC, this thesis research has been set up with the aim to find a mitigation measure that mitigates dynamic vibrations of the crane.



Figure 1.2: Jack-up Vessel [9]

1.1 Problem definition of the dynamic response of cranes for offshore wind turbine installation

The challenges that the offshore wind industry is facing due to growing wind turbines and expansion across the globe are an increasing length of the crane boom and installation in seismic prone areas. These two problems are elaborated below.

The required installation height for wind turbines is increasing as the wind turbines are growing. This requirement leads to an increased length of the boom which induces higher natural periods of the boom. This development is noticed in practice and can be substantiated by a simplified cantilever beam formula.

Prior analysis of general four-legged wind installation jack-up vessel shows that such jack-ups have three main natural periods close to each other. It is found that the corresponding modes of these natural periods correspond to the transverse, longitudinal and torsional direction of the hull. The natural periods of these modes vary between 3 and 6 seconds depending on case specific parameters, such as water depth and variable weight on board.

The increasing natural period trend of the crane causes the crane to align with the natural period of the jack-up. This is an undesired event by which resonance starts to occur as the motion of the jack-up excites the crane in its natural frequencies and vice versa. Larger deflections and forces will arise in the structure when the combination of the jack-up and the crane start to move in one frequency.

GustoMSC is an engineering company that designs mobile offshore engineering units and equipment. Globally, they have been noticed for their expertise in the design of jack-ups and are a market leader in this industry for many years. To meet the installation requirements for the future generation wind turbines, GustoMSC is

designing a telescopic boom crane with an extendable part. With this solution, that is new to the offshore wind industry, the crane can reach out to higher installation heights.

Recently, GustoMSC conducted research on the response of this telescopic crane in operational sea states. Based on their research, GustoMSC concludes that the operational sea states contain insufficient energy to excite the combined system of the jack-up and crane in such a way that it would lead to noteworthy responses of the crane in the longitudinal direction. However, for the transverse direction, their research concludes that there are operational configurations that exist that lead to some dynamic excitation of the crane. Although, the significant acceleration values of the boom in the transverse direction are still well below the design limit.

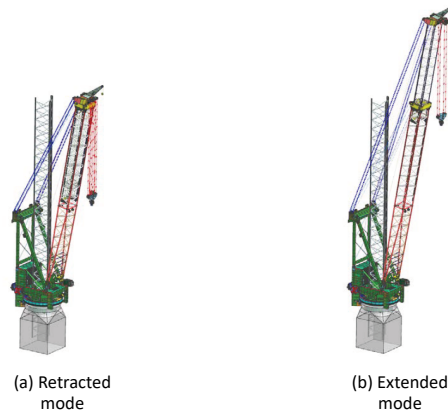


Figure 1.3: Telescopic Boom Crane by GustoMSC [9]

Next to the operational sea states, extreme level earthquakes need to be considered in the design of bottom founded offshore structures that are located in seismically active zones. This is required by the ISO19901-2 standard to ensure safe offshore operations. This ISO-standard states that the extreme level earthquake is comparable to an extreme environmental event. This extreme environmental event describes more ferocious conditions than the operational sea state conditions for which the crane has been investigated. Therefore, it is expected that the design requirements related to seismic conditions overshadow those related to the present operational sea states.

In addition to this, sea states can be predicted prior to an operation. This means that precautionary measures can be taken which lowers the risk significantly. However, no precautionary measures can be taken for earthquakes as these cannot be predicted prior to the execution of an operation. This means that the jack-up and crane will be hit in its operational state and the risk cannot be mitigated upfront.

Recent studies of GustoMSC have created a detailed and representative model of a jack-up for seismic analysis. With this model, the performance of a jack-up subjected to seismic vibrations is investigated. Next to that, research was conducted on the application of mitigation measures in the jack-up structure to improve the performance of the jack-up. Although the results of these studies are promising, one should keep in mind that these studies include the crane in a simplified manner and not as a substructure. Furthermore, the motion of and the forces in the crane itself have received little-to-non attention. Since the crane is a relatively large substructure on board of the jack-up, a potential collapse due to seismic activity carries large human and financial risks.

1.2 Objectives of this thesis

The main objective of this thesis is:

"To determine the best solution to mitigate the dynamic response of cranes for offshore wind turbine installation in seismic prone areas"

This main objective is divided into four objectives. The first objective is to investigate the influence of modelling the crane as a substructure on the motion of the jack-up. This is interesting since the current seismic analysis of jack-ups include the crane in a simplified manner. Namely, as a mass distribution over the hull nodes. It is thought that fully modelling the crane as a substructure attached to the jack-up might result in a different motion response of the jack-up. Furthermore, this is interesting as it is preferred to use these seismic induced jack-up motions as input for the seismic analysis of the crane.

The second objective is to investigate and review existing solutions to mitigate seismic induced vibrations in offshore and land-based structures. The aim is to select feasible mitigation measures with a high potential for mitigating the dynamic response of the crane.

The third objective is to find a possible implementation method for these measures in the crane. This is important as the measure should be implemented in such a way that the crane is still able to operate but mitigates the response in an optimized manner.

The fourth objective is to investigate the influence of these mitigation measures on the seismic performance of the crane. The performance of the crane can indicate its probability of survival and its stability during installation. An increase in these two will result in great safety and economic benefits. Therefore, the influence on this performance is interesting because it indicates the safety and economic benefits that this measure can deliver for GustoMSC.

1.3 Methodology for the investigation in this thesis

This thesis aims at finding a solution that mitigates the dynamic response of the crane that is caused by seismic vibrations. After reviewing existing mitigation measures an investigation will be performed to the influence of the most promising mitigation measures on the performance of the crane. For this investigation, a software package called Opensees will be used to perform simulated experiments. This is an open source software framework for earthquake engineering simulations.

Prior to this thesis, a model of a jack-up and crane has been created in this software. These models will be adjusted and improved to correctly consider the combined structure as a whole and to consider multiple configuration cases. This thesis will address a variety of configuration cases to capture the divergence of configurations in which the jack-up and crane will operate.

To ensure safe operations, the ISO19901-2 [5] requires that bottom founded offshore structures in seismic prone areas will be analyzed for extreme level earthquake events, i.e. ELE events. The seismic analysis of these structures needs to be done for multiple ELE events to capture the randomness in earthquakes correctly. Therefore, in this thesis, we will use a database with ELE events as input for the simulated experiments. This database consists of actual Japanese earthquake data that has been scaled to location dependent parameters such as site class and seismic zone. This database enables seismic analysis for a variety of locations.

Since it is desired to conduct research with a model that is as simple as possible to avoid unnecessary side effects it is interesting to investigate whether the resulting jack-up motions can be used for a stand-alone crane model. In addition to that, there are doubts over the correctness of the jack-up motions of the current model. These doubts arise due to simplifying the crane as hull mass distribution over the hull nodes instead of fully modeling the crane as a substructure on the jack-up. For these two reasons, we will investigate the influence of

fully modeling the crane as a substructure instead of including the crane as a mass distribution on the motion response of the jack-up.

In this investigation two models will be compared based on the lateral motions of the jack-up. The first model will represent the current jack-up model in which the crane is included as a mass distribution over the hull nodes. In the second model the crane will be fully modelled as a substructure on the jack-up to include for the dynamic response of the crane and the associated interaction with the jack-up. From this investigation it can be verified whether simplifying the crane as a mass distribution is correct and whether the jack-up motions can be used as input for a stand-alone crane model.

Thereafter, we are going to review existing mitigation measures that mitigate seismic induced vibrations in the crane. First, an overview of existing measures will be created based on literature and expert's opinion. Then, the most promising measures will be selected for implementation in the model and further investigation. This selection will be based on their feasibility for implementation on the crane and their potential to reduce the response of the crane during seismic loading.

Once the measures are selected, they will be applied in the crane model for which their implementation method is discussed. An investigation to the performance of the crane will be conducted by comparing a crane model without mitigation measures to a crane model with mitigation measures. The benefits these measures deliver for the survival performance and stability of the crane during seismic vibrations will be indicated by the difference between the maximal force response in the boom hinge and maximal motion response in the jib respectively. Potential benefits on the performance of the crane during environmental loading, such as wave load, may be initiated by the decay of the crane response over time.

This thesis will be concluded with an advice on which mitigation measures to use in the crane, substantiated with the performance improvements that are expected to be achieved by this solution.

1.4 Structure of this thesis

This thesis is structured as follows. Chapter 2 provides an overview of the state of the art and the associated literature. Chapter 3 presents the model description for the jack-up and crane used in this research. Chapter 4 investigates the influence of the crane on the motion of the jack-up. Chapter 5 elaborates on the implementation of the mitigation measures applied in the crane. Chapter 6 investigates the influence of the mitigation measures on the performance of the crane. Chapter 7 presents the conclusion and elaborates on the recommendations for further research.

1.5 Nomenclature of crane parts

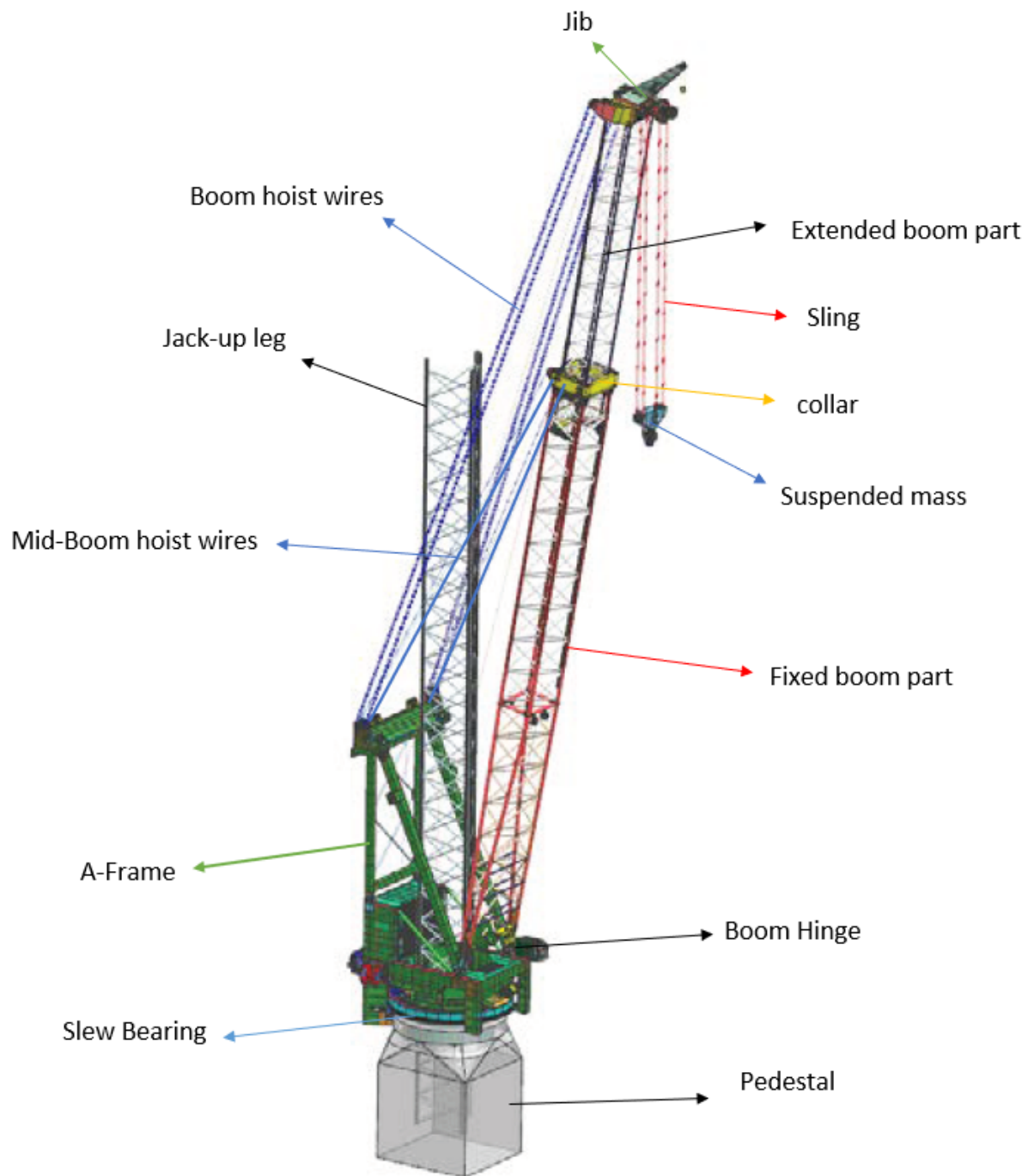


Figure 1.4: Telescopic boom crane by [9]: Nomenclature of parts of this crane for this thesis

2

The state-of-the-art of the seismic analysis of jack-up vessels and their cranes

This chapter discusses the state-of-the-art of the seismic analysis of jack-up vessels and elaborate on possible mitigation measures which can be applied in the crane to suppress its dynamic behavior. A general history of jack-up vessels is provided and the requirements for seismic analysis of offshore structure are discussed. The most up to date GustoMSC models for seismic analysis are explained and an overview of existing mitigation measures is given.

2.1 General history of jack-up vessels

The origins of the offshore industry can be found in the 1920s when the oil and gas industry started to move offshore to exploit new areas with great potential. The offshore industry experienced a fast pace of innovation ever since.

In the early 1950s, jack-up platforms were introduced for shallow water operations. A jack-up platform consists of a buoyant hull fitted with a number of movable legs. These legs can be lowered to the sea floor and enable the platform to raise its hull over the surface of the sea. In the early days, these platforms were dependent on support vessels for their mobility. Later on, in order to improve mobility, jack-up platforms were designed as vessels with their own propulsion system. Figure 1.2 in the introduction gives an example of such a jack-up vessel.

Over the years, jack-up platforms started to face deeper waters and harsher environmental conditions. In the 1970s, multiple disasters occurred which caused the loss of lives and had large environmental consequences. As a result, both government and industry recognized that there was a need for regulation and legislation.

The regulations that were put in place, forced the offshore industry to take environmental conditions, such as wave and wind loads, into account in the structural design of their platforms. These regulations mitigate the risks that are induced by these environmental conditions.

Over the years, the offshore industry expanded to seismic prone areas where tremors and earthquakes occur. These additional environmental conditions and corresponding risks resulted in new regulations. Following these regulations, the dynamic behavior and seismic analysis of these structures must be taken into account in platform design.

Although seismic shocks can induce risks for offshore structures, these risks can be relatively small for oil and gas jack-up platforms since these types of structures are generally compliant. This means that the vibrations induced by the seabed can be captured and absorbed relatively well by the flexibility of the legs of the structure.

In 1991, a new offshore industry originated in Denmark with the installation of the first offshore wind farm. Many European countries followed which fostered technological developments in the offshore wind industry. Over the past decade, the offshore wind industry has expanded to other regions around the world. This resulted in an exponential growth of global offshore wind energy production.

In contrast to oil and gas jack-up platforms, wind jack-up vessels consist of a structure that is generally less compliant. This is necessary to deliver the required stability for wind turbine installation. Since these structures are less compliant, they are generally more vulnerable seismic activity. Therefore, it is important to take seismic analysis into account when designing wind turbine installing jack-up vessels and this is required by regulations.

A jack-up vessel is the most common structure used for wind turbine installation due to its stability during lifting operations combined with its relocation mobility. This thesis focuses on these kinds of jack-up vessels. For convenience, we refer to a jack-up wind installation vessel as a 'jack-up' in the rest of this thesis.

2.2 Design requirements for jack-up vessels

The offshore wind industry is relatively young, and innovations are introduced every year. Therefore, the regulations in this industry are lagging the state of the art. This results in an industry that sets its own requirements to guarantee the safety of personnel and to mitigate operational, environmental, and financial risks. One of those requirements is related to seismic activity. Since jack-ups are subjected to severe earthquakes in countries such as Japan and Taiwan, seismic analyses are required in the design process. The current requirements that the industry sets for such areas are usually copied from oil and gas regulations. An example of this is ISO 19901-2 [5]:

“Structure located in seismically active areas shall be designed for the ultimate limit state (ULS) (...) using different levels of earthquakes. The ULS requirements are intended to provide a structure which is adequately sized for strength and stiffness to ensure that no significant structural damage occurs for a level of earthquake ground motion with an adequately low likelihood of being exceeded during the design service life of the structure. The seismic ULS design event is the extreme level earthquake (ELE). The structure shall be designed such that an ELE event will cause little or no damage. Shut-down of production operations is tolerable, and the structure should be inspected subsequent to an ELE occurrence.”

A time history analysis is required by ISO 19901-2 [5]. In this method:

“...the base excitations shall be composed of three motions, i.e. two orthogonal horizontal motions and the vertical motion. Reasonable amounts of damping compatible with the ELE deformation levels are used in the ELE design. The International Standard applicable to the type of offshore structure shall be consulted. Higher values of damping due to hydrodynamics or soil deformation (hysteretic and radiation) may be used, however the damping value used shall be substantiated with special studies. The foundation may be modelled with equivalent elastic springs and, if necessary, mass and damping elements; off-diagonal and frequency dependence can be significant. The foundation stiffness and damping values shall be compatible with the ELE level of soil deformations.

(...)

If the time history analysis method is used, a minimum of 4 sets of time history records shall be used to capture the randomness in seismic motions. The earthquake time history records shall be selected such that they represent the dominating ELE events. Component code checks are calculated at each time step and the maximum code utilization during each time history record shall be used to assess the component performance. Satisfactory performance shall be achieved for either the greater of four or half the total sets of time history records. Satisfactory performance of a given time history record, constitutes all code utilizations being less than or equal to 1,0.

(...)

If 7 or more time history records are used, global structure survival shall be demonstrated in half or more of the time history analyses.”

This implies that a structure located in a seismic prone area shall be designed such that ELE-events cause little or no damage. This can be demonstrated with a seismic time history analysis method. Current GustoMSC research does this kind of analysis for 7 relevant time history records of which half or more should demonstrate global survival.

Another related ISO code, ISO 19902[7], states:

“The assessment load case, F_d , shall be determined using the following generalized form in which the partial factors are applied before undertaking the structural response analysis to ensure that the non-linear behaviour is properly captured as given in Formula(8.8-1):

$$F_d = \gamma_{f,G}G_F + \gamma_{f,V}G_V + \gamma_{f,E}(E_e + \gamma_{f,D}D_e) \quad (2.1)$$

(...)

The partial action factors for ELE analysis are given below:

$\gamma_{f,G} = 1.0$ and is applied to actions due to fixed load;

$\gamma_{f,V} = 1.0$ and is applied to actions due to variable load;

$\gamma_{f,E} = 0.9$ and is applied to ELE actions;

$\gamma_{f,D} = 1.0$ and is applied to inertial actions induced by ELE ground motion($E_e = 0$);

This implies that the dynamic forces resulting from an ELE analysis should be multiplied by a factor of 0.9 to capture the non-linear behavior properly.

Next to that, the ISO19905-1 [6] states that:

“In computing the dynamic characteristics of braced, pile-supported fixed steel offshore structures, a modal damping ratio of up to 5 % of critical may be used in the dynamic analysis of the ELE event. Additional damping, including hydrodynamic or soil induced damping, shall be substantiated by special studies.”

This implies that up to 5 % damping can be used in the model.

In this study, we use the above stated requirements to evaluate the effect of seismic shocks and vibrations to jack-up vessels and its crane.

2.3 GustoMSC: The seismic analyses of jack-up vessels

GustoMSC conducts research on the seismic performance of wind installation jack-up vessels and their compliance to the ISO 19901-2 [5] regulation as mentioned before. For this purpose, GustoMSC created a model which

has been improved over the past years. This model was used in multiple studies to investigate the structural design of jack-up vessels. Some of these studies are discussed below.

Latooi (2018) [16] created a four-legged bar stool model which contains simple spring foundations. Although, this model can be used for the static analysis of jack-ups, it should not be used for transient analysis due to unrealistic dynamic behavior as a result of an oversimplified hull mass distribution.

According to Linthorst [13] the mass and stiffness distribution of the jack-up is important for an accurate response when constructing the jack-up model. He states that a slight eccentricity in the mass of the jack-up leads to a very different response. Therefore, he added a crane and a substructure for the hull to the bar-stool model of Latooi (2018) to ensure that mass distribution and eccentricity are incorporated.

Blankenstein (2020) [3] introduced mitigation measures to the jack-up model in order to reduce their vulnerability to seismic activity. A description of existing mitigation measures and their purpose is provided in the next section of this thesis.

Blankenstein (2020) investigated which mitigation measures may be suitable for jack-ups subjected to earthquakes. Based on a large literature study, interview with employees of GustoMSC and a qualitative analysis Blankenstein (2020) concluded that two mitigation measures are most promising. The first measure is a tuned liquid damper in the hull of the jack-up. The second measure is a friction pendulum at the bottom of the four legs. Subsequently, Blankenstein (2020) evaluated these two measures in a model similar to Linthorst (2019). Blankenstein concluded that both measures are very promising solutions.

One difference between the model of Linthorst (2019) and Blankenstein (2020) is that the first implements the crane as a substructure and the latter uses a fixed crane mass distribution to incorporate the crane in the hull mass. Since actual jack-up vessels comprise of two large elements, namely the jack-up and the crane, it is interesting to investigate what the benefits of each approach are.

Next to these studies, GustoMSC suspects that the mass, dimensions, and corresponding dynamic behavior of the crane relative to the jack-up vessel may have little or even dampening effects on the motion of the jack-up structure. This has not yet been proven by research.

In this thesis we investigate the effect of the crane as a substructure on the dynamic behavior of the jack-up. Thereafter we evaluate the effect of an implementation of mitigation measures on the crane's dynamic behavior. With this, we built upon and add to the existing literature and thereby progress the field of offshore wind energy engineering.

2.4 Literature on important considerations in the seismic analysis models of GustoMSC

The current model that is used by GustoMSC for the seismic analysis is an improved version of the model of Linthorst (2019) [13]. This model uses a couple of specific design decisions and analysis settings of which the background is explained in this chapter. Further design considerations of this model are discussed in Section 3.3

In general, Timoshenko beams are used to connect nodes in this model. The classical Euler-Bernoulli beam theory provides a means for calculating the load-carrying and deflection characteristics of beams. This theory is only valid for small deflections of a beam that are subjected to lateral loads. In addition to this theory, the Timoshenko beam theory takes shear deformation and rotational bending effects into account. This makes it suitable for describing the behavior of thick beams[17]. The added mechanisms for deformation effectively

lower the stiffness of the beam. This results in a larger deflection under a static load and lower predicted natural frequencies for a given set of boundary conditions.

As stated in the ISO-standards in Section 2.2, the seismic analysis of the structure needs to be done based on a time-history analysis. In such a time-history analysis, the governing equations of motion of a structure are solved for each time step in the time-trace. This model uses the Hilbert-Hughes-Taylor integration method and the Modified Newton-Raphson iteration algorithm to advance to the next time step.

The Hilbert-Hughes-Taylor integration method makes a numerical approximation of the displacements, velocities, and accelerations of the structure in the next time step of the analysis [14] [11]. It is a one-step implicit integration method for solving the transient analysis which attempts to increase the amount of numerical damping present without degrading the order of accuracy. This method ensures that Rayleigh damping is properly considered.

According to ISO 19905-1 [6], a modal damping ratio of 5 % of the critical damping is used in the current model. This is applied in the form of numerical damping called Rayleigh damping. This Rayleigh damping is a combination of stiffness and mass-proportional damping. Different structural response frequencies lead to different damping ratios, therefore the Rayleigh damping is can be tuned to two specific response periods.

The Newton-Raphson iteration algorithm is a root finding algorithm which produces succeedingly better approximations to the solution of the structure's displacement, velocity, and acceleration [14] [4]. The algorithm keeps on adjusting its solution till a certain precision of this solutions has been reached, i.e. convergence has been reached. The adjustment for the next iteration is based on the current iteration's solution and its tangent.

Due to this iteration algorithm the non-linear P-delta effect is taken into consideration within this model. P-Delta is a second order effect which is created by a first-order initial deflection of the structure in reaction to acentric loads. P-Delta is a moment found by multiplying the first order deflection by the force that is a direct result of the weight of the structure. The iteration algorithm enables the structure to experience additional deflection because of this P-Delta moment [14].

2.5 Existing measures to limit earthquake damage

The dynamic response of the crane can be reduced by applying a mitigation measure to this substructure. This measure might be an increase of the structural ductility to increase the damping of the structure itself. Or it can be in the form of a device which can be added to the structure. These devices are designed to act as energy dissipating systems, to isolate the structure from ground motion, to mitigate dynamic response through the momentum exchange or to include a combination of the effects above.

The in-depth engineering book, called 'Modern Earthquake Engineering for offshore and land-based structures', contains a very extensive discussion on the mitigation of the dynamic response of structures. In this book, the measures are subdivided in categories based on their working mechanisms. No other mitigation measures have been found according to experts' opinions. This indicates that this book describes a rather complete overview of available measures. Therefore, an overview of these measures is created and a brief explanation is given in the following sections.

2.5.1. Ductility through structural configuration

The conventional approach requires that structures can passively resist seismic loading through a combination of redundancy, strength, deformability, and energy absorption. In an earthquake prone area, a ductile structural

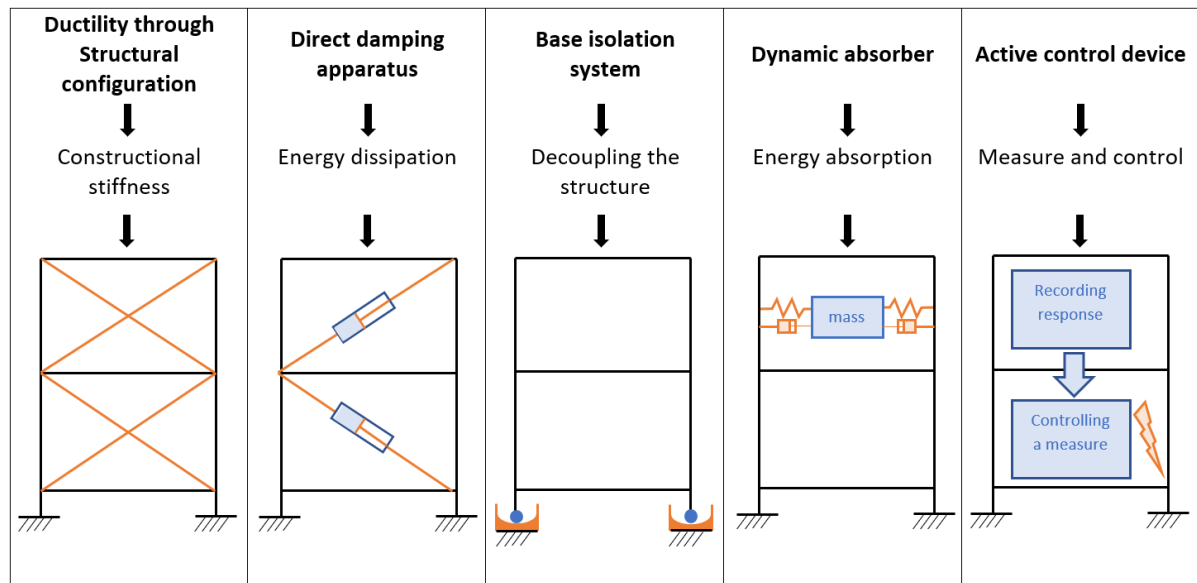


Figure 2.1: Overview of existing mitigation measures

system with minimal weight is preferred and is often the main design principle. Therefore, it is normally easier to meet the criteria with steel structures. There are plenty of engineering realizations of steel brace frames which are economical and add high lateral stiffness.

2.5.2. Direct Damping Apparatus

Damping apparatuses have been recognized as an effective technique to mitigate dynamic seismic and wind induced response for structures. A wide range of damping apparatuses are commercially available and rely on viscous, dry friction, hysteric effects, or a combination of these effects. It should be noted that damping apparatuses are normally not designed as static load bearing members but as a part of structural elements subjected to dynamic loading.

Under low amplitude of dynamic loading, they have sufficient stiffness to behave elastically. However, dampers deform significantly when they are subject to large amplitude of dynamic loading, and in the meantime, absorb the seismic energy transmitted from other parts of the structure. Through the energy absorption, the loads applied on primary load bearing structural members can be dramatically decreased, and the safety of the structure is therefore ensured.

2.5.3. Base Isolation Systems

The base isolator possesses of three essential elements: 1; a flexible mounting so that the period of vibration of the total system is lengthened sufficiently to reduce the force response. 2; a damper or energy dissipator so that the relative deflections structure and substructure can be controlled to a practical design level. 3; a means of providing rigidity under low (service) load levels due to mild wind and minor seismic ground motions.

Nowadays, in earthquake prone areas, land-based structures are located on base isolators that allow the ground to move laterally back and forth beneath the structure while the accelerations of the structure are rather limited and free from damage. This requires the base isolators to not only provide the vertical load transmission, but also, if possible, enable active re-centering of the structure during and after an earthquake.

2.5.4. Dynamic Absorbers

To absorb the kinetic energy produced by dynamic loading such as by waves, wind, earthquakes, and ice loading on a structure, one can install a mechanism called a dynamic absorber. For the optimal performance, this measure should be installed at an anti-node location of a dominating normal mode of the main structure.

The mass of such a dynamic absorber is only a percentage of the mass of the main structure. The stiffness should be tuned such that the natural frequencies of both, the dynamic absorber and disturbing force applied by the main structure, are equal. Therefore, the resonance of the mechanism with the vibration of the main structure facilitates the vibration energy of the main structure to be efficiently transferred into the absorber, and the main structure's dynamic response is reduced in an optimized manner.

2.5.5. Active control device

A control mechanism can be introduced to increase the damping efficiency of a measure. The parameters of a mitigation measure are adapted to respond to the changes in the vibrating structure and achieve more optimal damping. This leads to the application of semi-active and active measures, which can control vibration systems with a smaller size of measure.

Semi-active and active measures usually utilize hydraulic or electro-mechanical actuator systems driven by an appropriate control algorithm. The major difference is that the semi-active damper only changes the damping level and does not add any other external mechanical energy to the system and therefore semi-active systems are more energy efficient.

2.5.6. Discussion on mitigation measures

The mitigating measures described above are assessed later in this thesis, in Section 5.1. This assessment is based on three criteria: their potential for mitigating forces, their potential for mitigating motions and their feasibility for implementation in the crane. From this assessment it is concluded that a base isolation system and a dynamic absorber are the most promising measures to reduce the response of the crane. Therefore, the next section elaborates in more depth on the physical working mechanism of these two measures.

2.6 A more detailed elaboration on the Base Isolation systems & Dynamic absorbers

From the assessment of the existing mitigation measures in Section 5.1 it is found that the base isolation system and the dynamic absorber are the most promising measures to apply in the crane. Therefore this section elaborates on their physical working mechanism.

2.6.1. Base Isolation Systems

Base isolation systems separate the response of a structure from the period of the underlying base. This is established by a low horizontal stiffness between the structure and the foundation. As this leads to an increase in the structure's natural period, it induces an effective reduction of the spectral excitation. Besides lengthening the structure's period, this system is capable of dissipating energy through friction.

Both damping effects can be seen in Figure 2.2 below where the response spectrum of such structures is given. This plot shows the response of the structure to different periods of the external force acting on the structure.

Base isolators ensure that energy is captured as displacements in the isolation system itself rather than as deformations of the main structure. It is found that these systems are most effective when the natural period of

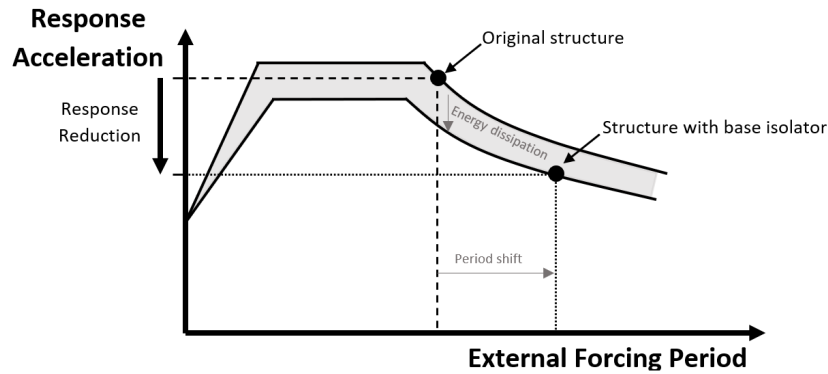


Figure 2.2: Acceleration response reduction due to a base isolation systems

the structure coincides with or is close to the period of the under-lying base.

Generally, there are two types of base isolators: elastomeric bearings or sliding isolation systems. The elastomeric bearing converts kinetic energy to thermal energy which can easily be dissipated. The sliding isolation system provides energy dissipation through friction and limits the forces being transferred to the superstructure due to a maximal friction force.

The latter is of interest for this thesis due to two reasons. Firstly, it provides sufficient stiffness at small displacements for daily service levels of environmental loading. Secondly, a typical ball sliding system can resist much higher vertical loads and overturning moments than a rubber elastomeric bearing due to a 5-10 times higher compressional stiffness.

A sliding base isolation system utilizes the frictional sliding mechanism between the structure and the foundation. On the one hand, the mechanism requires a low friction to partially cut the load transmission path. On the other hand, the mechanism also provides friction to dissipate energy.

Displacements within such a system need to occur to absorb the energy. However, these displacements can add up over time if they do not oppose each other. A high-tension spring or a curved sliding surface can be applied and tuned to create a restoring force when displacements occur. This equals the principle of a pendulum that wants to go back to its initial equilibrium position. The restoring force counteracts displacements since it is always pointed in the direction of its equilibrium position and the force increases with the magnitude of the displacement. In this way the displacements within such a system can be kept under acceptable limits. An example of such a sliding base isolation system with a curved sliding surface is a friction pendulum bearing.

The displacement curve of a friction pendulum bearing is shown in Figure 2.4 below. The load transmission path through this bearing is cut off when slip occurs. Slip occurs when the lateral force with respect to the normal force exceeds a certain slip threshold. i.e. Saying that the friction between the surfaces no longer can resist the lateral force between the top and bottom part of the bearing.

The slip threshold is determined by the friction coefficient. This coefficient can be calculated with different methods. These differ by including or excluding certain parameters which influence the behavior of the coefficient of friction. Such parameters are the absolute sliding velocity and the pressure on the contact area.

The slipping behavior of such a friction pendulum bearing is tuneable via the combination of the curvature and the radius of the sliding surface. The curvature determines the restoring force in a similar way as a pendulum. A larger displacement leads to an exponentially increased restoring force. The radius determines the maximum

possible displacement within this bearing.

The initial stiffness (K_{init}) should provide sufficient stiffness for daily service level load and captures the pre-slip deformation. The effective radius (R_{eff}) of the concave sliding surface ensures the restoring force.

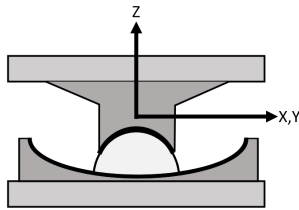


Figure 2.3: Schematic view of a friction pendulum

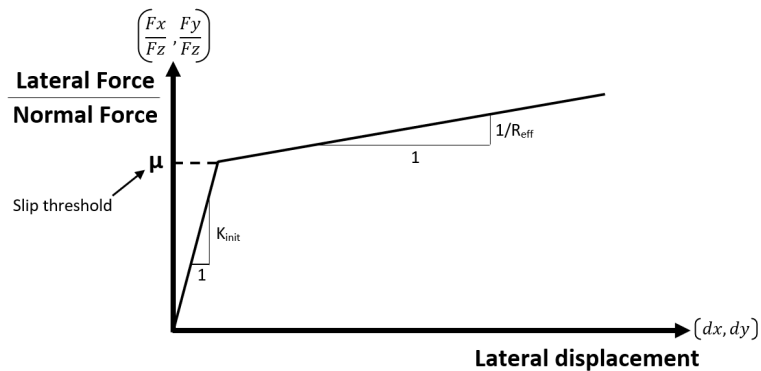


Figure 2.4: Displacement curve of a friction pendulum

An example of this measure applied in an offshore structure can be found in one of the largest offshore engineering projects in the world, the 'Sakhalin II project'. To overcome extreme dynamic loads, a friction pendulum bearings is proposed between the topside and the legs of this structure. This makes the topside a floating deck during strong seismic motions. It is estimated that the seismic risk comprises of almost 50% of the total risk. After implementation of the measure, this has reduced to only 26%.

2.6.2. Dynamic Absorber

A dynamic absorber imparts indirect damping to the structure by modifying its frequency response. Besides this modification of the frequency response, additional damping can be added to dissipate more energy. This can be done by connecting a viscous damper between the main structure and the absorber itself. The dynamic absorber can be viewed as an energy sink, where excess energy that is built up in a structure is transferred to the mass of an absorber. The damping effects of a dynamic absorber can be seen in Figure 2.5 where the response spectrum of such structures is given. This plot shows the response of the structure to different frequencies of the external force acting on the structure.

A dynamic absorber can drastically reduce the resonance response in a narrow frequency band and is therefore most effective for periodic excitations and structures under dominated self-vibrations. Ideally, the frequency of a dynamic absorber is tuned closely to the natural frequency of the dominant self-vibrations.

The most optimal location for such a dynamic absorber is a location where the largest motions of the structure occur. To be more precisely, this is an anti-node location of the vibration mode which has the largest influence on the structural dynamic response of the structure.

The resonant vibration of the dynamic absorber is out-of-phase with the vibration of the main structure as shown in Figure 2.7. This phase lag is influenced by the connection between the absorber and the structure. When only connected by a damper the phase angle is 90° and when connected by both a spring and a damper, the phase angle is less than 90° .

Dynamic absorbers do not require an external power source to operate and do not interfere with vertical and horizontal load paths. Therefore, dynamic absorbers are relatively convenient to implement in new structures

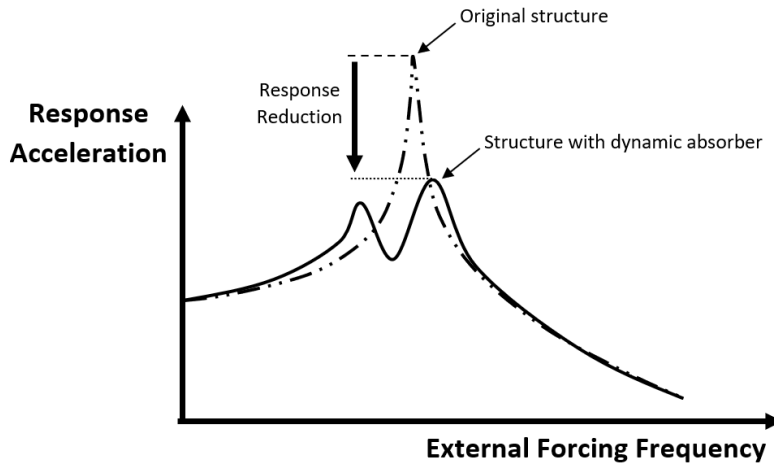


Figure 2.5: Acceleration response reduction due to a dynamic absorber

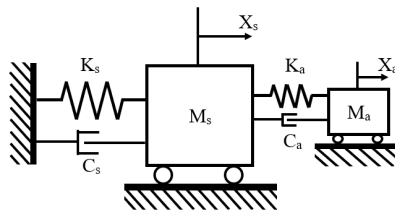


Figure 2.6: Schematic view of a dynamic absorber

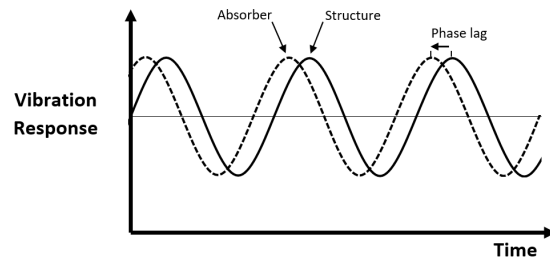


Figure 2.7: Phase lag of the dynamic absorber

and to retrofit in existing structures. Furthermore, dynamic absorbers can be combined with active control systems to function as hybrid systems in a relatively easy manner.

Generally, there are two types of dynamic absorbers: tuned mass dampers (TMD) or tuned liquid dampers (TLD). As the name already indicates the difference between the two is within the state of the mass. A TMD has a solid mass and a TLD has a liquid mass which uses sloshing of the liquid to generate additional damping.

The dynamic behavior of such absorbers can be tuned by adjusting the absorbers mass (M_a), stiffness (K_a), and damping (C_a) characteristics as indicated below. A schematic overview of the system is given in Figure 2.6.

A larger mass ratio between the absorber and the structure lead to a more effective reduction of the vibrations of the structure. However, in practice it is found that it is more economic to use an absorber mass between 1 and 5 % of the effective modal mass of the structure.

The stiffness of the absorbers should be tuned such that the natural frequency of the absorber equals the natural frequency of this mode, this can be done using Equation (2.2). Afterwards, additional damping can be added to the absorber. Realistic amounts of additional damping are in the range of 10% of the critical damping. The amount of damping required can then be calculated with the following equation:

$$K_a = \omega_s^2 * M_a \quad C_a = \zeta_a * 2 * \sqrt{K_a M_a} \quad (2.2)$$

An example of such a dynamic absorber is investigated for the use in offshore wind turbines[1]. It is stated that

these are rather flexible structures which make them vulnerable to excessive vibrations. During this research a tuned liquid column damper (TLCD) is considered and the model is subjected to waves, wind and seismic loading. The effect of the severity of earthquakes on the performance of the structural control device is investigated. The results suggest that the use of an optimal TLCD with a mass ratio of 2.5% reduces the fragility of the system by as much as 6% and 12% for operational and parked conditions, respectively.

3

Simulation model for the seismic analysis of a jack-up with a crane

For the seismic analysis of jack-up structures we use a simulation model. This chapter starts with a description of the structural dynamics that govern the structure and how they are modeled. After which, this chapter explains how the model is implemented in the software framework 'OpenSees'. Subsequently, this chapter explains why some adjustments of the existing jack-up and crane model of GustoMSC are necessary to make it suitable for our research goals. Finally, this chapter presents the natural period of the crane in this model and compares it with an analytical model.

3.1 Structural dynamics and finite element analysis

Structural dynamics is the field of engineering that covers the response of structures subjected to a dynamic loading. This dynamic loading refers to the force that is applied on the structure by time dependent external factors (e.g. wind, waves, seismic activity). The response of complex structures is studied with finite element analysis.

In finite element analysis, any physical structure can be simplified by bodies and elements. The bodies are defined by the structural mass ' \mathbf{M} '. The elements are defined by the stiffness of the structure that can be described as structural springs, ' \mathbf{K} ', and dampers, ' \mathbf{C} '. Each body has its own degrees of freedom that determine the directions in which the body can move independent of other directions. The motion of these bodies is defined by a system of equations that describe their motion over time (Equation (3.1)). In this system of equations, the dynamic loading on the structure is equal to the sum of forces that depend on the acceleration, velocity, and displacement of the structure.

$$\mathbf{M}\ddot{x} + \mathbf{C}\dot{x} + \mathbf{K}x = \mathbf{F} \quad (3.1)$$

Such a system of equations can be solved with finite element software. For a dynamic analysis, this system is solved for every time step with the associated time-varying force vector that represents the dynamic loading. Recent seismic analyses of jack-up vessels have been conducted by GustoMSC using a software framework called 'OpenSees'. The next section explains how this software solves the governing system of equations.

3.2 Opensees as solver for the governing system of equations

OpenSees, the Open System for Earthquake Engineering Simulation, is an object-oriented, open source software framework. It allows users to create finite element computer applications for simulating the response of structural and geotechnical systems subjected to earthquakes and other hazards. The OpenSees framework is composed of the model, the domain, the analysis, and the recorder.

In the model, a structure can be created which is then added to the domain. The domain contains both the current time step model (t) and the next time step model ($t+dt$). The analysis translates the state of the current time step model to the state of the next time step model. Finally, the recorder records user-defined parameters during this translation. In the subsections below this is discussed in more detail.

3.2.1. Opensees - Model builder

The model is defined in a global reference framework with 3 spatial dimensions and 6 degree of freedom. A structure is created by defining nodes and connecting them with elements. Each node is defined by its nodal coordinate and nodal mass. Each element is defined by two nodes and parameters that describe their relationship. The mass of the structure is divided over the nodes and the elements define the structural stiffness. Constraints can be assigned to certain nodes to include the boundary conditions.

By creating the structure, OpenSees automatically defines the following system of equations of motion:

$$F_I(\ddot{x}) + F_R(\dot{x}, x) = F_E \quad (3.2)$$

This is the same equation as Equation (3.1), just written differently. F_I represents the acceleration-dependent inertial force vector. F_R represents the resisting-force vector consisting of the velocity (damping) and displacement-dependent (stiffness) force vectors. F_E represents the external applied-force vector.

3.2.2. Opensees - Analysis

The time domain analysis advances through time by solving the system of equations. The predictive step towards the next time step ($t+dt$) is determined with an integration method that uses the tangent of the current step. This tangent describes the change in parameter values of the equation of motion for the current time step. Thereafter, an iteration algorithm solves the equations for the next time step by decreasing the residual vector through adjusting the tangent matrix. This vector is a result from the difference between the current state and the next state. A convergence test is performed to check whether the iterated solution is within a user set difference limit.

3.2.3. Opensees - Recorder

Recorders monitor the response of the structure during the analysis and generates output for the user. Displacements, velocities, and accelerations can be recorded for nodes. Reaction forces can be recorded for both nodes and elements.

3.3 Model design considerations for solving the governing system of equations

In 2019, Linthorst (2019) [13] created a new jack-up model in OpenSees to represent the design of the NG-14000XL. This is a GustoMSC jack-up vessel for wind installation purposes. Linthorst used this model for seismic analyses of the jack-up. The model has been verified with different methods and it was concluded that the model is an accurate, simplified representation of a jack-up. In the past two years, improvements to the model have been made based on the findings of GustoMSC employees interns[3].

The model of Linthorst (2019) uses a transient analysis with a constant time step. The Hilbert-Hughes-Taylor integration method is used to predict the step to the next time increment. The Modified Newton-Raphson iteration algorithm is used to adjust this predictive step towards a more precise numerical solution. These methods allow for energy dissipation, second order accuracy and the consideration of the P-Delta effect. A more elaborate explanation of these methods is provided in Section 2.4.

Linthorst (2019) applied Rayleigh damping to account for structural damping during the analysis. Rayleigh damping is a viscous damping method which is proportional to a linear combination of mass and stiffness. As recommended by ISO 19902 and explained in Section 2.2, a damping percentage of 5% is used. Moreover, Grasso et al(2017)[1] state that it is of high importance that the mass utilization ratio of the analyzed modes for the Rayleigh damping is above 90%. Therefore, the damping is tuned to the first and 12th mode.

The P-Delta effect is introduced to account for geometric non-linearities. This P-delta effect means that the jack-up in the model start to deflect due to an off-set of the eccentricity of the jack-up. As this deflection leads to a larger off-set a secondary moment is created by which the model should deflect some more. This is included by iterating at every time step until convergence is reached and therefore no more deflection is introduced by the secondary moment.

The time analysis starts by adding weight of the structure in multiple steps. This can deform the structure. This weight is kept constant for the rest of the time domain. For the rest of the time domain, a tri-axial time trace defines the excitations of the environment in two orthogonal horizontal directions and one vertical direction. These excitations enter the structure through the foundation where the model is connection to the environment.

Further design considerations for the jack-up structure and the crane structure are discussed in the following two subsections.

3.3.1. Model design of the current jack-up model

As mentioned above, the jack-up model of Linthorst (2019) represents the design of the NG-14000XL. This is a GustoMSC jack-up for wind installation purposes. This jack-up can operate in water depths up to 65 meters and possesses of a hull with a length of 130 meters and a width of 50 meters. The model of this jack-up consists of 4 legs and a hull as can be seen in Figure 3.1.

The truss legs of the jack-up are simplified and modelled as a beam, consisting of Timoshenko beam elements which are defined by pre calculated truss leg parameters. Each leg is connected to the environment by their lowest node. This connection is modelled as a spring dashpot to represent the spudcan interaction with the environment. The leg-to-hull interface is modeled as a spring that connects the leg to the jack house. The spring defines the stiffness in six degrees of freedom to represent the lower and upper guides and the jacking system. The jack house is composed of four stiff diagonals which ensure that forces and accelerations from the leg are well spread over the four corners of the jack house.

The hull structure consists of thick beams, such as bulkheads, girders and hull edge beams. This structure has been modelled by Timoshenko beam elements since they represent the behavior of thick beams well. These Timoshenko beam elements are located in such a way that they represent the hull well. To ensure a representative mass and eccentricity of the vessel, a tool is used, to generate a hull mass distribution. The result of such a hull mass distribution is shown in Figure 3.2. This tool includes the mass of fixed items ranging from the steel structures such as the hull, deck house, and crane, to paint and furniture. Next to the fixed items, it includes variable deck loads such as lifting tools and wind turbine components.

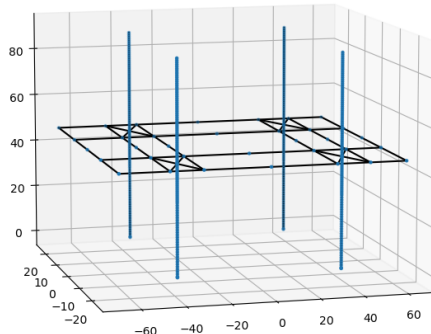


Figure 3.1: Structure nodes and elements in the current jack-up model for time domain analysis

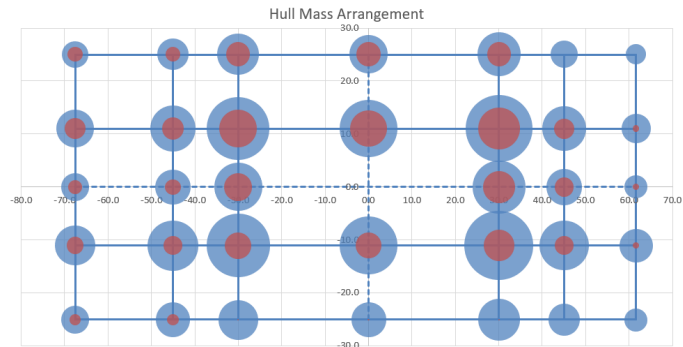


Figure 3.2: Hull mass distribution
Blue dots represent fixed weight
Red dots represent the variable weight

3.3.2. model design of the current crane model

The crane model of Linthorst (2019) [13] represents a new type of crane that is designed for the offshore wind market. This is the so-called Telescopic Boom Crane (Figure 1.3) [9]. Its name refers to the telescopic part which can be extended from the fixed part of the boom as can be seen in Figure 3.4. In retracted mode, the crane boom has a length of 100 meters and a lift capacity of 2500 tons. In extended mode, the crane boom has a length of 150 meters and a lift capacity of 1250 tons. The crane is modeled with Timoshenko beams to ensure that shear deformation and rotational bending effects are considered[17]. The complete crane model is shown in Figure 3.3 and composed of a pedestal, A-frame, boom, jib, suspended mass, and the hoist wires.

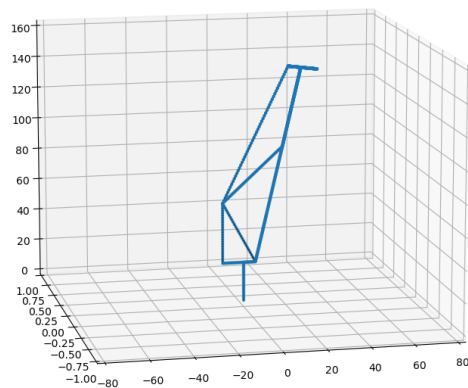


Figure 3.3: Structure nodes and elements in the crane model of Linthorst (2019)[13]

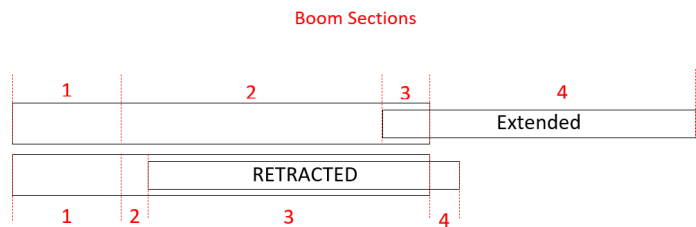


Figure 3.4: Distribution of the boom sections in the crane model

The pedestal is modelled as a beam which is connected to the starboard stern leg of the jack-up. It is attached to same stiff diagonals which connect the hull to the leg to ensure for force and acceleration distribution over the jack house corners. The pedestal has a height of 25 meters.

The double parallel A-frame of the actual crane is modelled by a single A-frame consisting of three beams that form a triangle. These beams represent the stiffness properties of the double A-frame. The single A-frame is a solid steel structure with a hinged connection to the boom. While this hinge allows all forces to be transferred, it only allows for the transfer of moments in the x- and z-direction. The A frame has a height of 38 meters and horizontal length of 15.6 meters.

The boom consists of four sections as can be seen in Figure 3.4. This accommodates the telescopic capabilities of the crane. It ensures that the mass division and stiffnesses of the crane adapts to the length of the crane.

The first section has a fixed length and mass. The length of the other three sections is depended on how far the telescopic part is extended. The second section has an equal mass and stiffness distribution as the first section but differs in length. The third section defines where the telescopic part of the boom overlaps with the fixed part of the boom. This section has the weight and stiffness of the fixed part plus the telescopic part. The fourth section has the mass and stiffness of the telescopic part. When the telescopic part is fully extended, section three does not exist, and so does section four not exist when the telescopic part is fully retracted. In extended mode, the boom has a length of 150 meters. In retracted mode the boom has a length of 100 meters.

The jib is connected to the tip of the boom and consists of an upper and a lower jib. The suspended mass that is lifted by the crane has been modelled as an extra node at the end of lower jib. This node is connected to the lower jib by a spring in horizontal direction and is fixed to jib in vertical direction. This stiffness of the spring represents the horizontal stiffness of a simple pendulum with a certain sling length. In vertical direction, this model neglects the relative motion between the suspended mass and the jib.

The main hoist wire runs from the top of the A-frame to the backside of the jib. The mid hoist wire runs from the top of the A-frame to the collar, which is located at the end of the fixed part of the boom (end of boom section 3). The connections of these hoist wires to the crane are modelled as hinges. These hinges enable the transfer of forces but not of moments. This ensures the transfer of axial forces in the hoist wires only. For model simplicity, these hoist wires are also modeled as Timoshenko beams and use the specifications that represent 24 wires for the main hoist and 8 wires for the mid hoist.

This model is assumed to be only relevant for a crane that is in operation since the dynamic response of the boom changes drastically when it is supported by its boom rest (as is the case when not in operation). The validation of this model is done with a simplified existing analytical model of which the natural periods and mode shapes are compared.

3.4 Corrections to the crane model

Two deficiencies in the crane model of Linthorst (2019)[13], as described in the previous section, were revealed when analyzing its dynamic response. First, an unexpected high natural frequency of the crane was found. Second, a convergence error occurred for slew angles around 90 degrees. Another deficiency was found while implementing the crane on the jack-up. The crane introduced significant modes which cause the Rayleigh damping to be tuned incorrectly. Therefore, a new crane model is necessary which addresses these deficiencies. The adjustments which lead to this new model are discussed in the following subsections.

3.4.1. Correction of the boom hinge stiffness

In order to verify whether the model approximates reality well, we investigate the natural periods of the model of Linthorst (2019). The results of this investigation for a short legged jack-up model are presented in Table 3.1. As can be seen in the first column, for a jack-up without a crane, the three modes with the highest natural periods have a natural period of approximately 3 seconds. These modes have significantly higher natural periods than the other modes. They represent the motion of the jack-up in the three lateral directions, namely the x, y and torsional direction. This corresponds to findings in prior research which indicates that this model is suitable to use.

The implementation of the crane on the jack-up results in four additional significant modes for the combined structure, as can be seen in the second column of Table 3.1. These four additional modes represent the suspended mass modes in two horizontal directions and the crane modes for the in-plane and out-of-plane direction.

Although these additional modes are expected to be present, the period of the out-of-plane mode is surprisingly high (15.82 seconds). This is related to the fact that the rotational stiffness of the zero-length-element that represents the boom hinge is lower than it should be. In the actual crane, the boom hinge is a very stiff component that does not allow for any other rotation than the luffing angle to occur. This is the angle by which the boom can be lowered. In the crane model, this luffing angle equals the rotation around the x-direction of the boom hinge element. Therefore, the rotational stiffness around the y and z axes of this boom hinge element should be modeled as infinitely stiff. This is not the case in the model of Linthorst (2019). Therefore, we chose to incorporate an infinite stiffness in our model.

To determine what level of stiffness is sufficient to represent this infinite stiffness we execute a convergence test. In this test, we gradually increase the rotational stiffness of the boom hinge. Figure 3.5 present the results of this convergence test. It shows that convergence is reached when the boom hinge has a stiffness of 10E7 MNm/rad. Therefore a value larger then this is used in our crane model to incorporate this infinite stiffness.

Table 3.1: Highest ten natural periods present in the OpenSees models

Mode no.	J* [s]	*J+C [s]	J+C* Corrected [s]
1	3.22	15.82	8.97
2	3.15	8.97	8.97
3	3.07	8.97	3.97
4	0.69	3.33	3.32
5	0.62	3.21	3.11
6	0.57	3.00	2.99
7	0.53	2.60	2.60
8	0.50	0.68	0.68
9	0.50	0.67	0.63
10	0.50	0.63	0.61

J*: Jack up without crane

J+C*: Jack up with crane

This table represents the natural periods of a jack-up model and a crane model. The jack-up model represents the NG-14000XL in shallow(30m) water and the crane model represents the telescopic boom crane.

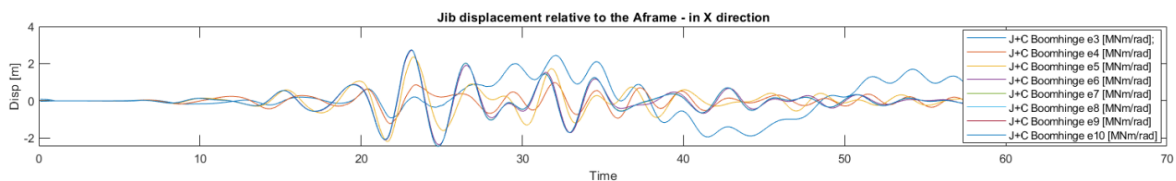


Figure 3.5: Convergence study to the stiffening of the boom hinge.

The input signal this convergence study is an earthquake which has its focus between 20 and 30 seconds.

3.4.2. Correction of the boom hinge orientation

The second correction to the crane model has to do with its orientation. During the analysis, a convergence error occurs for slewing angles close to 90 or 270 degrees. The response of the crane becomes divergent and so to speak, the crane flies away. To find the cause of this problem, the displacements of several nodes that are conveniently distributed over the crane are recorded and presented in Figure 3.6.

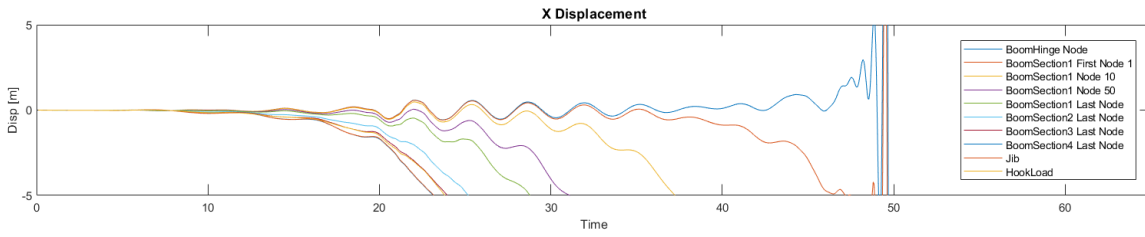


Figure 3.6: Divergent behaviour of the crane due to improper modelling of the boom hinge stiffness.

It is found that the displacements of the A-frame node that is the closest to the boom remain limited while the first boom node clearly shows unexpected divergent behavior. Therefore, we find the origin of the convergence error in the hinge of the boom.

As explained in the previous section, the boom hinge element is a zero-length element. Compared to other elements, this element does not automatically consider geometric transformations. Normally, these transformations translate the local reference system, that is defined by the two adjacent nodes, to the global reference system. Since the local reference system for a zero-length element cannot be defined, the model uses the global reference system to define this element.

Therefore, a change in the slew angle will not result in a change of the orientation of these stiffnesses of the boom hinge. Modelling the boom hinge in this way is incorrect since the stiffness of the boom hinge has a different magnitude for each rotational direction.

To include the slew angle and thus the orientation of the boom hinge in the correct manner, the zero-length elements has been provided with a predefined orientation vector. Hereby we manually define the local reference system based on the slew angle that has been set upfront. The part of the vector that determines the x- and y-axis of the local reference system are shown in Equation (3.3). The z-axis of this element does not need to be predetermined as it equals the z-axis of the global reference system.

In this way, the model possesses of a proper implementation of the boom hinge and the analysis completes its run without convergence errors.

$$X_{Localaxis} = \begin{bmatrix} \cos(\alpha_{slew}) \\ \sin(\alpha_{slew}) \\ 0 \end{bmatrix} \quad Y_{Localaxis} = \begin{bmatrix} -\sin(\alpha_{slew}) \\ \cos(\alpha_{slew}) \\ 0 \end{bmatrix} \quad (3.3)$$

3.4.3. Correction of the Rayleigh damping

As explained in Section 3.3, the Rayleigh damping is applied to the jack-up model by fitting it to the first and 12th mode to ensure a mass participation percentage of more than 90%. The damping coefficients curve resulting from this is given in Figure 3.7 by the green line. As mentioned before, adding the crane to the model results in four additional significant modes. Two of these modes relate to the horizontal motions of the suspended mass. It is found that these modes have a relatively large natural period compared to the significant modes of the jack-up. In this section, we refer to these large suspended mass modes as “sling modes”.

Fitting the Rayleigh damping in the combined model on the same modes as done for the jack-up model, result in an under damped system that is conservative and unrealistic. Since the sling modes have a relatively large natural period, tuning to the first mode results in a much lower damping for the significant jack-up modes as can be concluded from the blue line in Figure 3.7.

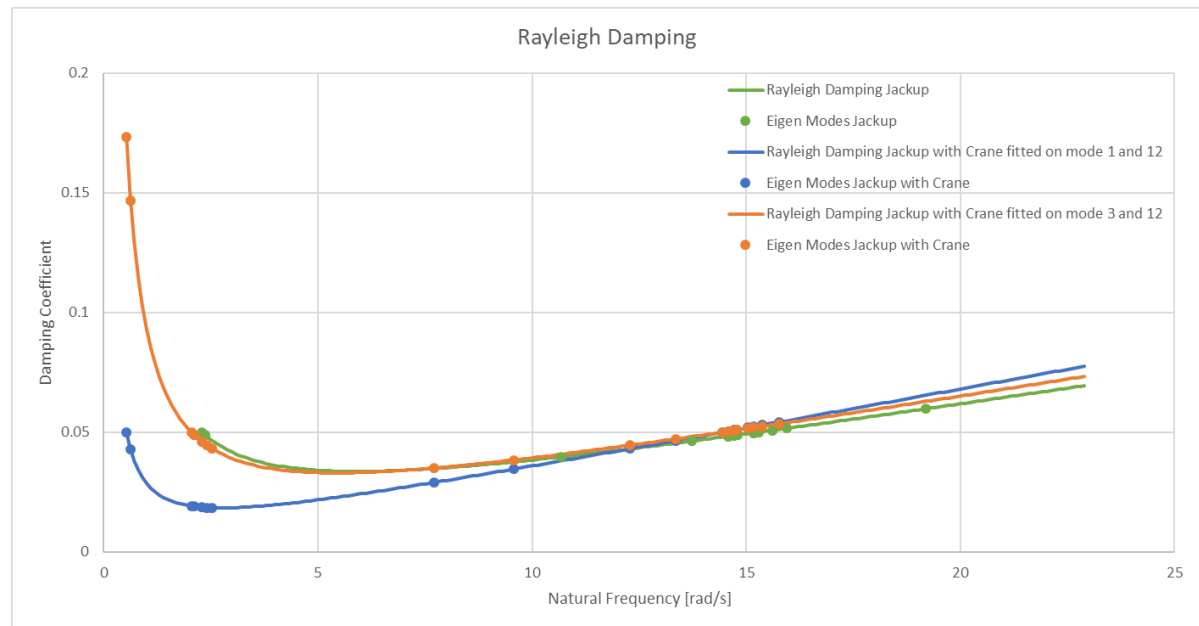


Figure 3.7: Rayleigh damping tuned to 1th & 12th mode or tuned to 3rd and 12th mode.

Another issue is that the natural periods of the sling modes vary with the sling length of the suspended mass. This makes fitting on the first mode incorrect as the damping in the jack-up would then become variable of the sling length of the suspended mass.

It is found that the combined mass participation percentage of the significant jack-up modes is 71% while this is below 1% for the suspended mass modes. To make sure that the structural damping stays realistic without being too conservative, the Rayleigh damping can be tuned to the 3rd and 12th mode instead. Tuning in this way, still results in a mass participation percentage of more than 90% while the under damping due to the sling modes is mitigated. The orange line in Figure 3.7 represents this case.

Although, one consequence of fitting the Rayleigh damping to the 3rd and 12th mode is that the sling modes become heavily over damped. Since the actual sling possesses of minimal damping, it has been chosen to exclude the sling modes in the application of the Rayleigh damping. In this way, the sling is conservatively modelled which we assume to be acceptable for the research in this thesis.

3.5 Verification of the crane model

The crane model is verified with a simplified analytical crane model. This analytical model considers the A-frame and the pedestal to be infinitely stiff. Furthermore, it does not consider the mid hoist boom wires connecting to the A-frame. In this analytical crane model, the crane is investigated for the in-plane and out-of-plane direction of the boom. These directions in the analytical crane model are visualised in Figure 3.8. The in-plane direction has two degrees of freedom, namely the boom hinge angle and the sling angle. The out-of-plane direction has 4 degrees of freedom, three are distributed over the boom and one defines its sling angle.

The natural periods that are found with this analytical model can be compared to the significant natural periods of the OpenSees crane model that is described before. For this comparison, the parametric values in the OpenSees crane model are set identical to that of the analytical model. The natural periods of both models and their relative difference is presented in Table 3.2. Since we find reasonably small differences, we assume this model to be verified.

Table 3.2 is representative for the configuration of the original analytical model. In this configuration the boom has a length of 150 meters, a luffing angle of 80 degrees, a sling length of 9.81 meter and a suspended mass of 115 tons. Varying the latter two input values for both models does not result in a larger relative difference change than 1.5%. Therefore, we concluded that the crane model is a representative model for various configurations in which the crane can be positioned.

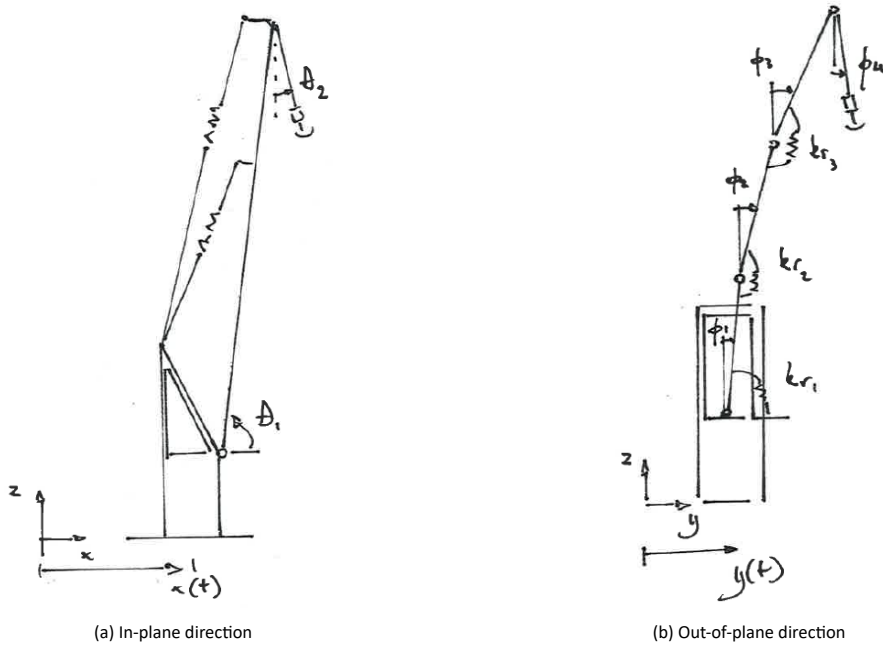


Figure 3.8: Analytical model of the telescopic boom crane

Table 3.2: Verification of the natural periods of the crane model with an analytical model

Mode Explanation	Analytical [s]	OpenSees [s]	Difference [%]
Sling mode (Out-of-plane)	7.49	7.42	-0.9
Sling mode (in-plane)	6.79	6.70	-1.4
Crane mode (Out-of-plane)	4.16	4.16	0.1
Crane mode (in-plane)	3.58	3.50	-2.3

The crane model is set to equal the parameters that define the analytical model. Such parameters are: a boom length of 150 meter, suspended mass weight of 115 tons and a sling length of 9.81 m.

3.6 Adjustments of the hull mass distribution of the jack-up model

Next to the corrections that are made to the crane model, some adjustments need to be made to the jack-up model to ensure for a proper mass distribution.

3.6.1. Adjustment to counter a duplicate crane mass

As explained in Section 3.3.1, the current jack-up model accounts for the crane as it is included in its hull mass distribution. In this distribution, the crane contributes to the Elevated Light Ship Weight (ELSW) calculations. The ELSW represent the fixed mass of the vessel. Using the crane model in combination with the jack-up model results in a duplication of the crane mass and an incorrect eccentricity of the combined model.

This mistake can be avoided by excluding the crane from the ELSW. In this way the crane is also excluded in the

hull mass distribution of the jack-up model. Using the crane model in combination with the jack-up model now results in a proper crane mass distribution. Table 3.3 describes the calculation of the mass and eccentricities of the new ELSW; the first column indicates the currently used ELSW, the second column indicates the crane contribution to this ELSW and third column indicates the ELSW from which this crane contribution is excluded.

Table 3.3: Change of the hull mass distribution for implementation of the crane

		ELSW	Crane _{ELSW}	ELSW _{subtracted}
Weight	[t]	22250	2400	19850
LCG	[m]	-0.82	-30.19	2.73
TCG	[m]	-2.01	-16.78	-0.22

ELSW: Elevated Light Ship Weight
 LCG: Longitudinal Center of Gravity
 TCG: Transverse Center of Gravity

3.6.2. Adjustment to represent the crane model in the hull mass distribution

The next chapter of this thesis investigates the influence of the dynamic response of the crane on the motion of the jack-up. For this investigation we model the crane as substructure on the jack-up model and compare the jack-ups response to that of a jack-up in which the crane is included in the hull mass distribution. We refer to this latter jack-up model as the benchmark model.

For correctness of the comparison, both models need to consider a similar crane mass and eccentricity. This is established by adjusting the hull mass distribution of the benchmark model. Similar to previous section, we first subtract the current crane mass from the distribution(ELSW_{subtracted}). Then we determine the mass and eccentricity of the crane model(Crane_{OpenSees}) and add this to the hull mass distribution in which no crane mass is present(ELSW_{subtracted}). The result is a adjusted ELSW(ELSW_{Adjusted}) that is used for the calculation of the hull mass distribution of the benchmark model. Table Table 3.4 presents an overview of these calculations for the case that the crane model has an similar configuration to that of the crane in the hull mass distribution.

Since the crane is investigated for multiple operation configurations, the calculations of the ELSW_{Adjusted} for various crane configurations are automated with a tool. This tool is an addition to the tool that calculates the hull mass distribution and enables the slew angle, luffing angle, and suspended mass to change.

Table 3.4: Change of the hull mass distribution of the benchmark jack-up model

		ELSW	Crane _{ELSW}	ELSW _{subtracted}	Crane _{OpenSees}	ELSW _{Adjusted}
Weight	[t]	22250	2400	19850	1872	21722
LCG	[m]	-0.82	-30.19	2.73	-30.19	-0.11
TCG	[m]	-2.01	-16.78	-0.22	-16.78	-1.65

ELSW: Elevated Light Ship Weight
 LCG: Longitudinal Center of Gravity
 TCG: Transverse Center of Gravity

In this table, Crane_{OpenSees} represents a similar orientated crane as the Crane_{ELSW}



Influence of the dynamic response of the crane on the motion of the jack-up

To study the influence of the dynamic response of the crane on the response of the jack-up structure, we implement the crane as a substructure in the jack-up model and compare the simulated dynamic responses to those in a model with a fixed mass distribution representing the crane. We do this because we would like to use the jack-up motions of the benchmark model as input for a stand-alone crane model. This is desired as model simplicity eliminates unnecessary side effects of the jack-up during further investigation in this thesis.

This chapter starts with a description of the methodology and models that are used in this investigation. After that, this chapter explains how we obtain useful data from the output of these models. Subsequently, this chapter gives an analysis of the data based on distribution and scatter plots. In the last section of this chapter the conclusions of this investigation are presented and discussed.

4.1 Methodology: Measuring the influence of dynamic modelling of the crane

As previously stated, the motion of the jack-up model is preferred to be used as input for a stand-alone crane model. However, these motions need to be validated as they might differ due to the dynamic implementation of the crane as a substructure on the jack-up. Therefore, we investigate the influence of dynamic modelling of the crane on the jack-up by comparing the motions of the jack-up for the combined model and the benchmark model. For these models we use the jack-up and crane model as explained in Chapters 3 and 4.

The first model combines the jack-up with the crane model. In this way, the crane is implemented as substructure on the jack-up and the dynamic response of the crane is considered. Since the jack-up model includes the crane mass in its hull mass distribution, this need to be removed to prevent the consideration of the crane mass twice. The second model is the jack-up model in which the crane mass is included in the hull mass distribution. We use the mass and eccentricity of the crane model in this hull mass distribution to make the two models comparable. This second model neglects the dynamic response of the crane and is used as benchmark model. Figure 4.1 provides a schematic view of the two models.

Actual operations address various configurations of this jack-up and crane. This may induce a different interaction behavior of the two structures. In this investigation, we use a certain spectrum of possible configuration cases to account for this variation. Next to that, we simulate our models for multiple earthquake events to consider for seismic randomness as stated in ISO 19901-2 [5] in Section 2.2. Such an investigation method in which

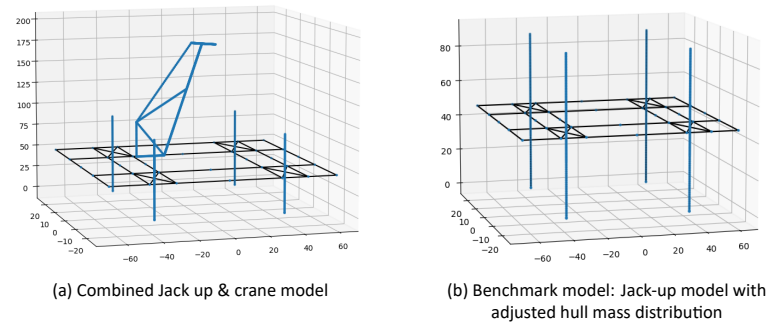


Figure 4.1: Models used in this investigation

a physical process is simulated for multiple starting conditions is also referred to as a Monte Carlo simulation. The next two sections take a closer look at the variation that has been considered during this Monte Carlo simulation. Since the legs of the jack-up have relatively low bending stiffness compared to its axial stiffness, larger lateral motion than vertical motions of the jack-up occur. Intuitively, larger motions of the jack-up have larger potential to damage both the jack-up and the crane. This potential damage can have severe consequences (e.g. the loss of human life and financial costs). Since large motions carry more risks, we use the maximum lateral motion of the jack-up as an indicator for the influence of dynamic modelling of the crane on the motion of the jack-up.

The lateral motions of the jack-up are described by the motion in the longitudinal, transverse, and torsional direction of the center point of the jack-up. This center point describes as imaginary location in the model at the center of the hull of the jack-up.

In our simulation model, motions in opposite direction are expressed as positive and negative motions, respectively. Since we are interested in the maximum lateral motion in either direction, we first take the absolute value of the lateral motion of the jack-up and then calculate the maximum.

We evaluate the influence of the dynamic implementation of the crane on the response of the jack-up by comparing the combined model with the benchmark model based on the maximum absolute displacement of the center point of the jack-up.

We evaluate the influence of the dynamic implementation of the crane on the response of the jack-up by comparing the maximum absolute motions jack-up displacement for the combined model and the benchmark model. We use two indicators for this comparison. The first indicator is referred to as the '*displacement difference*' ($\Delta X_{max,[MN]}$) and is defined as the difference between the maximum absolute displacement of the center point of the jack-up. The second indicator is referred to as the '*displacement ratio*' ($\Delta X_{max,[\%]}$) and is defined as the *displacement difference* weighted by the maximum absolute displacement in the benchmark model. These indicators are defined by the following equations:

$$\Delta X_{max,[m]} = \max(|X_{Dynamiccrane}|) - \max(|X_{Benchmark}|) \quad (4.1)$$

$$\Delta X_{max,[\%]} = \frac{\Delta X_{max,[m]}}{\max(|X_{Benchmark}|)} * 100\% \quad (4.2)$$

4.1.1. Variation of the Monte Carlo simulation

As explained above, multiple configuration cases and multiple earthquake events need to be considered during this investigation for which a Monte Carlo simulation is performed.

Each configuration case is defined by a unique combination of several configuration parameters. The configuration parameters are parameters that define the configuration of the model and that change for each operation that is executed. The parameters that are assumed to have an influence on the dynamic response of the structure are considered as variable in the Monte Carlo simulation.

Influential configuration parameters for the jack-up are the water depth, the variable weight on deck and some stiffness parameters that define the spudcan interaction with the soil. For the crane, we vary the slew angle, the boom angle, and the weight of the suspended mass. An overview of these variables and their values is provided in Table 4.1

Important to note is that the probability of occurrence of each case is set to be equal during this Monte Carlo simulation. This does not represent the actual occurrence of configurations. However, as each case is very plausible to occur, it is assumed that this distribution of cases gives a good representation of the most common operation configurations.

Due to prior research to this jack-up model, an upper and lower bound case for the natural period of the jack-up is known. The lower bound case consists of a water depth of 30 meters, has a relatively low variable weight and a relatively high stiffness for the spudcan interaction with the soil. The three main natural periods for this lower bound jack-up approximate 2.7 seconds. The upper bound case consists of a water depth of 65 meters, has a relatively high variable weight and a relatively low stiffness of the spudcan interaction with the soil. The natural period of this upper bound case, approximate 5.8 seconds.

For the crane, the most common operation configurations are used to create a limited set of crane configuration cases. These most common configurations are determined based on a data set which holds the records of actual executed operations during the construction of a wind farm. These records capture a period of 2 months of installation operations and only include the data of the moments when the crane is out of its boom rest. The slew and boom angle data that are retrieved from this data set are visualized in Figure 4.2. It can be concluded that the most common operation configurations consist of a slewing angle of 10, 165, 230, 280 or 325 degree and a boom angle of 80 or 70 degree. Therefore, these values are used as variation in the Monte Carlo simulation.

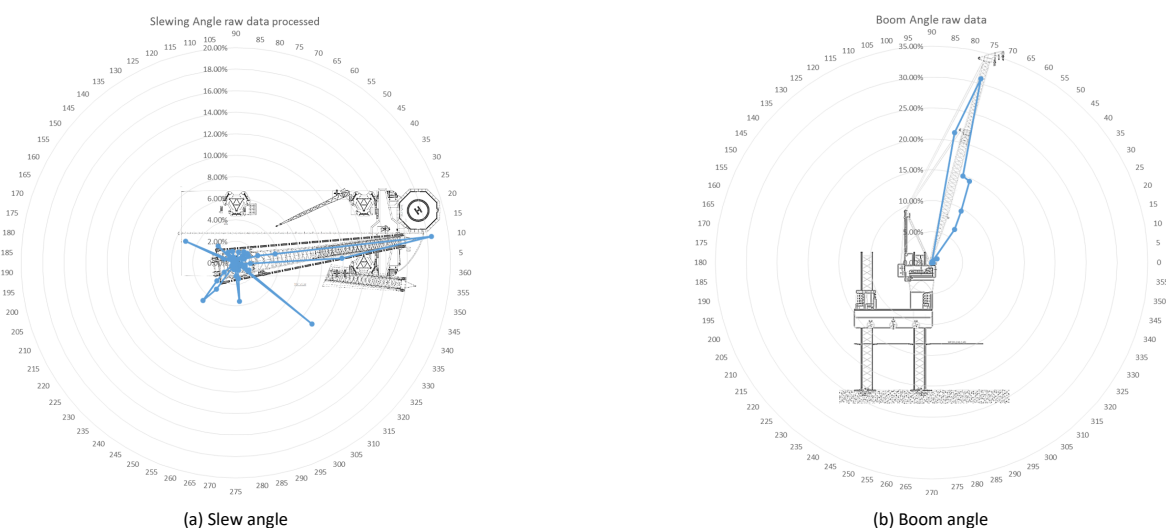


Figure 4.2: Distribution of occurrence during a wind turbine installation period of 2 months.

For the weight of the suspended mass it has been chosen to use the lower and upper limit for which the extended crane is designed. The lower limit is defined by the case without any lifting load in the hook. Since the hook

and the lower block have a weight of 115 tons, the suspended mass is defined as 115 tons for this case. The upper limit case is defined by the maximum liftable mass in extended mode, this equals a mass of 1250 tons [9]. Therefore, the suspended mass of this case is defined as 1365 ton.

Table 4.1: Variation in test cases

Variable	#	Possible values
Seismic Zone	3	0.3g 0.4g 0.5g
Earthquake	7	1, 2, 3, 4, 5, 6, 7
Jack up case	2	low, high
Slew Angle	5	10, 165, 230, 280, 325
Boom Angle	3	70,80
Hook load	2	0, 1250
Total	840	Possible Cases

This table presents the possible configuration cases

Next to the configuration cases, we vary the Monte Carlo simulation with multiple earthquake events. We do this by varying the input signal that prescribes the domain of the model. This input signal represents an earthquake event and defines its seismic ground accelerations over a certain time span in which this earthquake occurs.

As stated in the ISO 19901-2 [5], seismic analysis of offshore structures should demonstrate global survival in at least four dominant extreme level earthquake(ELE) events to capture seismic randomness. Such an ELE event is defined by the seismic zone and soil characteristics of the location in which the structure is located. However, as the dominating ELE events cannot be chosen unambiguously, GustoMSC uses seven rather dominant ELE events for their seismic analysis of their jack-ups. This is also a valid investigation decision that is described in the ISO 19901-2 [5].

An earthquake database that is frequently used by GustoMSC is provided for this thesis. This database describes variation of seven ELE events that are recorded nearby Japan. These variations scale the ELE events to different seismic zones for a certain location. The variation of these ELE events have been created with the software Seismomatch and match a specific target response spectrum using the Wavelets Algorithm. A more in-depth description of this method is provided in the thesis of Linthorst(2019)[13]. Each ELE event consist of a tri-axial time history vector that defines the ground acceleration in two orthogonal horizontal components and one vertical component. Figure 4.3 provides an example of such a tri-axial time history vector.

Due to large computational time for the simulation of the model, it has been chosen to limit the variation of simulation cases to three seismic zones, 0.3g, 0.4g, 0.5g. These numbers indicate the intensity of the ELE event for a certain location. Prior research from GustoMSC shows that this range of seismic zones result in severe internal forces of the jack-up. Below this range, no severe internal forces and motions occur and the analysis for earthquakes becomes less relevant. Above this range, the internal forces experience a large likelihood to exceed the structural limits of the jack-up. This indicates that the jack-up has a large likelihood of failure and is therefore not interesting for this thesis.

4.2 Data collection and processing

The lateral displacement of the jack-up are obtained from the records of the lateral displacement of the hull-to-leg nodes. The output of these records consists of three orthogonal time dependent vectors that represent the displacements in the x, y, z-directions of the global reference system (i.e. the domain).

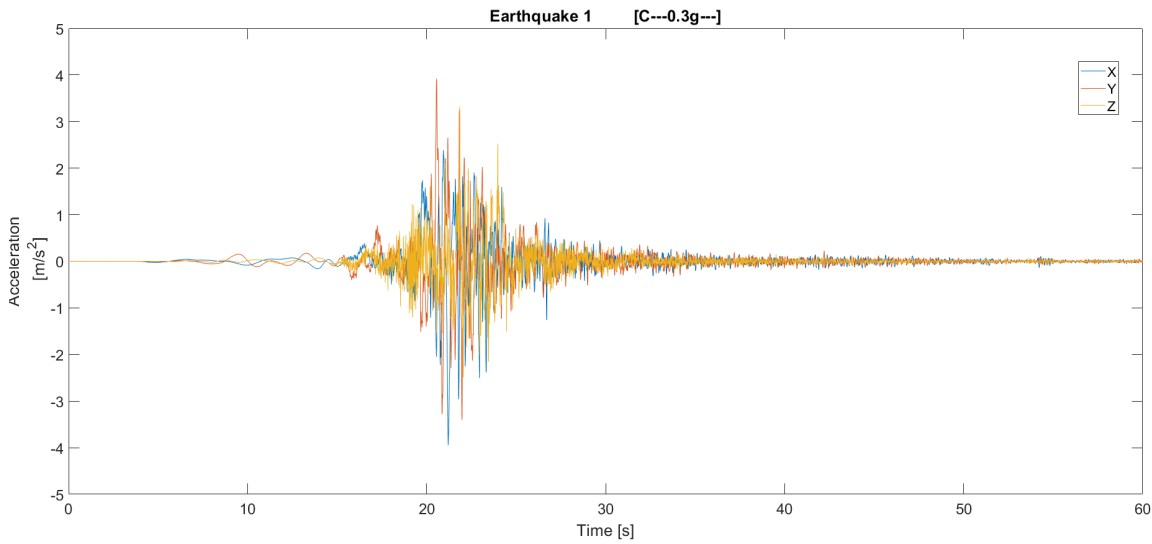


Figure 4.3: Earthquake time trace: Tri-axial ground acceleration record

As previously stated, the lateral displacement of the jack-up is defined by the longitudinal, transverse, and torsional direction of the center point of the jack-up. We refer to these directions as X , Y and T respectively. Figure 4.4 provides an overview of these directions

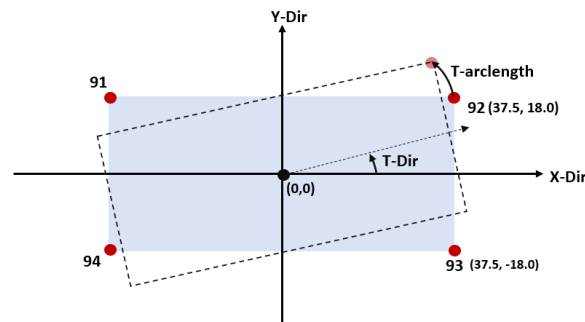


Figure 4.4: Schematic top view of jack up indicating the motion directions.

The longitudinal (X) and transverse (Y) displacement of the center point of the jack-up is obtained by averaging the displacements records from the four hull-to-leg nodes. The torsional rotation(T) of the center point of the jack-up is obtained with a goniometric function. These mathematical transformations are defined by the following equations:

$$X_{Centerpoint} = \frac{X_{91} + X_{92} + X_{93} + X_{94}}{4} \quad (4.3)$$

$$Y_{Centerpoint} = \frac{Y_{91} + Y_{92} + Y_{93} + Y_{94}}{4} \quad (4.4)$$

$$T_{Centerpoint} = \tan^{-1}\left(\frac{((Y_{92} + 18.0) + (Y_{93} - 18.0))/2}{((X_{92} + 37.5) + (X_{93} + 37.5))/2}\right) \quad (4.5)$$

An initial displacement of the jack-up occurs during the first period of the simulation. This is a result of the p-

delta effect and the self-weight of the structure that induce a deformation of the structure and a settlement in the ground. This initial displacement is subtracted from the signal as we are interested in the dynamic response part only.

To make the *displacement differences* for the three lateral direction comparable, we define the torsional rotation as a unit of length. This unit of length equals the length of a circle arc that is defined by the torsional rotation and a radius. To make the unit of length representative as indicator of the lateral displacement of the jack-up, this radius is chosen as the distance from the center point of the jack-up to one of the four legs. Figure 4.4 shows this circle arc.

We assume that an equal displacement in each of the three lateral directions cause an equal risk for the jack-up. As larger displacements induce larger risks, we determine the maximum of the three lateral directions to indicate the highest risk that governs a case.

The three lateral displacement vectors and their maximum vector represent the simulated displacements of the jack-up and are now ready to be evaluated following the methodology described in the previous sections.

4.3 Analysis of the displacement differences of the jack-up

This section visualizes the recorded and processed data of the *displacement differences* and *displacement ratios* with distribution graphs and scatter plots. These figures enable the analysis of and the discussion on the influence of the dynamic absorber on the crane.

For clarification of the figures below it should be noted that: A *displacement difference* larger than zero indicates a case in which the first model, that considers the dynamics of the crane, provides a larger maximum absolute displacement than the benchmark model. These cases are referred to as 'worse response' and are displayed with a red color in the figures below. A *displacement difference* smaller than zero indicate that the first model provides a smaller maximum absolute displacement than the benchmark model. These cases are referred to as 'better response' and are displayed with a green color in the figures below.

4.3.1. Displacement difference

As explained in Section 4.1, we use the *displacement difference* as an indicator to investigate the influence of dynamic modelling of the crane on the response of the jack-up. Figure 4.5 presents the distribution of the *displacement differences* for each of the three lateral directions. Figure 4.6 presents the distribution of the maximum of the three directional *displacement differences*.

The distributions for each of the lateral directions show a normal distribution shape. The average *displacement differences* are close to zero and the range of the *displacement differences* has an order of magnitude of about plus and minus 0.1 to 0.2 meters.

When we take a closer look, it can be noticed that the *displacement differences* for the longitudinal direction have averages below zero and a slightly lower range than the *displacement differences* for the transverse and torsional direction. Furthermore, it can be noticed that the distribution in the longitudinal direction shows a relative flat-peak normal distribution by which about 90% of the cases fall within the range of plus and minus 0.05 meters. For the other two directions, the distributions show a sharp-peak normal distribution with a clear symmetric exponential distribution.

The distribution difference between the cases is probably caused by the fact that legs have a larger spacing in longitudinal direction than in transverse direction. The larger spacing in the longitudinal direction induces a

larger bending stiffness of the jack-up in this direction than in the transverse or torsional direction. Due to this higher stiffness, any adjustment to the jack-up itself will result in a lower absolute *displacement difference* for this longitudinal direction than for the other directions.

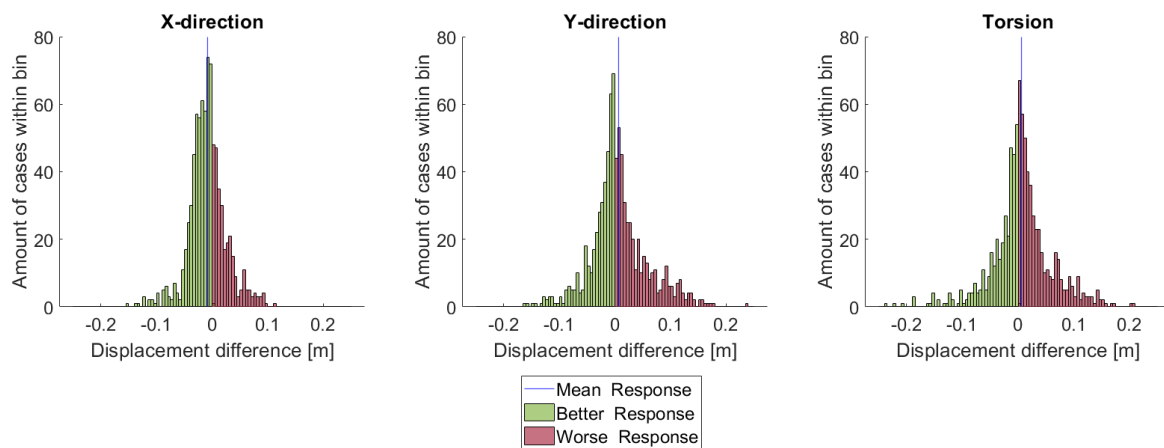


Figure 4.5: *Displacement difference* distributions for each of the lateral directions.

Contradictory to the three directional distributions, the distribution for the maximum of the three directional *displacement differences* shows a right skewed distribution. The average of this distribution is positive with a value of 0.03 meters. The distribution ranges from minus 0.05 meters till plus 0.2 meters. About 80% of the cases describe a *displacement difference* of the maximum of the directional *displacement differences* that is above zero. This indicates that dynamic modelling of the crane generally results in higher amplitude displacements of the jack-up.

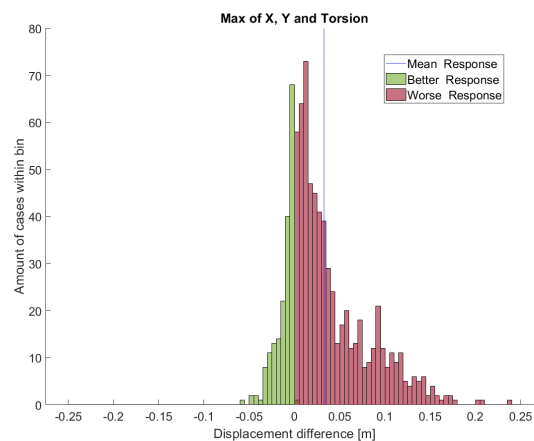


Figure 4.6: Distribution of the maximum of the three directional *displacement differences*

4.3.2. Displacement ratio

As explained in Section 4.1, another indicator to investigate the influence of dynamic modelling of the crane on the response of the jack-up is the *displacement ratio*. Figure 4.7 presents the distribution of the *displacement ratios* for each of the three lateral directions. Figure 4.8 presents the distribution of the maximum of the three directional *displacement ratios*.

The overall impression of these *displacement ratios* is that the distributions show a similar shape to the *displace-*

ment differences. The distribution for each of the three lateral directions show a normal distribution shape while the maximum distribution shows a right skewed distribution.

The averages of the directional *displacement ratios* are close to zero compared to its range. The range of the *displacement ratios* have an order of magnitude of about plus and minus 30% to 40%.

When we take a closer look, it can be noticed that the *displacement ratios* for the longitudinal direction have averages below zero and a range that is lower than the transverse and torsional direction. As expected, this in line with the distribution of the *displacement difference*.

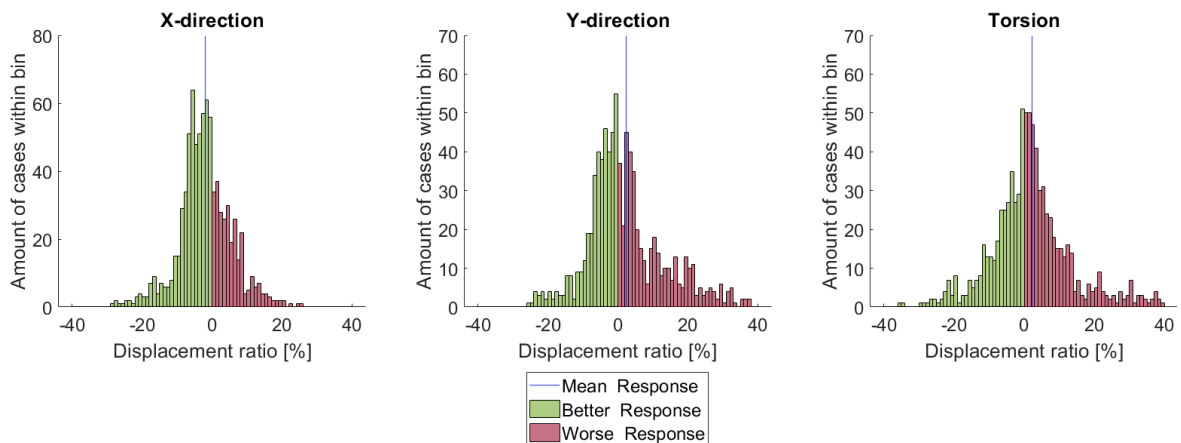


Figure 4.7: *Displacement difference* distribution for each of the lateral ratios

The average of the right skewed distribution for maximum of the three directional *displacement differences* is a positive value of 8.2%. The distribution ranges from minus 10% till plus 57%. This indicates that dynamic modelling of the crane generally results in higher amplitude displacements of the jack-up.

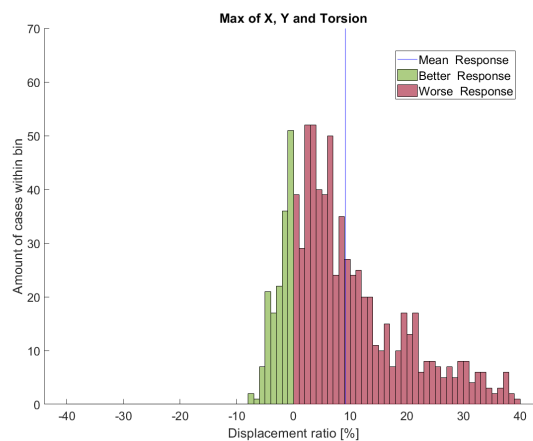


Figure 4.8: Distribution of the maximum of the three directional *displacement ratios*

4.3.3. Displacement difference vs displacement ratio

Figure 4.9 presents a scatter plot of the *displacement difference* vs the *displacement ratio*. This plot describes the relation of the distributions shown above. It indicates the significance of each case and certain outliers, i.e., a case with a high *displacement ratio* may seem to be significant, however, when the *displacement difference*

is very small, the case is definitely not significant.

The relation between the two indicators seems to describe a somewhat linear curve for which a higher *displacement difference* lead to a higher *displacement ratio*. Relative significance is shown for all cases as no obvious outliers are present. The cloud of cases has a higher density of cases close the zero, the axis intersection, which is in line with the distributions described above.

This plot clearly indicates that for the vast majority of cases (78%), the dynamic modelling of the crane leads to worse motion response of the jack-up. Furthermore, as indication of the significance, 26% of all cases have a difference above 0.05 meter and a ratio above 10%.

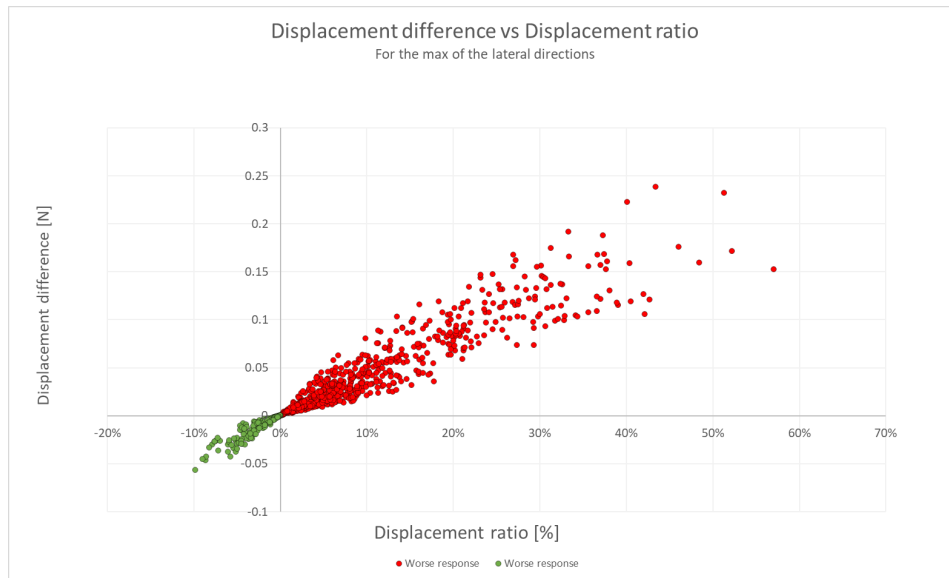


Figure 4.9: Scatter plot of the *displacement difference* versus the *displacement ratio*

4.3.4. Influence of the variables on the distributions

The share of each variable to the distributions is investigated to find the reason for the worst or best cases. This is investigated based on the maximum lateral displacement distribution of the *displacement difference*. From this distribution a case specific distribution can be made for each variable. We refer to these as 'variable distributions' and can be found in Appendix C.

Most of the variable distributions do not show a difference that is worth mentioning. However, for the jack-up configuration and the slew angle some differences can be distinguished.

Figure 4.10 presents the variable distributions for the lower and upper bound case of the jack-up that refers to a low and high eigen period of the jack-up, as mentioned in Section 4.1.1.

Comparing these two distributions indicates that the lower bound case has a higher mean *displacement ratio* that is accompanied by a higher range. The range of the distribution in the lower bound case is approximately double the range of the upper bound case. This indicates that dynamic modelling of the crane results in worse differences when the lower bound case is used. For clarification, the cases are defined by relative low water depths that indicate relative short leg lengths, a relatively low variable weight and a relatively high stiffness for the spudcan interaction with the soil.

It is assumed that this difference is present due to the difference in lateral stiffness of the jack-up. A higher

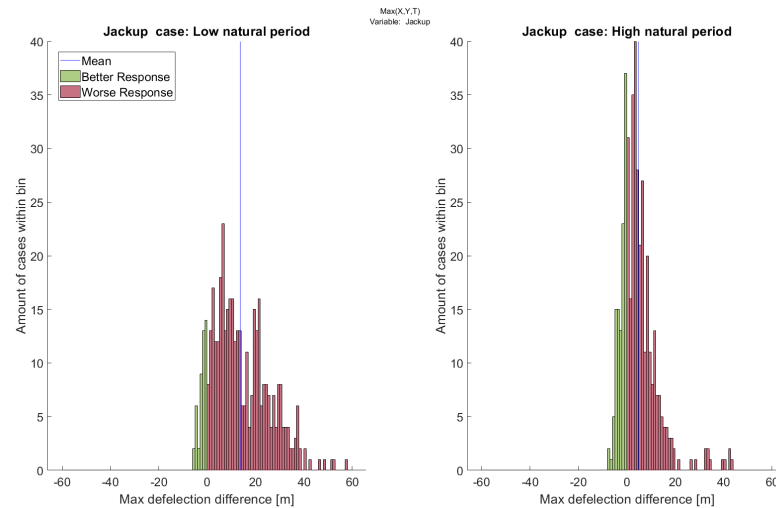


Figure 4.10: Distributions of the difference ratios for each of the jack-up configuration cases.

stiffness ensures larger accelerations of the jack-up as response to the ground accelerations. These larger accelerations of the jack-up are transferred to the crane what leads to larger accelerations of the crane. As larger accelerations of the crane occur in the lower-bound case of the jack-up, the dynamic modelling of the crane is assumed to play a more dominant role in the response of the jack-up.

During the investigation of the jack-up case influence, another interesting issue came to light. For the 10% highest maximum absolute displacement cases, the mean *displacement difference* is well below zero. This indicates that for the cases in which extreme large displacements occur, the dynamic modelling the crane on the jack-up gives a beneficial influence on the amplitude of the displacement of the jack-up. The upper-bound case of the jack-up ensures all these large displacement cases. This can be explained by the lower lateral stiffness in the upper bound cases and that the jack-up starts to resonate at the end of the earthquake.

Next to the differences for the jack-up configuration cases, the slew angle cases indicate a slight difference as well. An overview of directions of the five slew angle case is presented in Figure 4.11. The variable distributions of the slew angle cases are presented in Figure 4.12.

Comparing these distributions indicate that the 165° and the 230° cases have the highest average value and for which nearly all cases indicate a difference above zero. The 10° case and the 325° case have the lowest average value and for which multiple cases indicate a difference below zero. Case 280° presents a distribution that is in between these other cases.

The difference between these distributions indicate that for the 165° and the 230° case the dynamic modelling of the crane results in worse *displacement differences* of the jack-up. It is assumed that this can be explained by the fact that these cases are pointed towards the aft of the ship. This results in a larger distance between the center of gravity of the crane and the center of gravity of the jack-up. This larger distance means that the arm of the forces of the crane to the jack-up result in a larger moment of force on the jack-up. As the larger moments of force are generated for these cases, the influence of the dynamic moment of forces of the crane on the jack-up should be larger.

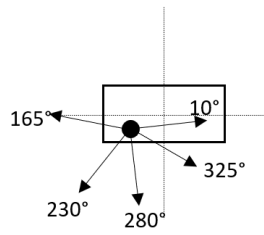


Figure 4.11: The relative orientation of the slew angles with respect to the jack-up

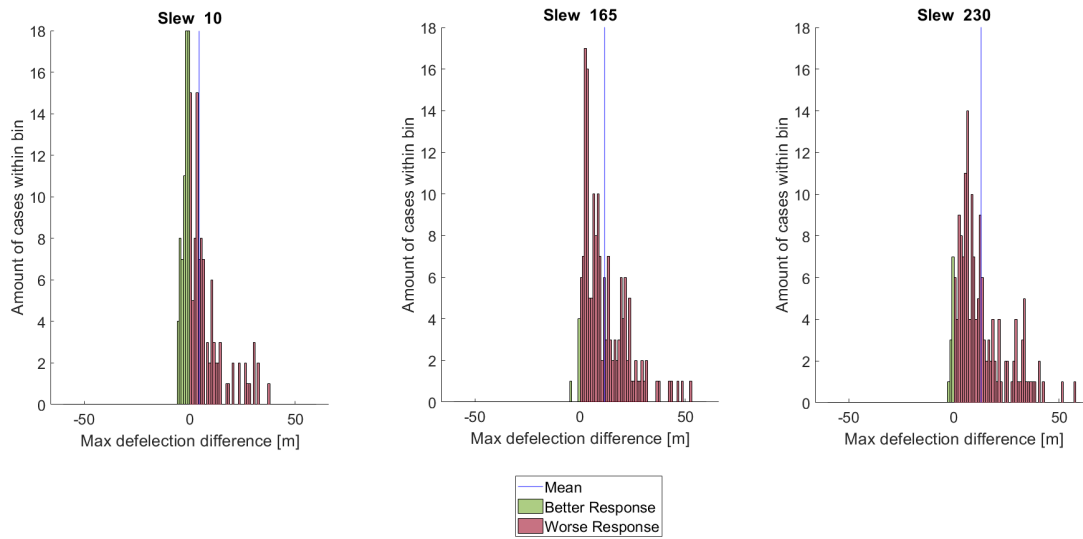


Figure 4.12: Distributions of the difference ratios for each of the slew angle configuration cases. (10°, 165° and 230°)

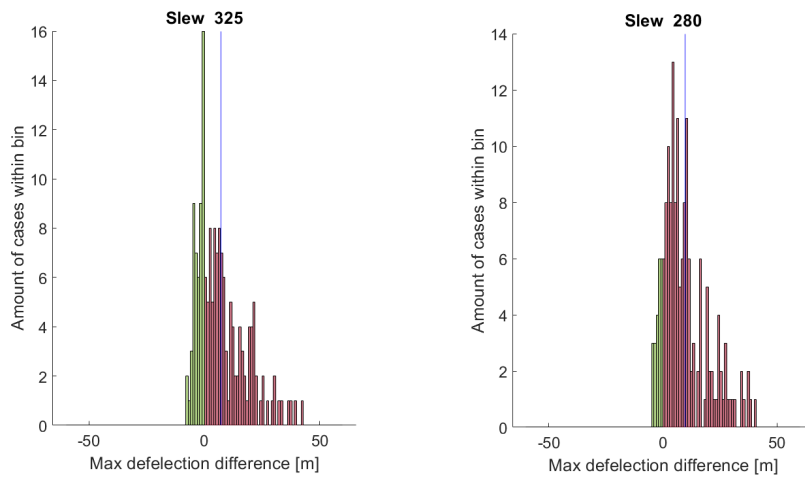


Figure 4.13: Distributions of the difference ratios for each of the slew angle configuration cases. (325° and 280°)

4.4 Conclusion: Influence of the crane on the motion of the jack-up

In this chapter, we have studied the influence of the dynamic response of a crane on the response of a jack-up structure that is subjected to seismic activity. We did this by implementing the crane as a substructure in the jack-up model and comparing the simulated dynamic responses to those of a model in which a fixed mass distribution over the hull nodes of the jack-up represents the crane.

Our findings were that for the vast majority of simulated cases, namely 78%, the dynamic response of the crane leads to larger motion responses of the jack-up structure. Maximum motion differences were found up to 0.24 m and this was equal to 43% of the amplitude of the displacement. We observed that two variables influence the characteristics of this increased dynamic response of the jack-up.

First, we observed that jack-ups with a low natural period are generally more effected by the dynamic response of the crane. This can be explained by the higher lateral stiffness of these jack-ups that induces a larger dynamic response of the crane.

Second, we observed that jack-ups on which the boom of the crane is oriented away from the center of the jack-up are generally more affected by the dynamic response of the crane. This can be explained by the larger distance between the center of gravity of the crane and the center of gravity of the jack-up. This larger distance induces a larger moment for the dynamic forces of the crane on the jack-up.

As this is not conservative and , we concluded that using the jack-up motions as input for our investigation to the crane is not valid. Therefore, we have used the integrated model during the rest of our research

We conclude that the motion response of the current jack-up structure is not conservative since most cases show a worse response with the crane model integrated as substructure on the jack-up model. As the maximum absolute motion of the jack-up has been used for this comparison and we found that a fourth of the cases have a worse displacement than 10%, we assume that these jack-up motions are not valid for the use as input for a stand-alone crane model. Therefore, we choose to implement the crane as a substructure in the jack-up models that we use in our investigation into mitigation measures for the dynamic response of the crane.

Next to that, this conclusion indicates that the jack-up model that is currently used by GustoMSC to calculate the probability of survival of jack-ups in seismic prone areas may give too optimistic outcomes. The reason for this is that the dynamic response of the crane, which we find to be present in a worsening way, is not included in their model.

For further research, it may be interesting to investigate whether the accuracy of this fixed mass distribution model that GustoMSC uses can be improved. One promising option for this is related to the fact that the suspended mass is relatively decoupled from the crane itself in the lateral directions. Therefore, this suspended mass may be neglected when the crane mass, as defined in the hull mass distribution, is applied to the lateral degrees of freedom of the jack-up nodes. Although, as we did not find a clear difference between the lower and upper limit case of the suspended mass, we assume this to be a minor mistake.

5

Review of Mitigation measures and their implementation

Existing mitigation measures that limit the response of structures to earthquake are presented in Section 2.5. This chapter starts with reviewing these mitigation measures based on literature, expert opinion, and two criteria. We find two of these mitigation measures to possess a high potential to mitigate the response of the crane. After which, the second and third sections elaborate on the implementation of these mitigation measures in the crane model. The last section presents the conclusions of mitigation measures and implementations.

5.1 Review of mitigation measures

Since the mitigation measures described in Section 2.5 differ widely from mitigation method, they are assessed in an appropriate but superficial manner. The measure should be able to minimize the seismic induced loads in the crane to improve the probability of survival. Next to that, as the measure is intended to be used in practice, this measure should be feasible for installation in new crane structures as well as to retrofit it in existing crane structures. Based on these criteria, the existing mitigation measures are discussed below.

5.1.1. Ductility through structural configuration

Adjusting the structural configuration of the crane is an excellent method to achieve a lower dynamic response of the crane. However, this measure is rather unpractical as it is not suitable for retrofitting. Besides, changing the structure of the boom is not in line with the scope of this thesis. Therefore, this measure is not considered further on.

5.1.2. Direct Damping Apparatus

A direct damping apparatus dissipates energy due to friction that is caused by a relative motion within this measure. Within the frame of the boom these relative motions are very small. The damping potential of this measure is considered as low due to this reason. This makes the direct damping apparatus not a potential candidate for application within the crane boom itself.

Since the relative motions at the base of the crane are larger, this measure might result in larger damping potentials at this location. Therefore this measure might give some additional damping to a base isolation system.

5.1.3. Base Isolation Systems

A base isolation system decouples parts of structures by cutting of the load path during high load peaks. Loads are captured as displacement in the base isolation system rather than as forces in the crane. Base isolation systems have a high potential to reduce dynamic responses that are caused by extreme load peaks. This measure is located at the base of the crane. However, the benefits from this measure are assume high enough to overcome these challenges.

5.1.4. Dynamic Absorbers

A dynamic absorber absorbs energy from the structure by transferring it to a secondary system. Kinetic energy in a structure is partly transferred to the mass of the absorber rather than to be captured as forces in the crane. The structures dynamic response can be reduced in an optimized manner by tuning the absorber to the frequency of the structure force. This measure has a proven feasibility for implementation and retrofiting.

5.1.5. Active control device

An active control device records a certain motion or load and actively controls a mitigation system to mitigate this recorded response. In fact, this system can be seen as a passive mitigation measure that is actively adjusted during operations. However, active measures are more complex for application. Next to that, they require more maintenance and support. Additionally, active measures are dependent on electric systems which makes them less reliable.

Adjusting the passive measure in front of an operation is not considered as an active control device as the reliability of the system is not at stake. Due to these reasons, the aim of this thesis becomes to find the best passive measure for the crane.

5.1.6. Conclusion: Promising mitigation measures

From this review, it is concluded that the base isolation system and the dynamic absorber offer the best prospect in decreasing the dynamic response of a crane. The implementation of these two measures in the model, is discussed in the next sections.

5.2 Implementation of a base isolation system

The goal of a base isolator is to reduce the dynamic response of the crane by cutting of the load path during high load peaks. A more in-depth elaboration of the physical working mechanism of a base isolator is explained in Section 2.5.

Two specific elements from the OpenSees library are considered during the implementation of the base isolator in the crane model. The so-called single friction pendulum bearing element ('singleFPBearing') and the flat slider bearing element ('flatSliderBearing'). This section discusses the implementation method of these elements in the crane model and multiple configurations of the base isolation system to account for the overturning moment of the crane.

This chapter investigates the implementation of the base isolator based on a certain test case. This test case is defined by a slew angle of 270° , a boom angle of 80° , a relative light suspended mass of 115 tons and a relative shallow water depth of 30 meters. For each simulation with this test case we vary the configuration of the base isolation system. A cross-section view of this configuration is present next to each simulation to indicate its configuration.

5.2.1. Location of the base isolator in the crane model

As previously mentioned, the location of a base isolation system should be anywhere within the primary load path to cut-off the transfer of loads between the jack-up and the crane. Three possible locations of interest are considered. These locations in the crane are presented Figure 5.1 and are referred to as: below the pedestal at the deck level, just above the slew bearing, or below the boom hinge.

The location below the pedestal does not consider for the rotation, i.e. slew angle, of the crane. This means that the normal forces, and therefore slip behavior, of the base isolator become variable with the slew angle in which an operation is executed. It results in a system that need to be designed for the worst possible overturning moment in every direction.

The complexity and size of such a system can be mitigated by locating the base isolators above the slew bearing. In this way, the location of the base isolators is relative to the orientation of the crane. The overturning moment that needs to be captured by the system becomes independent the orientation of the crane. The implementation under the boom hinge is expected to result in issues at low boom angles. For example, when the crane is lowered to its boom rest, the lateral force in the boom hinge increase significantly due to the hoist wires pulling the boom back. The high lateral force causes the occurrence of slip, which is not preferred in such a case. Figure 5.2 presents an indication of this case.

This makes the location above the slew bearing the preferred spot to implement the base isolation system. In the model, we implement the base isolation system on the topside of the pedestal and rotate the system with the slew angle of the crane.

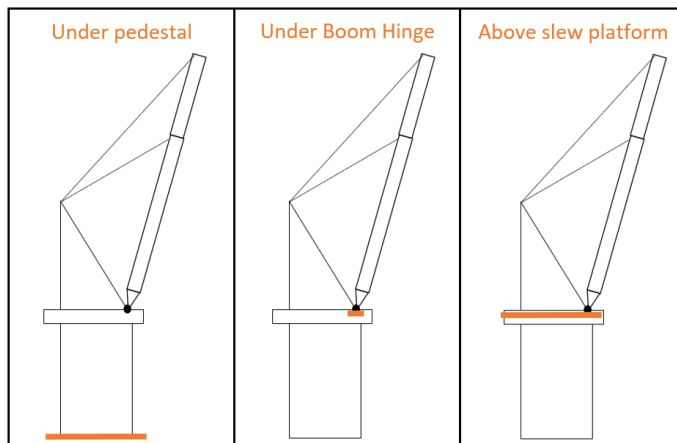


Figure 5.1: Possible locations of the base isolation system

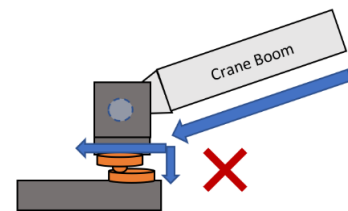


Figure 5.2: Lowering the boom: Example case in which the base isolation system would lead to issues.

5.2.2. Parametric description of the base isolation system

As explained before in Section 2.5, the response of a base isolator is defined by a bi-linear lateral stiffness between the surface area. The stiffness curve is defined by the friction coefficient, ' μ ', the initial stiffness in local shear direction ' K_{init} ', and the effective radius of the concave sliding surface, ' R_{eff} '.

Coulomb's law of friction is used to determine the friction coefficient ' μ '. The law states that that kinetic friction is independent of the sliding velocity and that the friction coefficient is independent of the pressure between the interacting surfaces. The friction coefficient is considered as conservative due to these reasons. Velocity or pressure dependent friction models exist and may be more representative in a later design stage. The value of the friction coefficient is set as 0.13. This is assumed as an industry average for coated steel to steel interfaces

[2, 10].

Slip occurs during the moments that the lateral force (F_L) exceed the normal force (F_N) within the base isolator. These moments are defined by the following equation.

$$F_L > \mu F_N \quad (5.1)$$

Before slip starts to occur, the initial lateral stiffness, ' K_{init} ', of the base isolator is defined by the relation between the shear force and the resulting shear. In physics, shear is referred to as the deformations that occur within the interacting surfaces. These shear deformations are very limited compared to the displacement that potentially occurs during slip. Therefore, we assume that the shear deformations can be neglected during this stage of the research to the implementation of a base isolator on the crane. To do so, the initial lateral stiffness is set to a very large number, $1E10$ N/m.

When slip occurs, the lateral stiffness of a friction pendulum as base isolator is defined by the effective radius of the concave sliding surfaces, ' R_{eff} '. Since the aim of a base isolator is to cut off the load path, the stiffness during this slip period should be low. A low stiffness is obtained by a large effective radius. However, an argument for higher stiffness, and thus smaller radius, is its re-centering ability. Yet, the effective radius is set to 40 meters, which is relatively large, since the re-centering capabilities are not the main design driver for the investigation. For the flat slider as base isolator, no lateral stiffness is present during slip. This is comparable to an infinite effective radius.

Within the model, the base isolator element has no length, i.e. zero-length element. The compressive stiffness of the base isolator is set to infinite to ensures that no vertical deformation occurs within the element. In an opposite manner, the tensile stiffness of the base isolator is set to infinitely small by the software to include uplift behavior.

5.2.3. Change of iteration algorithm

Due to the bi-linear stiffness curve of the base isolator, abrupt localized stiffness changes occur when the slip threshold is met. The prior used Modified Newton algorithm is not able to solve for these abrupt stiffness changes. Instead, we use the Krylov-Newton algorithm. This algorithm uses a Krylov subspace accelerator to accelerate the convergence of the Modified Newton algorithm [4]. This method is explained below.

The iteration algorithms advance the initial state of the structure to the state of the structure in which equilibrium is satisfied for the externally applied loads. This executed by adding the initial displacement vector (U_0) and the computed successive displacement increments (V):

$$U_{k+1} = U_k + V_{k+1} \quad (5.2)$$

The Krylov acceleration algorithm decomposes the displacement increment into two vectors. The standard Modified Newton component (q) of the displacement increment and the Krylov acceleration component (w).

$$V_{k+1} = w_{k+1} + q_{k+1} \quad (5.3)$$

The Krylov acceleration component, w_{k+1} , advances only to the degree of freedom where the largest change of state occurs. In case of our model, towards the base isolator element as no other non-linearity's are modelled

(except for the P-Delta effect). Thereafter, the Modified Newton component advances the solution to the degree of freedom where small changes of the state occur. In this way the amount of iterations reduces drastically, and the model is able to converge for abrupt stiffness changes.

5.2.4. Confirmation of the slip behavior of an implemented base isolation system

The base isolator element is investigated for proper response to confirm its working mechanism. This is done by implementing the friction pendulum bearing element on the crane model and recording the forces and displacements. The elements capability to capture moments is set to infinite during this investigational phase to exclude the overturning moment by which the crane otherwise tips over.

For this investigation, we use the test case as mentioned before. A model with a friction pendulum element is compared to a model with a rigid element implementation. We record the lateral forces and relative displacements that occur between the upper and the lower node of these elements. We assume that the rotation of the local reference system remains small. This means that normal force in the element equals the recorded force in vertical direction and that the lateral displacement equals to the recorded displacements in the two horizontal directions. The slip threshold can be calculated based on the normal force and the friction coefficient, μ .

Figure 5.3 presents a period of the test run for which slip occurs. A large relative displacement (blue) is found during the moments that the lateral force of the rigid element model (yellow) exceeds the slip threshold force (black) of the friction pendulum element model. This indicates the slip occurrence in the friction pendulum element. Next to that, during these slip moments, the lateral forces (red) in the friction pendulum element are limited to the slip threshold force (black). This indicates that the lateral forces are correctly cut off by the friction pendulum element. Therefore, the working mechanism of the friction pendulum element is confirmed.

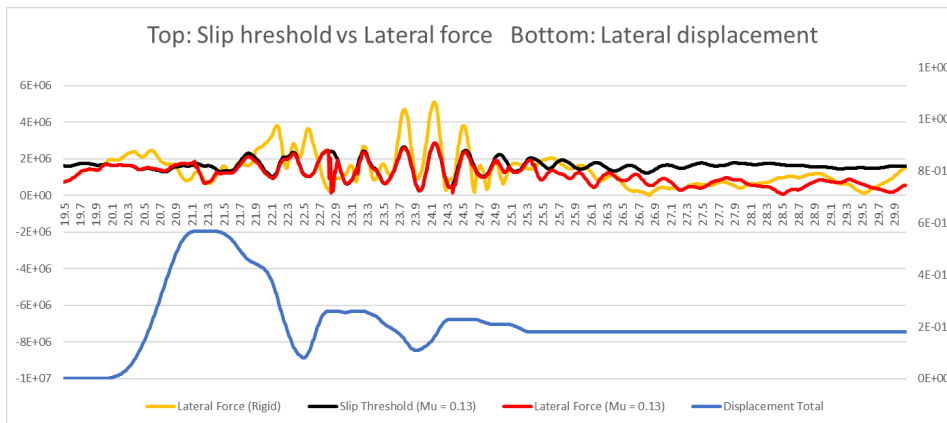


Figure 5.3: Test case: Confirmation of slip occurrence

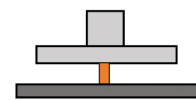


Figure 5.4: Cross-section view: Friction pendulum element without the consideration of moments

5.2.5. Accounting for the overturning moment that is present in the crane

Since the center of gravity of the crane is not aligned with the center of the slew bearing, a static overturning moment is present at the base of the crane. This implies that the crane would tip over to the front side when the load transmission path is cut off. Next to this static overturning moment, a dynamic overturning moment is present due to the dynamic response of the crane. Since a base isolator only ensures for the transfer of forces, but not for the transfer of moments, a configuration with multiple bearing elements, with relative spacing, is required to capture the overturning moments.

Since the actual base of the crane encircles the leg of the jack-up, the bearings should be placed in a circular pattern. The configuration needs to capture the overturning moment in both the in-plane and out-of-plane

direction of the crane. Due to this reason and for model simplicity, we implement four bearings that have an angular spacing of 90° . We refer to the front side bearing as the bearing that is in the same direction as the orientation direction of the boom. This ensure that the configuration is relative to the slew angle, as explained in Section 5.2.1. The circular pattern has a radius of 7.2 meters as this equals the radius of the actual slew bearing. Figure 5.5 presents an illustration of this configuration.

For the practical implementation in real life, it might be preferred to add multiple bearings in each direction to distribute the forces on each base isolator. Figure 5.6 presents a distribution of such a case. However, as both the lateral and normal forces are distributed over the bearings, we assume that incorporating only one bearing on each of the four quarters is a good approximation for this investigation.

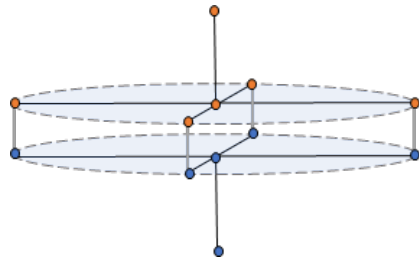


Figure 5.5: Schematic view of the circular configuration

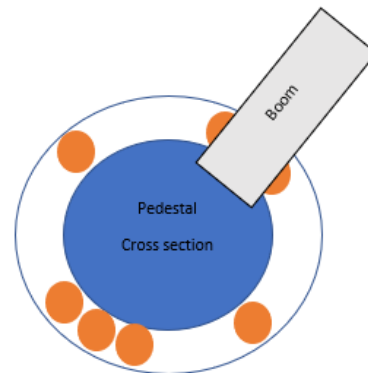


Figure 5.6: Top view: In practice multiple bearings may be installed for each direction

The full transfer of forces and moments, from the pedestal to the outlying bearing elements, is ensured by modelling the horizontal connecting elements as infinitely stiff. A verification of this configuration is performed by recording the forces in the boom hinge and using rigid beams instead of base isolators. The infinite stiff modelling of the horizontal elements is verified since no differences occurs between the model with and without the bearing system.

Next to this verification, we investigate the vertical forces in the bottom nodes of the rigid modelled configuration to check these forces with the expectations from the static overturning moment. Figure 5.3 presents the forces during the test run. As expected, there is a compression on the front side (black) and a tension on the aft side (red) of the system. However, as stated above, the base isolating elements do not allow for tension to occur as this causes uplift behavior. This indicates that the overturning moment cannot be captured when we apply base isolators instead of rigid beams.

When the slip threshold of one of the bearings is exceeded, the exceeding lateral force is transferred to the other bearings. This is ensured by the infinitely stiff horizontal elements that connect the bearings. The moment that slip occurs in all four bearings is later referred to as 'total slip'. At this moment the load path is cut off, meaning that any additional lateral force results in a relative displacement within the bearings.

The following sections elaborate on possible methods to mitigate this problem. The first method considers the implementation of pre-tension to the bearings. The second method considers the implementation of the aft bearing on the top side of the crane part. The third method considers an encased configuration with friction plates on both the top as bottom side of the crane part of the bearing.

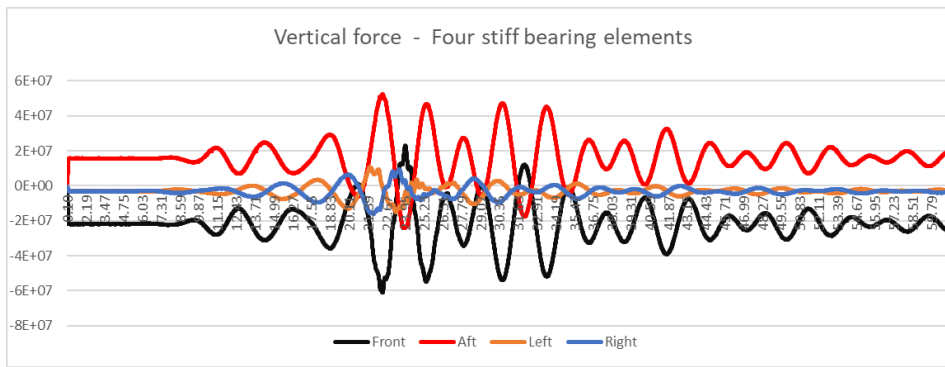


Figure 5.7: Test case: Defining the vertical forces in the bearings

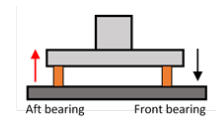


Figure 5.8: Cross-section view: Rigid bearing elements

Implementing pre-tension to the bearings

The uplift behavior that is caused by the overturning moment can be mitigated by applying a load that counters the overturning moment. A solution that generates these loads, without adding to much mass, is pre-tensioned cables between the upper and lower part of the base isolator. Figure 5.9 presents an illustration of such a solution.

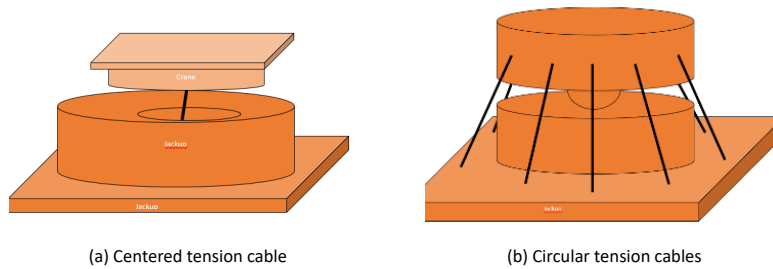


Figure 5.9: practical implementations of applying pre-tension

The pre-tension that is required to capture the overturning moment can be divided in a static and a dynamic part. The static moment mainly results in a vertical force in the front and aft bearing due to the configuration of the crane. A pre-tension in the aft bearing is applied to counter its uplift behavior. This pre-tension is equals to the static moment divided by the radius.

For the test case, the required static pre-tension equals approximately 30 MN. This is considered as a huge force that may not be easy to apply in real life. However, this implementation challenge is ignored during this thesis as the aim is to prove the concept of a base isolator.

In the model, the pre-tension is applied to the aft bearing as a vertical force that works downwards in the upper node and upwards in the lower node. Figure 5.11 presents the vertical force response of the bearing elements during the test run. It shows that all four bearings experience a compressional force during the first period of the run. This indicates that the static overturning moment is indeed captured by this pre-tension force. Furthermore, it can be noted that the model stops after 20 seconds. This happens due to uplift behavior which is caused by the dynamic overturning moment.

Contrary to the static overturning moment, this dynamic moment effects all four bearings. An additional pre-tension of approximately 30 MN is required in each bearing to counter the uplift behavior due to the dynamic moments. Figure 5.13 presents the vertical forces during the test run. From this figure it can be seen that each of the four bearing elements experiences compression during the entire run. This means that no uplift behavior

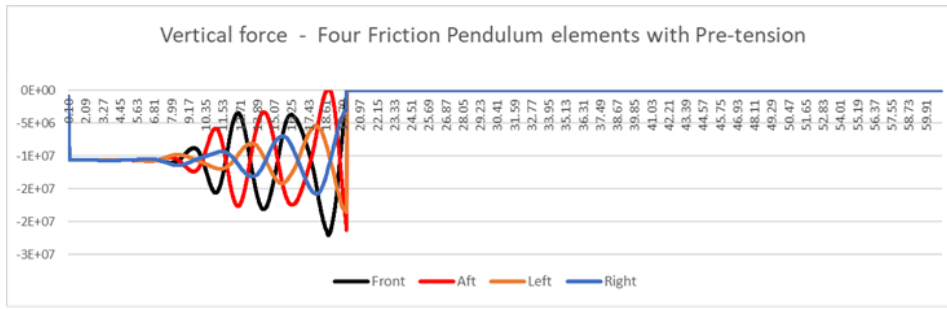


Figure 5.10: Test case: Friction pendulum bearings with 'static' pre-tension

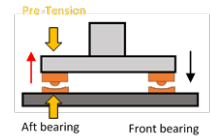


Figure 5.11: Cross-section view: Friction pendulum bearings with 'static' pre-tension

occurs and implies that total overturning moment is captured by the pre-tension.

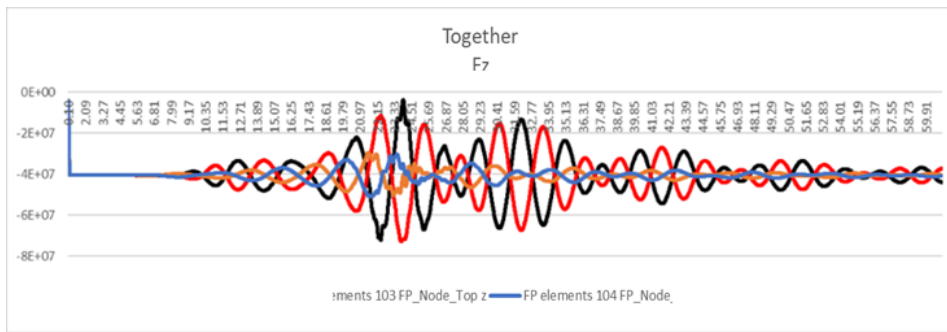


Figure 5.12: Test case: Friction pendulum bearings with both 'static and dynamic' pre-tension

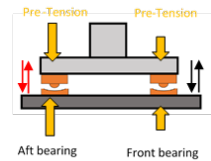


Figure 5.13: Cross-section view: Friction pendulum bearings with both 'static and dynamic' pre-tension

However, no slip occurs during the test run as no significant displacements are recorded. Next to the mitigation of the overturning moment, the pre-tension also causes higher natural forces in the bearings. These higher forces result in a slip threshold that is too high to be exceeded by the lateral forces that act on the bearings. Figure 5.14 presents both the slip thresholds and the lateral forces from which this is concluded. Since this method to mitigate the problem of the overturning moment does not favor the capabilities of the base isolator, other methods need to be investigated.

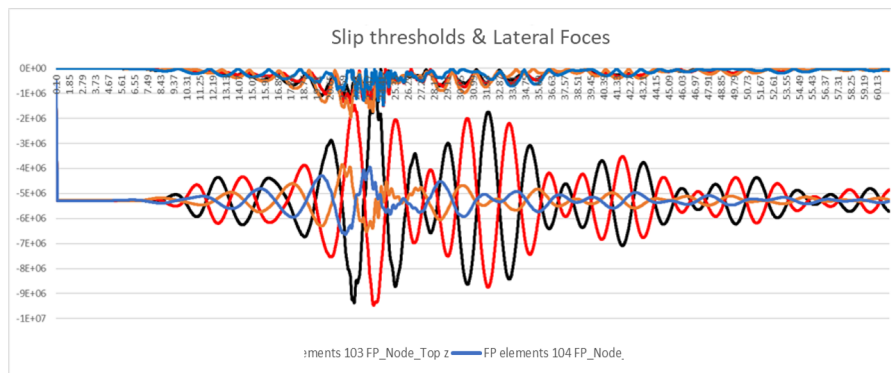


Figure 5.14: Test case: Slip thresholds vs lateral forces

→ Lateral Forces

→ Slip Thresholds

Implementing the aft bearing on the topside of the crane part

Another method to mitigate the issue with the overturning moment is to implement the aft bearing on the topside of the crane part. In this way, the crane is not able to tip over to the front and the static overturning moment is mitigated. Figure 5.16 presents a cross-section view of this encased configuration.

However, the dynamic overturning moment causes upward behavior in the side bearings and a downward behavior in the aft bearing. To mitigate this problem, pre-tension is again added to the bearing. As the dynamic moments need to be mitigated only, the resulting pre-tensions are lower. Figure 5.15 presents the resulting vertical forces of this method on the test case. It shows that compression occurs during the entire run in each of the four bearing elements.

The vertical forces on the side bearings are relatively low compared to the vertical forces on the front and aft bearings. This implies a lower slip threshold for these bearings. Since the slip thresholds of the front and aft bearings are still high, no total slip will occur.

Next to this, it is noticed that the forces on the front and aft bearing run in parallel. This is in itself a logical consequence of implementing the aft bearing on top of the crane part. Due to the parallel behavior, slip will only occur in one direction and will be periodic with the staggering of the crane boom. It implies that slip could only occur for the moments when the crane is on its heels.

As the displacements of the slip add up over time, this is a dis-preferred scenario. Therefore, it is concluded that this method is not in favor of the slip behavior of the system and that another method needs to be investigated.

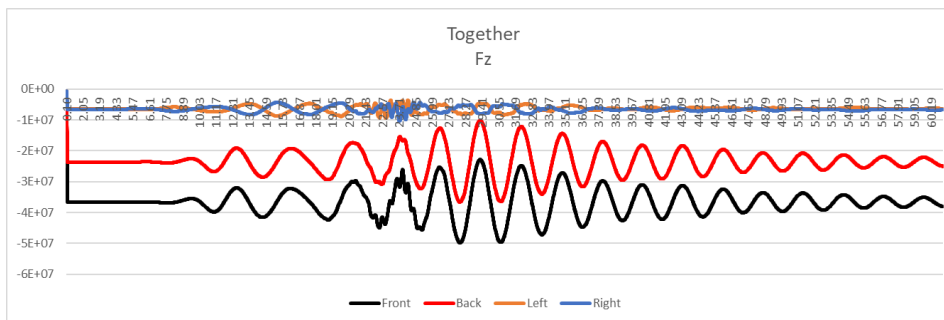


Figure 5.15: Test case: Friction pendulum bearings, aft implementation on top side

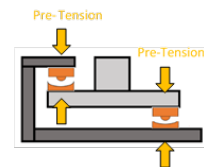


Figure 5.16: Cross-section view: Friction pendulum bearings, aft implementation on top side

Accounting for the overturning moment by encasing the crane part with friction plates

The third method that is investigated to mitigate the overturning moment, is to encase the crane part of the system with friction plates on both the top as bottom side. In this way, both the static as the dynamic part of the overturning moment can be captured. Figure 5.17a presents schematic cross-section view of this encased configuration in the model.

As the name suggests, the motion of a friction pendulum is defined by a path that can be described by a pendulum. The concave sliding surface induces a vertical motion when a horizontal motion occurs. Therefore, implementing two of these friction pendula, above and below the crane part, will result in clamping of these bearings when slip should occur. However, as friction plates have a flat sliding surface, slip will not result in a vertical motion for this type of bearings. Therefore, these friction plates are used to encase the crane part of the base isolation system. Figure 5.17b presents a cross-section view of this configuration.

The vertical forces that result from the test case for this configuration method are similar to the vertical forces in the rigid elements as bearings, Figure 5.7. However, for this encased configuration the upward pointing forces result in compression in the top bearings and downward pointing forces result in compression of the bottom bearings.

The occurrence of slip is investigated by comparing the lateral force and the slip thresholds for each bearing.

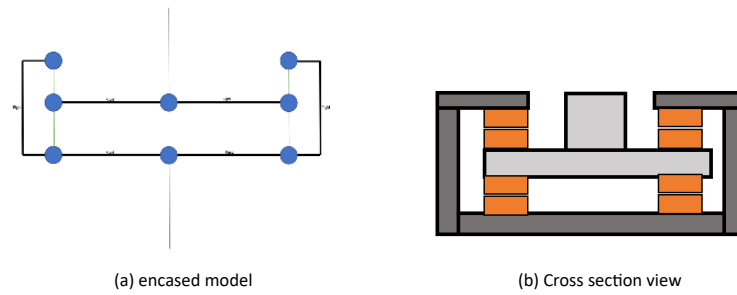


Figure 5.17: Friction plates on both top as bottom side

Figure 5.18 presents this comparison for the aft bearing and it indicates slip occurrence by highlighting the time intervals in which the difference between lateral force and the slip threshold is very low. The figure shows that slip occurs multiple times.

During a period of relatively large lateral forces, the slip threshold determines whether slip occurs since their values oscillate due to the staggering motion of the crane. These oscillations cause slip to occur in a rather periodic behavior. This indicates that slip will only occur at the moments that the crane is near to its equilibrium state as the overturning moments and thus the vertical forces are then close to zero.

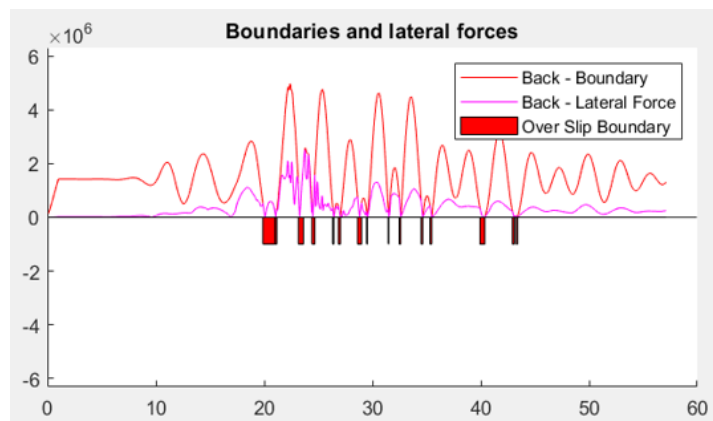


Figure 5.18: Vertical motions, lateral forces and slip occurrence

As mentioned before, total slip will only occur when all four bearings are slipping at the same time. Figure 5.19 presents these moments of total slip and it indicates that total slip only occurs for a limited amount of times.

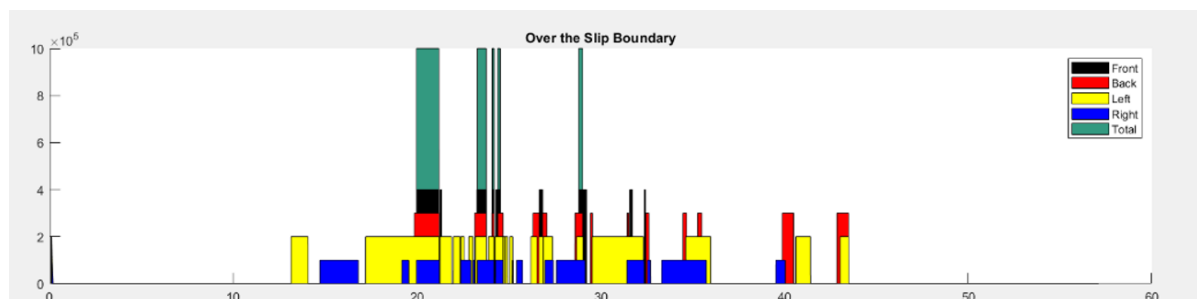


Figure 5.19: Slip occurrence at each bearing & Total slip occurrence

When these total slip intervals are presented in combination with the lateral displacements, as shown in Figure 5.20, it can be confirmed that slip only occurs during significant displacement intervals. Besides this confir-

mation, a lateral offset can be noticed after the earthquake. This indicates a side effect of the friction plates, namely that they do not present a restoring force that limits the displacements over time.

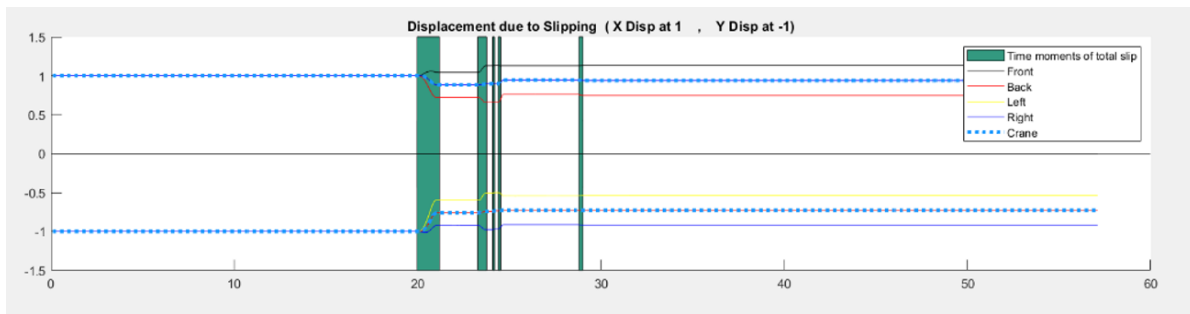


Figure 5.20: Offset after the earthquake

Next to the displacements in the bearings itself, we study the forces in the boom hinge since we use these in the next investigation which simulates the effect of the mitigation measures for multiple model configurations. We find a sudden surprisingly high peak force in boom hinge shortly after a long moment of slip. Figure 5.21 present these findings and points out the peak force

This peak force is assumed to be cause by the moment that the bearings regain their friction control after slip occurrence. Slip occurs to cut of the force transfer of the jack-up to the crane, however, this also causes a relative velocity between the crane and jack-up. After this moment of slip, the base isolators suddenly regain their grip and the relative velocity is no longer present. During the very short time interval in which the relative velocity decreases, a high acceleration in the opposite direction of the velocity is experienced by the crane. Intuitively, we assume that these high decelerations of the crane to regain its grip result in the peak forces in the boom hinge.

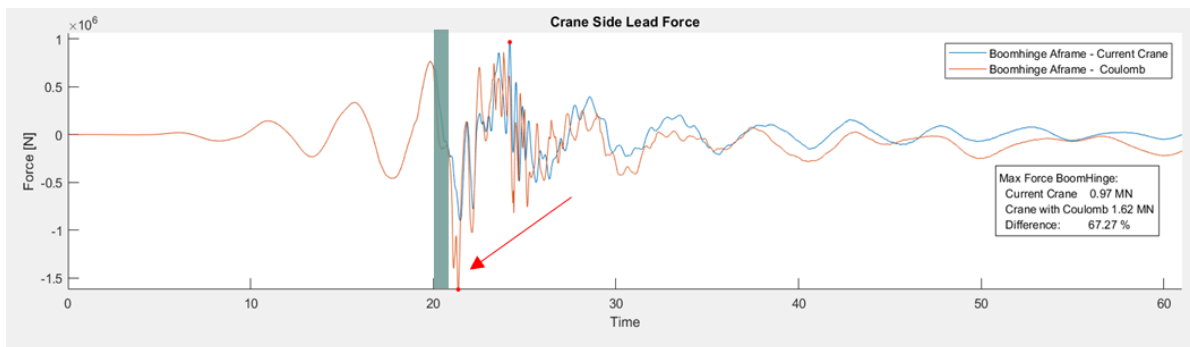


Figure 5.21: Vertical motions, lateral forces and slip occurrence

The peak force and the lateral offset of this configuration case counteract the aim of reducing the crane's dynamic response. As these peak forces may be prevented when the slip occurs more often during a shorter time interval, we mitigate the overturning moment once again by implementing a pre-tension to the aft bearing in order to reduce the slip thresholds.

Next to this pre-tension, to mitigate the lateral offset after the earthquake, we implement lateral springs in the bearings to act as restoring force. The stiffness of this spring is derived from the assumption that the maximal force that needs to be encountered for is 1 MN and that the bearing then should have an associated maximal offset of around 0.25 cm. This is a quick assumption to investigates the effect of lateral springs on the offset after the earthquake.

The effect of the implementation of the lateral stiffness and the pre-tension is investigated based on the test case. Figure 5.22 and Figure 5.23 present the displacements in the bearings and the forces in the boom hinge respectively. As expected, these figures indicate that slip occurs more often, and with shorter time intervals and that the offset after the earthquake and the peak force after the long period of slip are mitigated. Although the system seems to work, the maximum boom hinge force does not decrease significantly. In addition, the oscillating dynamic overturning moment still governs the periodic slip behavior of the bearings. Instead of being determined by large lateral forces, the slip is determined by the moments when the crane is near to its equilibrium state. As the main objective of reducing the dynamic response of the crane is not obtained, we deem this configuration case as unfeasible.

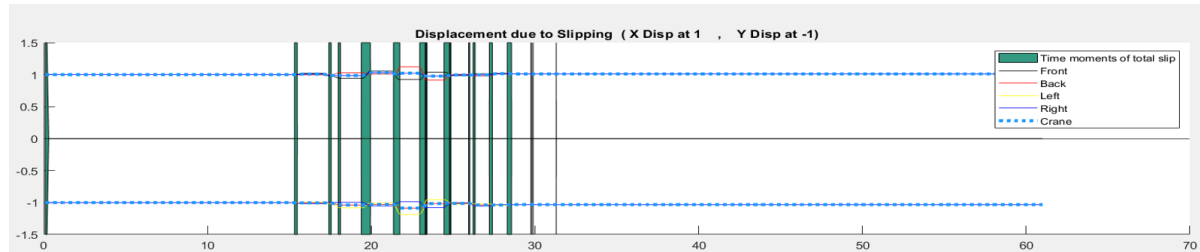


Figure 5.22: No permanent offset is found.

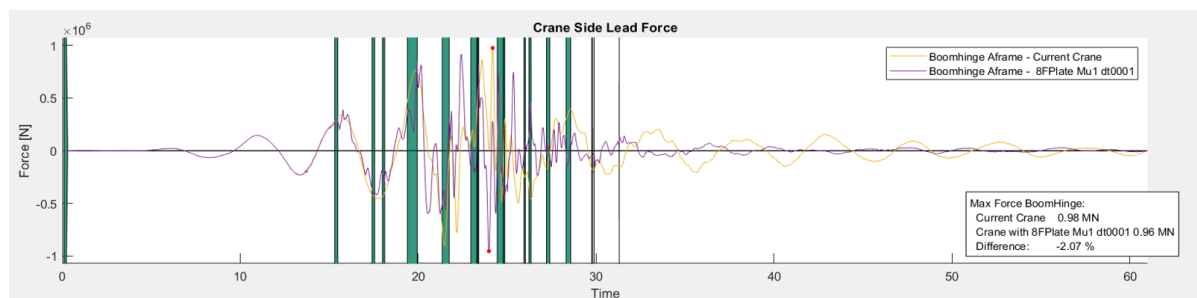


Figure 5.23: Out of plane forces in the boom hinge

5.2.6. Check the Base isolation system for a lower friction coefficient

A final attempt is made to make one of the encased configurations as stated above to show a mitigating effect on the response of the crane. During the prior investigations, we use a friction coefficient value of 0.13 as we assume this to be an industry standard for coated steel to steel interfaces. During the final attempt, we significantly lower the friction coefficient to 0.01. This lowers the slip threshold that must be exceeded by the lateral forces in order for slip to occur.

Figures 5.24 and 5.25 present the records of the test case with the encased configuration that does not have an additional lateral spring or pre-tension. These figures indicate the slip occurs very often and that the peak forces in the boom hinge are very well mitigated. However, a very large off-set is present after the earthquake. Therefore, we also investigate the case with the lateral spring implemented to the bearing.

Figure 5.26 presents the boom hinge forces in both the out-of-plane and in-plane direction. We find reduction of forces for both directions. However, the reduction of the maximum force in the out-of-plane direction remains limited.

Next to this, we find that the total lateral offset of the crane remains limited after the earthquake. However, the offset of each bearing is significant and means that the crane is rotated around the vertical axis. Furthermore,

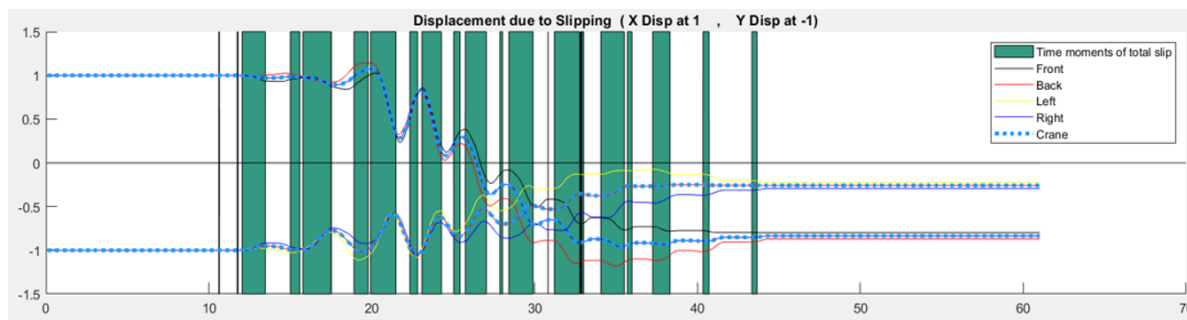


Figure 5.24: Test case: Friction coefficient set to 0.01 for encased friction plates, Displacement in the bearing

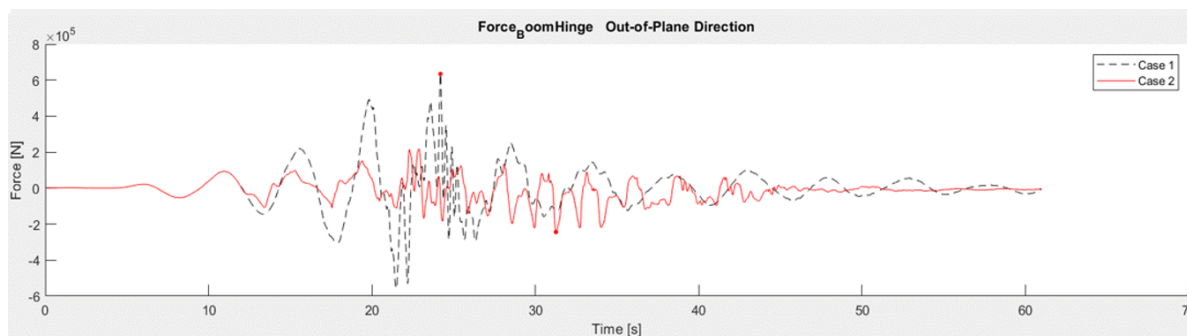


Figure 5.25: Test case: Friction coefficient set to 0.01 for encased friction plates, Out of plane forces in the boom hinge

the offset during the earthquake reaches amplitudes of one meter and is deemed as unacceptable high as an offset induces a very large overturning moment in the crane. When we try to mitigate this offset by increasing the lateral stiffness of the springs, we find that the boom hinge forces drastically increase and become twice as high as the crane without base isolation system.

As we are unable to find a configuration method that results in a mitigation of forces in the boom hinge of the crane, we deem the implementation of the base isolation system as unfeasible. Therefore, we do not further investigate the influence of this measure on the dynamic response of the crane in the next chapter.

5.2.7. Conclusion: Implementation of the base isolation system

We investigate the feasibility of the implementation of the base isolation system in the crane model such that it mitigates the dynamic response of the crane. We determine that we need to implement the base isolation system above the slew bearing as it than considers the rotation of the crane. For modelling purposes, we find that we need to use the Krylov-Newton algorithm instead of the Modified Newton algorithm to account for the non-linear behavior that is caused by the bi-linear stiffness behavior of the base isolation elements.

As a large overturning moment with dynamic dependency is present, we investigate multiple configuration methods to make the base isolation system a possible mitigation measure in this crane. These configurations consist of implementation of pre-tension to the bearings, implementing the aft bearing on the top side of the crane part, and the implementation of an encased configuration with friction plates. Next to this, we investigate adjustments of these configurations to counter the offset after the earthquake and to ensure for more slip occurrence.

We do not succeed in finding a potential configuration method that mitigates the dynamic response of the crane while keeping all other issues in mind. Next to that, it is found that during large lateral force the slip behavior is

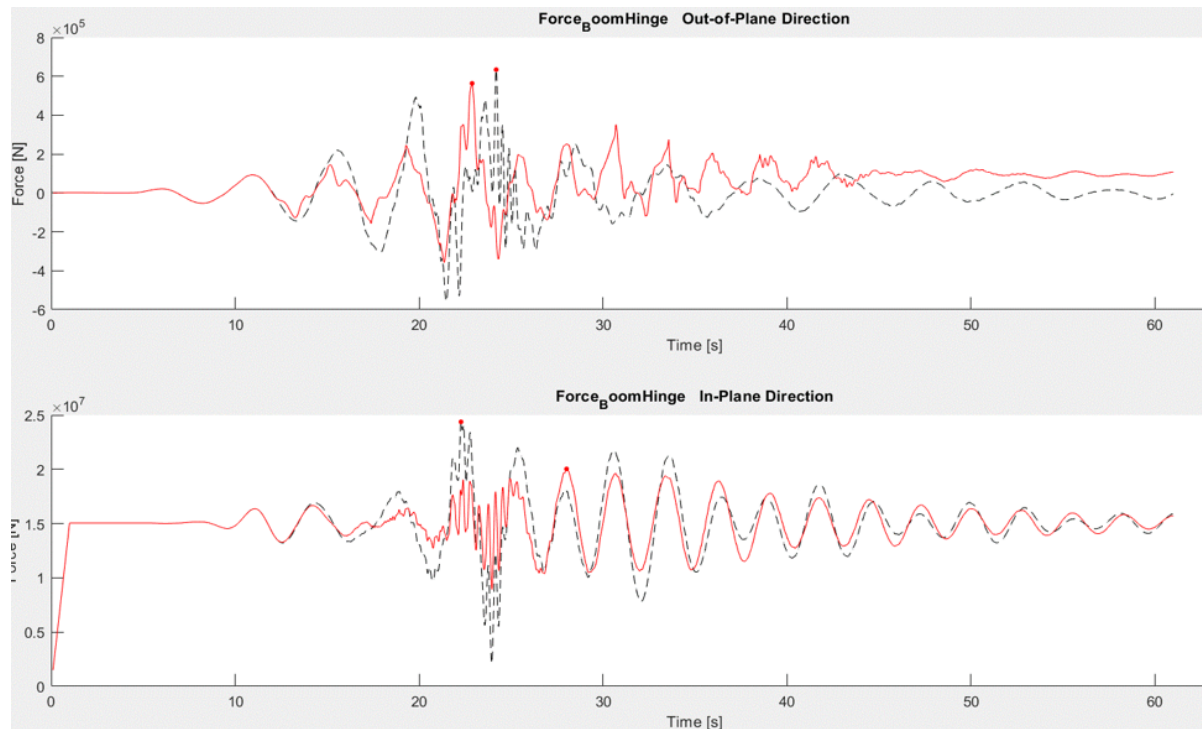


Figure 5.26: Test case: Friction coefficient set to 0.01 for encased friction plates and horizontal springs, In-plane and Out of plane forces in the boom hinge

highly dependent of the staggering motion of the crane. The base isolation system only slips at the moments in which the crane tips over its equilibrium position.

From these findings, we conclude that a base isolation system is not a feasible mitigation measure to counter the dynamic behavior of a crane on a jack-up. Therefore, we do not consider this mitigation measure in our further research.

5.3 Implementation of dynamic absorber

The goal of the dynamic absorber is to reduce the dynamic response of the crane by absorbing the kinetic energy that is build up in the structure. A more in-depth elaboration of the physical working mechanism of the dynamic absorber is explained in Section 2.5.

The implementation of a dynamic absorber in practice can be done in many ways. In this research, we choose to investigate the main working principle that is present in any practical implementation of the dynamic absorber. Namely the tuned mass damper mechanism. This section discusses the implementation of such a tuned mass damper in the crane model.

5.3.1. Location of the dynamic absorber

The literature in Section 2.5 states that the optimal location for dynamic absorber a location in the structure where the largest kinetic energy is present. To be more specific, this is an anti-node location of the vibration mode that has the largest influence on the structural dynamic response of the structure. In the case of our crane we find this location in the tip of the boom and implement the dynamic absorber at this location.

5.3.2. Parametric description of the dynamic absorber

As stated before, the dynamic absorber is implemented as a tuned mass damper. This system is defined by a mass of which the dynamic behaviour can be tuned by adjusting the springs and dampers connecting this mass to the structure.

In the crane model, these three elements are represented by a node, an elastic element, and a viscous damper element respectively. The initial nodal coordinates are set to the intersection of the boom and the jib. Thereafter, the elastic and viscous element connect the node with this intersection. The elastic and viscous elements are modelled such that they allow for lateral motion only. The parameters that define the mass and stiffness can be calculated to achieve an optimal mitigating performance. The method to calculate these parameters can be subdivided in three steps. An idealization of the continuous system, a simplification of this idealization, and the calculation of the optimal parameters of the dynamic absorber based on this simplification.

The first step is to idealize the continuous system that represents the crane as a discrete system with one degree of freedom. As field experts state that the out-of-plane motion has a higher likelihood to cause failure than the in-plane direction, we idealize the crane to the out-of-plane degree of freedom. This discrete system that is obtained from this idealization is comparable to a 'one sided clamped bending beam' or a so-called cantilever beam and can be seen in Figure 5.27.

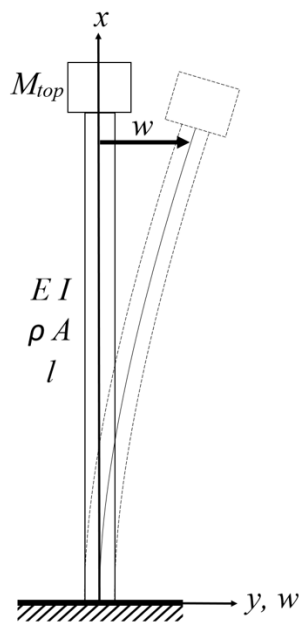


Figure 5.27: Idealized cantilever beam model

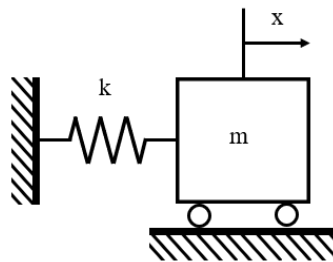


Figure 5.28: Simplified mass spring system

The second step is to simplify this cantilever beam into a discrete mass spring system as illustrated in Figure 5.28. Since the mass of the actual crane is distributed over various components, a cantilever beam with a simple uniform mass distribution is not a representative model. However, we assume that dividing the mass over two components, namely the boom and the jib, result in an adequate representation of the crane. The boom is then simplified by a uniform distributed boom mass and the jib is simplified as a concentrated mass in the tip of the boom.

Since two significant masses represent the crane in the cantilever beam model, a derivation of the simplified mass-spring system is not straight forward made.

To calculate the representative mass and stiffness of the simplified mass-spring system, an equivalent mass, M_{eq} , need to be calculated from this cantilever beam model. This equivalent mass can be calculated based on the stiffness of the cantilever beam and its natural frequency as explained below.

The stiffness of the cantilever beam can be deducted by combining Hooke's law:

$$F = Kx \quad (5.4)$$

With the deflection of single sided clamped cantilever that is subject to point load at its other end:

$$x = \frac{FL^3}{3EI} \quad (5.5)$$

When rewriting the above equations one can find the stiffness of the cantilever beam as:

$$K_c = 3EI/L^3 \quad (5.6)$$

Furthermore, as we know the natural frequency of the crane, we can use this to calculate the equivalent mass of the cantilever beam with the standard natural frequency formula:

$$\omega_c = \sqrt{K_c/M_{eq}} \quad (5.7)$$

Rewriting Equations (5.6) and (5.7) results in the equivalent mass that is defined as:

$$M_{eq} = \frac{3EI}{\omega_c^2 L^3} \quad (5.8)$$

This calculation of the equivalent mass is based on the parameters that are used in the crane model.

The third step is to calculate the parameters of the dynamic absorber. Literature states that even though a larger mass ratio between the absorber and the main structure may result in more effective mitigation, it is more economic to use a mass ratio in the range of 1 to 5% [6]. This agrees with the idea that it is undesired to add a lot of weight in the tip of the boom as the boom then needs additional stiffening to counter buckling. We consider a mass ratio of 5% in our investigation to obtain the best possible mitigation results. Therefore, the absorbers mass becomes:

$$M_a = 0.05 * M_{eq} \quad (5.9)$$

Subsequent is the calculation of the spring stiffness. Literature states that the optimal mitigation performance is achieved when the motion of the absorbers mass is tuned to the frequency of its disturbing force. In our case, the crane motion causes this disturbing force and therefore we tune the natural frequency of the dynamic absorber to that of the crane. The stiffness of the spring of the dynamic absorber can be calculated to achieve optimal tuning. For this calculation, we combine the absorbers mass and the natural frequency of the crane in an equation similar Equation (5.7):

$$K_a = \omega_c^2 * M_a \quad (5.10)$$

Since we model the dynamic absorber in two horizontal directions and since the crane has two different natural frequencies for these directions, the stiffness of the spring should be calculated for each direction separately. Next to this is the calculation of a realistic amount of damping in this system. This realistic amount of damping can be calculated with a certain damping ratio. This ratio expresses the level of damping relative to the critical

damping of a structure. The critical damping coefficient is calculated as follows:

$$C_{crit} = 2\sqrt{K_a * M_a} \quad (5.11)$$

Since we assume that a damping ratio of 10% is feasible, the damping of the viscous element of the dynamic absorber becomes:

$$C_a = 0.1 * C_{crit} \quad (5.12)$$

A schematic view of the total system with dynamic absorber is illustrated in Figure 5.29

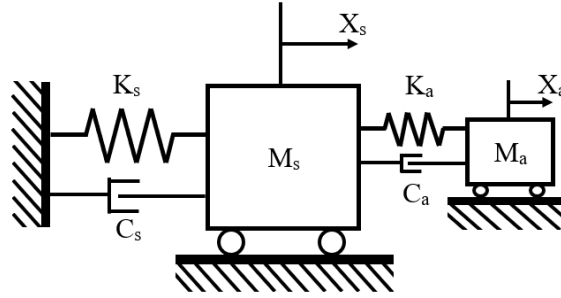


Figure 5.29: Schematic view of crane and dynamic absorber

5.3.3. Confirmation of the mitigation of dynamic response of the crane

As a first indication of the effect of the dynamic absorber on the dynamic response of the crane, we use the same test case as we used to investigate the base isolation system. First, we present the calculations of the parameters that define the dynamic absorber in the crane model then we discuss the findings of this dynamic absorber in the test case.

Based on Equation (5.8), the parameters of the crane and its natural frequency for the out-of-plane direction we find an equivalent mass of the simplified spring mass system of 343 tons.

$$E = 2.068E11Pa \quad (5.13)$$

$$I = 3.29m^4 \quad (5.14)$$

$$\omega = 1.33rad/s \quad (5.15)$$

$$L = 150m \quad (5.16)$$

$$M_{eq} = \frac{3EI}{\omega^2 L^3} = 343Tons \quad (5.17)$$

With a mass ratio of 5%, we calculate the mass of the absorbers(\$M_a\$) as 17 tons. Substantiated with expert opinion, we assume this mass to be an acceptable additional weight as it mitigates the dynamic response of the crane.

Thereafter, As the model finds \$\omega_{out} = 1.33rad/s\$ and \$\omega_{in} = 1.63rad/s\$ for the out-of-plane and in-plane natural frequency respectively, we can calculate the horizontal stiffnesses of the dynamic absorber with Equa-

tion (5.10):

$$K_{a(Out)} = \omega_{out}^2 * M_a \quad (5.18)$$

$$= 30.2kN/m \quad (5.19)$$

$$K_{a(In)} = \omega_{in}^2 * M_a \quad (5.20)$$

$$= 45.6kN/m \quad (5.21)$$

Subsequently, we can calculate the damping coefficient with Equations (5.11) and (5.12):

$$C_{a(Out)} = 0.1 * 2 \sqrt{K_{a(Out)} * M_a}$$

$$= 4.5kNs/m \quad (5.22)$$

$$C_{a(In)} = 0.1 * 2 \sqrt{K_{a(In)} * M_a}$$

$$= 55kNs/m$$

To give a first indication of the dynamic absorber on the response of the crane, we perform a simulation with the test case model in which the dynamic absorber, with the parameters calculated above is implemented. Figure 5.30 presents the boom hinge forces in out-of-plane direction that result from this model. As the forces are compared to the model without dynamic absorber, it indicates that the dynamic absorber has a mitigating effect on the response of the crane. Therefore, this dynamic absorber seems to be a feasible solution and it is interesting to investigate this measure over a wide range of configurations. To do so, the next section elaborates on the variation of the parameters for the dynamic absorber for the various crane configuration cases.

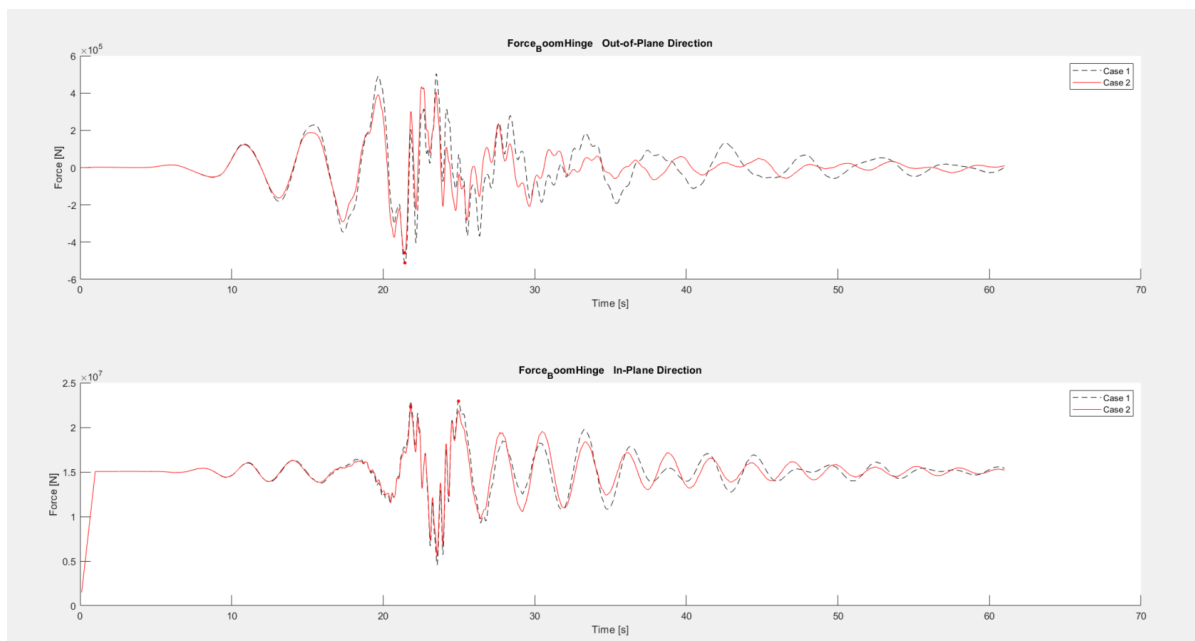


Figure 5.30: out-of-plane and in-plane boom hinge force.

5.3.4. Implementation of the dynamic absorber in multiple configuration cases

Since the implementation of the dynamic absorber in the crane is feasible, we investigate the dynamic absorber for multiple configuration cases in the next chapter. This section describes the changes that are made to the dynamic absorber due to various configuration case. The parameters are tuned to the natural period of the crane for each configuration case to obtain a more optimal response.

For the investigation in this thesis we choose to keep the mass of the dynamic absorber as a constant and use the stiffness as governing tuning mechanism. A practical example of such a dynamic absorber is a rigid mass that is suspended from a cable. The stiffness of this system can then be varied by changing the sling length of the cable. Prior, the motion response of the jack-up has been investigated for set of configuration cases that is described in Section 4.1.1. This set of variables is also used for the investigation to the influence of the dynamic absorber on the dynamic response of the crane. The natural periods of the crane are found to be depended of these configuration variables. As we use the natural periods, as frequency, to calculate the parameters of the dynamic absorber, we investigate the variation in the natural periods of the crane for the variation of configuration variables.

We find that the natural periods, and thus the natural frequencies, are most depended on the variables that define the weight of the suspended mass and the jack-up configuration case. The variation in the natural period of the crane due to these variables is summarized in Table 5.1. Next to this, it presents the associated optimal dynamic absorber parameters for each configuration case. We calculate these parameters based on the equations of Section 5.3.2 and use them in the investigation of the next chapter.

Table 5.1: Natural periods and absorber parameters for multiple configuration cases

Suspended mass	[t]	115	115	1365	1365
Jack-up natural period	[-]	Low	High	Low	High
$T_{n(out*)}$	[s]	4.68	4.43	3.29	3.19
$T_{n(in*)}$	[s]	3.82	3.62	3.25	3.16
M_{eq}	[t]	336	301	166	156
M_a	[t]	17	17	17	17
$K_{a(out*)}$	[kN/m]	30.6	34.1	62.0	65.9
$C_{a(out*)}$	[kNs/m]	4.56	4.82	6.49	6.69
$K_{a(in*)}$	[kN/m]	46.0	51.2	63.5	67.2
$C_{a(in*)}$	[kNs/m]	5.59	5.90	6.57	6.76

Out*: Out-of-plane direction of the crane

In*: In-plane direction of the crane

This tables gives an overview of the dynamic absorber parameters that we use for the investigation in the next chapter.

5.3.5. Conclusion: Implementation of the dynamic absorber

The aim of this section was to find the best way to implement the dynamic absorber in the crane model to mitigate the dynamic response of the crane. We have determined the tip of the boom to be the most suitable location for this dynamic absorber as is this is an anti-node location of the most dominant eigen mode of the crane. Therefore, this location possesses of the highest kinetic energy that can be mitigated. After determining this location, we have implemented the dynamic absorber as a rigid mass that is connected to the tip of the crane by an elastic and a viscous element.

We have calculated the stiffnesses of these elements by tuning them, and thus the dynamic absorber, to the natural frequency of the crane. We have done this based on an idealization and simplification from the actual

crane to a one degree of freedom spring-mass system.

Subsequently, we have investigated the dynamic absorber for a random test case and find that the dynamic absorber indeed effects and mitigates the response of the crane. From this we concluded that further investigation for multiple configuration cases was interesting and we calculated the stiffnesses of the dynamic absorber for the most common operation configurations in advance for the next chapter.

5.4 Conclusion: Implementation of mitigation measures

In this chapter, we have investigate which mitigation measures existed and are suitable for mitigating the dynamic response of a crane on a jack-up that is subjected to seismic activity. Thereafter we have implemented the two most promising mitigation measures to test them for feasibility in the crane.

Existing mitigation measures

From literature[12] we found the following existing mitigation measures that were to be all-encompassing according to in-field experts.

- Ductility through structural configuration
- Direct damping apparatus
- Base isolation systems
- Dynamic absorbers
- Active control devices

Based on arguments of both literature and experts we concluded the base isolation system and the dynamic absorber to be the most promising solution in reducing the dynamic response of a crane that is subjected to seismic activity. The other measures were considered to be less promising as they were unable to be retrofitted, offer a low potential of damping in case of this crane or that they need a complex system that carries more support, maintenance and risks.

Next, we have studied how the two promising measures can be implemented in the crane of a jack-up to test their feasibility.

Implementation of a base isolation system

We have not succeeded in finding a both feasible and mitigating implementation of the base isolation system on the crane.

The main issue with the base isolation system is that the crane tips over due to a static and dynamic overturning moment that pulls the bottom and top side of the base isolation system apart. We have countered this issue by: 1; implementing pre-tension 2; putting the aft bearing on top of the crane part 3; encasing the crane part on both the top and bottom side 4; or a combination of these three. However, this did not result in slip occurrence due to high slip-threshold that could not be exceeded by the lateral forces on the bearings, or it resulted in either large peak forces in the boom hinge or in unacceptable offsets that induced even higher overturning moments.

We attempted to counter the latter two issues by applying a horizontal spring to the bearing. Unfortunately, we still found high offsets or that the response of the crane did not decrease. Since we did not succeed in finding a mitigative implementation of this base isolation system while keeping the offset rather acceptable, we conclude that this measure is not feasible on a wind turbine installation crane due to its overturning moment.

Although we did not find a feasible solution in our study, base isolation systems are in general suitable for and perform well on land-based structures. Therefore, it may be interesting to further investigate possible implementations of base isolation systems for the offshore industry in further research.

Implementation of a dynamic absorber

For the dynamic absorber, we did find a feasible implementation method. Based on literature, we have implemented the dynamic absorber in the tip of the boom as this is an anti-node location (where the largest amount of kinetic energy is present) of the most dominant eigen mode.

Next to that, we have calculated the mass of the dynamic absorber as 5% of the equivalent mass of the dominant eigen mode of the crane since we saw from literature that this is an economic optimum in practice.

Additionally, we have tuned the natural frequency of the dynamic absorber to the natural frequency of the crane by calculating the stiffness between dynamic absorber and tip of the crane. These calculations were based on an idealization and simplification of the actual crane into a one degree of freedom spring-mass system.

After determining this location, mass and stiffnesses, we have implemented the dynamic absorber as a rigid mass that is connected to the tip of the crane by an elastic and a viscous element. Subsequently, we have investigated the dynamic response of the crane with this dynamic absorber for a random test case and found that the dynamic absorber indeed effects and mitigates the response of the crane.

From our findings, we conclude that only the dynamic absorber is a feasible and promising mitigation measure that can be implemented on a crane and further investigation of this measure for multiple configuration cases is interesting.

6

Influence of the dynamic absorber on the response of the crane

We study the influence of the dynamic absorber on the response of the crane by implementing it in the jack-up and crane model. We compare the resulting simulated performance with that of a benchmark model without the dynamic absorber. This chapter starts with a description of the methodology and models that are used in this investigation. Second, this chapter explains how we obtain useful data from the output of these models. Third, this chapter provides an analysis of this data based on distribution plots and scatter plots. Fourth, to illustrate the dynamics that govern the performance of the crane with dynamic absorber, this chapter provides an in-depth analysis of one specific simulation run. For this, we selected the case in which the dynamic absorber achieves the biggest force difference in the boom hinge. In the last part of this section the conclusions from this investigation are presented and discussed.

6.1 Methodology: Measuring the influence of the dynamic absorber

The influence of the dynamic absorber on the response of the crane is investigated by comparing two models for multiple configurations and earthquake cases. For these models we use the jack-up and crane model as one combined structure as explained in Chapters 3 and 4. The first model includes a dynamic absorber in the crane. The second model is without the dynamic absorber implementation and is used as a benchmark.

The dynamic absorber is implemented in the tip of the boom since this is the location in which the largest amplitudes occur and which possesses the highest kinetic energy. Therefore, this enables the largest potential mitigation of the crane response due to the implementation of the dynamic absorber in this location.

The variation between the cases that are investigated is similar to the variation that is used to investigate the motion response of the jack-up in Chapter 4. The main difference to the Chapter 4 variations is that the variation has been reduced slightly to save calculation time. Additionally, for this investigation the boom angle and seismic zone are fixed at 80 degrees and 0.3g, respectively. These values are chosen since they have the highest likelihood of occurrence. Figure 6.1 and Table 6.1 provide an overview of the model and the cases that are investigated.

The structural survivability of the crane is governed by the forces in the boom hinge according to GustoMSC experts. Intuitively, larger forces in the boom hinge have a larger potential to damage the crane. This potential damage can have severe consequences (e.g. the loss of human life and financial costs). Since large forces carry

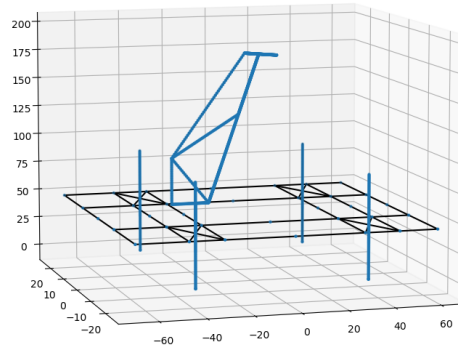


Figure 6.1: Combined model of jack-up with crane

Table 6.1: Variation in test cases

Variable	#	Possible values
Site Class	1	C
Seismic Zone	3	0.3g
Earthquake	7	1, 2, 3, 4, 5, 6, 7
Jack up case	2	low, high
Slew Angle	5	10, 165, 230, 280, 325
Boom Angle	3	80
Hook load	2	0, 1250
Total	140	Possible Cases

This table presents the possible configuration cases for this investigation

more risks, it is preferred to mitigate these large forces. Therefore, we use the maximum forces in the boom hinge as an indicator of the influence of the dynamic absorber.

In our simulation model, forces in opposite directions are expressed as positive and negative forces, respectively. Since we are interested in the maximum force in either direction, we first take the absolute value of the forces in the boom hinge and then calculate the maximum.

We evaluate the influence of the dynamic absorber on the response of the crane by comparing the maximum absolute boom hinge forces for the dynamic absorber model and the benchmark model. We use two indicators for this comparison. The first indicator is referred to as the '*force difference*' ($\Delta F_{max,[MN]}$) and is defined as the difference between the maximum absolute forces. The second indicator is referred to as the '*force ratio*' ($\Delta F_{max,[\%]}$) and is defined as the *force difference* weighted by the maximum absolute force in the benchmark model. These indicators are defined by the following equations:

$$\Delta F_{max,[MN]} = \max(|F_{withabsorber}|) - \max(|F_{Benchmark}|) \quad (6.1)$$

$$\Delta F_{max,[\%]} = \frac{\Delta F_{max,[MN]}}{\max(|F_{Benchmark}|)} * 100\% \quad (6.2)$$

6.2 Data collection and processing

The forces in the boom hinge are recorded during the simulations. The output consists of three orthogonal time dependent vectors that represent the forces in the x, y, z-directions of the global reference system (i.e. the domain).

As discussed in Section 2.2, the ISO standards state that the response forces that are found during earthquake time domain analysis should be multiplied by partial action factors. This implies that the static part of the response forces should be multiplied by a factor of 1.0 and that the dynamic part of the response forces should be multiplied by a factor of 0.9.

The dynamic part of the forces is obtained by subtracting the static part from the force vector. This static part is determined as the force that is present in the boom hinge right after the application of the weight of the structure itself. At this moment in the simulation, the structure is in static equilibrium and no dynamic forces are involved yet. Figure 6.2 gives an illustration of this processing for a force in the x-direction.

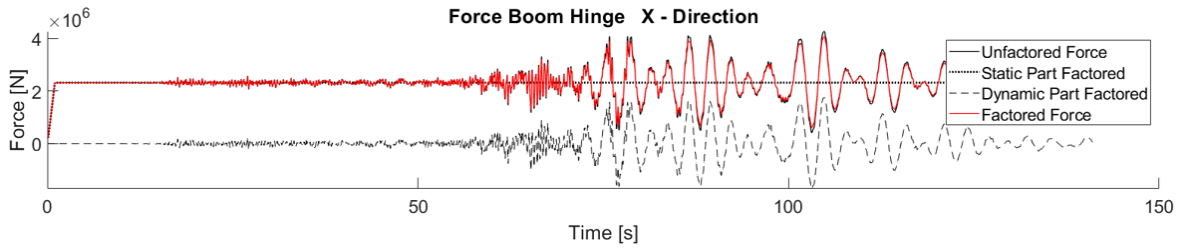


Figure 6.2: Consider the dynamic action factor: example case: EQ6 Low S165 B80 L115

The recorded force vectors are defined in the global reference system of the domain and do not align with the orientation of the local reference system of the crane. This alignment is necessary for the comparison of results.

The alignment of the force vectors with the local reference system is achieved by rotating them around the z-axis. For this purpose, we multiply the x, y and z force vectors by the rotation matrix (R_{z-axis}) that is dependent on the slew angle of the crane. After this rotation, the forces in the x-axis describe the forces that act in the same direction as the heading of the boom. The rotation matrix is defined as:

$$R_{z-axis} = \begin{bmatrix} \cos(\alpha_{slew}) & -\sin(\alpha_{slew}) & 0 \\ \sin(\alpha_{slew}) & \cos(\alpha_{slew}) & 0 \\ 0 & 0 & 1 \end{bmatrix} \quad (6.3)$$

We evaluate both the 'out-of-plane' and 'in-plane' forces in the boom hinge. The 'out-of-plane' forces ($F_{Out-of-plane}$) are defined as the forces in the local y-axis direction of the boom hinge. The 'in-plane' forces ($F_{In-plane}$) are defined by the root summed squared of the forces that are found for the local x- and z-direction. These forces are defined by the following equations:

$$F_{Out-of-plane} = F_{y-local} \quad (6.4)$$

$$F_{In-plane} = \sqrt{F_{x-local}^2 + F_{z-local}^2} \quad (6.5)$$

These two force vectors that represent the simulated forces in the boom hinge are now ready to be evaluated following the methodology described in the previous subsection.

6.3 Analysis of the force differences in the boom hinge

This section visualizes the recorded and processed data of the *force differences* and *force ratios* with distribution graphs and scatter plots. These graphs enable the analysis of and the discussion on the influence of the dynamic absorber on the crane.

6.3.1. Force difference

As explained in Section 6.2, we use the *force difference* as an indicator of the influence of the dynamic absorber on the crane. Figure 6.3 presents the distributions of these *force differences* in both the out-of-plane and the in-plane direction.

The distributions show an average of the *force differences* below zero. This means that the forces in the boom hinge reduce on average due to the implementation of the dynamic absorber. However, 12% of all simulated cases result in a *force difference* above zero. For these cases, the forces in the boom hinge increase due to the implementation of the dynamic absorber.

Important to note is that the magnitude of the *force differences* for the out-of-plane direction are a factor 10 smaller than that for the in-plane direction. Moreover, the mean *force difference* in out-of-plane direction is 65 KN and the mean for the in-plane direction is 620 KN.

Since the *force difference* is a nominal value it does not reflect the relation between difference and the amplitude of the maximum force in the boom hinge. The next section presents the *force ratios* to reflect on this relation.

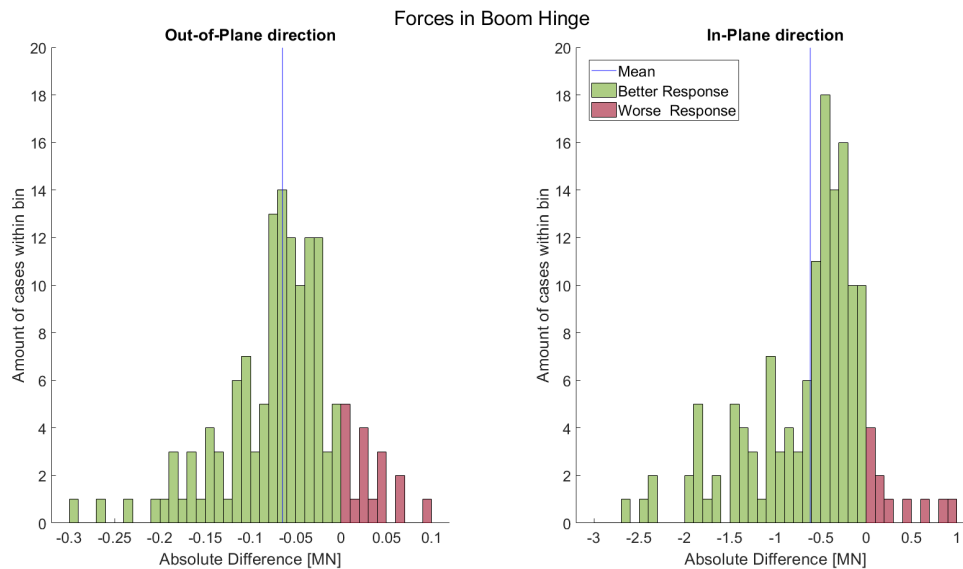


Figure 6.3: Distribution of the *force differences*

6.3.2. Force ratio

As explained in Section 6.2, another indicator of the influence of the dynamic absorber on the crane is the *force ratio*. Figure 6.4 presents the distributions of the *force ratios* in both the out-of-plane and in-plane direction. Note that the scales of the 'out-of-plane' and 'in-plane' *force differences* are different.

The distributions indicate an overall reduction of the forces while some cases indicate a force increase. This was to be expected based on the *force differences* discussed before. However, the range of the *force ratios* is a factor

2 to 3 larger for the out-of-plane direction than for the in-plane direction. Furthermore, we find a mean of -9.6% for the out of plane direction and a mean of -2.1% for the in-plane direction.

As the distributions of the *force differences* and the *force ratios* are somewhat comparable, it seems to indicate that there might be a relation between them. The next section makes scatter plots of the *force differences* and the *force ratio* to find the relation between the two.

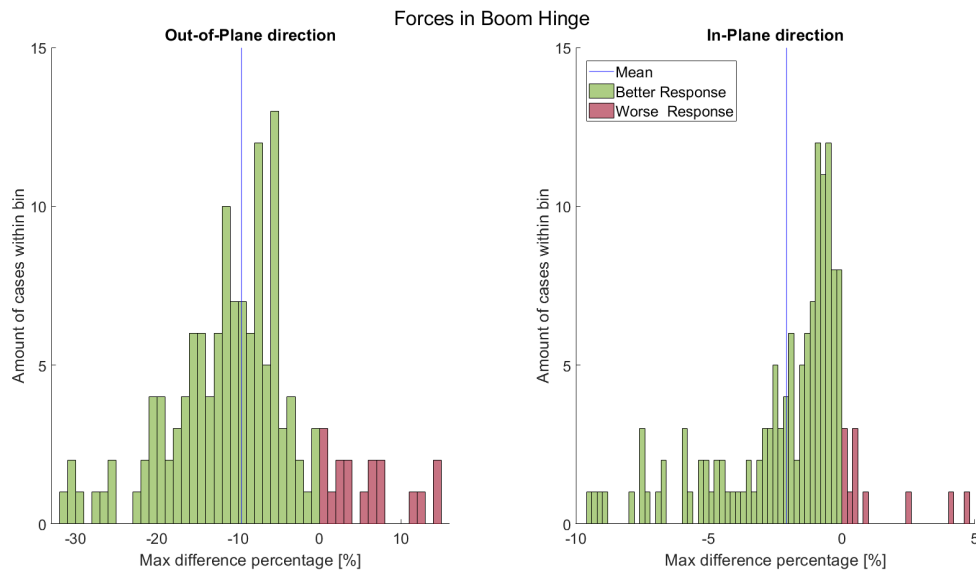


Figure 6.4: Distribution of the *force difference* ratios

6.3.3. Force difference vs force ratio

Each case has a certain *force difference* and *force ratio* values. We can find the relation between these two values by visualizing them in a scatter plots. Figure 6.5 presents the these scatter plots for both the out-of-plane and in-plane direction. Also here should be mentioned that the axes differ in range.

These scatter plots indicate the best mitigating results of the dynamic absorber in the lower left corner as that that quadrant indicates a reduction of forces in the boom hinge. Opposite to this. the worst mitigating results can be found in the upper right corner.

As expected, a relation can be distinguished from these plots. They indicate that the magnitude of the *force difference* increases with increasing *force ratios* as no clear outliers are found. For the in-plane direction, multiple variations of this relation can be distinguished. The cause of these variations has to do with the difference of the suspended mass between the cases.

We find that the relation is less steep for cases with a relative low suspended mass of 115 tons. The low and the high jack-up cases cause another slight distinguishment within these cases. Furthermore, we find a rather limited ratio distribution for the 1365 tons suspended mass cases, compared to the ratios for the 115 tons cases.

Additionally, we find found that for the out-of-plane direction, the ten worst cases all have a suspended weight of 115 ton.

As these cases vary in total applied weight it is interesting to investigate the influence of the amplitude of the force on the *difference ratio*. The next section presents this investigation and the findings.

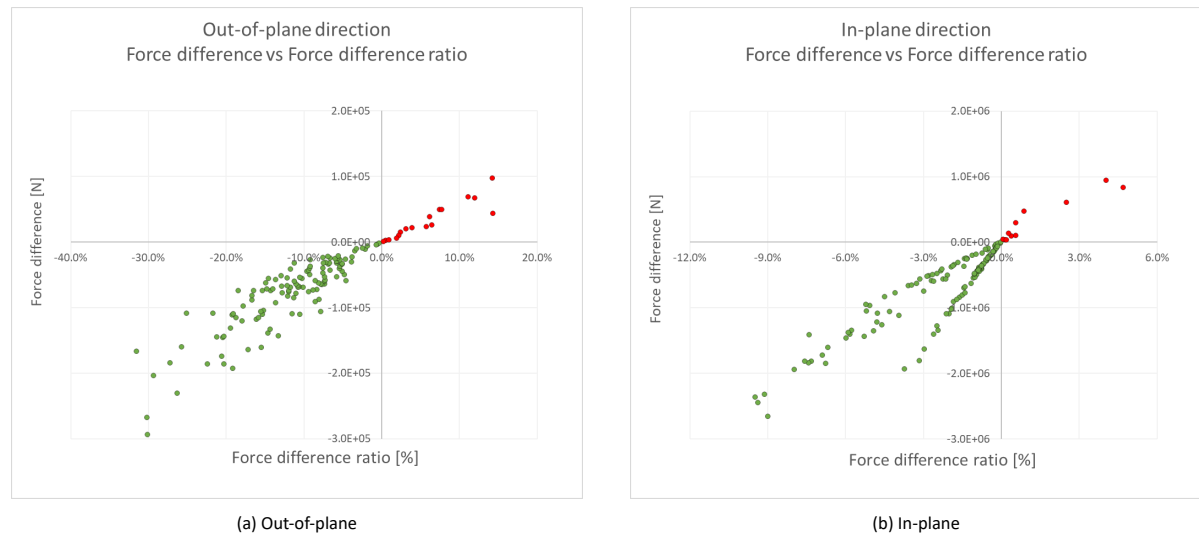


Figure 6.5: Scatter plots that visualises the distribution of the force differences and the forces difference ratio

6.3.4. Force ratio vs maximum absolute force of the benchmark model

We instigate the relation between the force ratios and the maximum absolute force of the benchmark by visualizing them in scatter plots. Figure 6.6 presents these scatter plots for both the out-of-plane and in-plane direction. Also here should be mentioned that the axes differ in range.

These scatter plots indicate two clear relations. For the out-of-plane direction, we find that a worsening influence of the dynamic absorber is only found for the cases in which the amplitude of the out-of-plane force remains limited. Since lower force amplitude indicates a lower risk case and since this worsening influence is only found for these lower risk cases, this may be acceptable. It is a very beneficial observation that the dynamic absorber solely has a mitigating effect in the cases with higher amplitude forces. This means that the highest risks are mitigated anyway.

After investigating the high force cases, we find that these high forces are caused by a very harmonic oscillation. As a dynamic absorber mitigates harmonic oscillations well, we only find a mitigating influence of the dynamic absorber for these high force cases.

For the in-plane direction, two clouds of cases can clearly be distinguished. These clouds represent the cases with a suspended mass of 115 ton or 1365 ton. This makes sense as the larger suspended mass results in a larger gravitational force that works in the vertical direction of the boom hinge. Next to that, since the suspended mass is positioned at a certain distance from the boom hinge, a larger suspended mass implies a larger overturning moment. This larger overturning moment is captured by an increased tension in the hoist wires and that results in an increased force on the boom hinge in in-plane direction.

Next to the distinction in amplitude of the force, it can be noted that the *range of force difference* is significantly smaller for the 1365 tons cases. This may be caused by two reasons. First, the smaller influence may be assigned to the fact that the amplitude of the boom hinge forces increase as its vertical component increases due to an increase of the suspended mass. Even if the horizontal forces in the boom hinge may be equal for both cases, this results in a lower *difference ratio* for a lower suspended mass anyhow. Secondly, the smaller influence may be caused by a smaller equivalent mass. A higher suspended mass causes a lower natural period of the crane. This lower natural period results in a smaller equivalent mass of the crane as can be derived from Equation (5.8). As the ratio of the effective mass versus the total mass of the crane is smaller this implies that the dynamic

absorber can dampen a smaller mass ratio of the crane. As a smaller mass ratio of the crane can be damped by the dynamic absorber, the range of difference percentages will be smaller for these 115 tons cases.

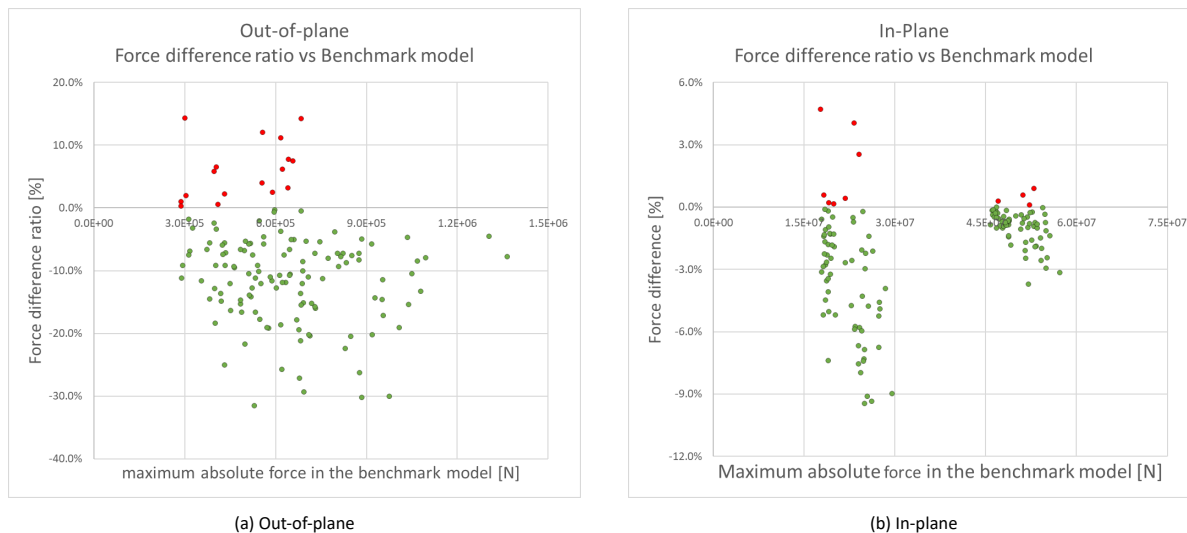


Figure 6.6: Scatter plots that visualises the distribution of the *force differences ratio* as function of the maximum absolute force of the benchmark model

6.4 Analysis of the case with the highest force difference in out-of-plane direction

In the previous section, the influence of the dynamic absorber is discussed based on distributions and scatter plots. These are generated from the maximum force that is recorded in the boom hinge. This offers a method to compare multiple configuration cases and gives an good overview of the degree of variation that can be distinguished between them. The influence of the dynamic absorber is hereby simplified to the maximum force amplitude only. However, the reason for this influence can only be discovered by comparing the entire time response of the crane.

This section performs such an entire time analysis for one specific case. It is assumed that a larger differences between incorporating a dynamic absorber or not makes it more easy to distinguish the reason for the absorbers influence. Furthermore, it is stated by field experts that the out-of-plane motion has a higher likelihood to cause failure than the in-plane direction. Therefore, it is chosen to use the case in which the largest *force difference* between the two models occur in the out-of-plane direction.

This specific case occurs during 6th earthquake from the earthquake list that is discussed before in Section 4.3.4 and is given in Appendix A. This case represents the low natural period configuration case of the jack-up. The jack-up consists of relative short legs (30 meters) and a relative low variable weight is present in the hull mass distribution. The suspended mass equals to 115 tons, this represents the mass of the lower block and the hook. The crane has a slew angle of 165 degree, meaning that its heading is to the aft of the jack-up. The natural periods found for the model with and without dynamic absorber are given in Table 6.2.

From this table can be seen that the dynamic absorber changes the natural periods of the crane. Each natural period of the crane is replaced by a natural period higher and lower than itself. This is an expected event as this is also shown in Figure 2.5. This figure shows the frequency response of a structure and its change due to the implementation of a dynamic absorber.

The analysis in this section investigates the earthquake input signal, the acceleration response of the base of

the pedestal, the force response in the boom hinge and the displacement response of the jib and the dynamic absorber.

Table 6.2: Natural periods of the modelled cases

	Without dynamic absorber [s]	With dynamic absorber [s]
Suspended mass	9.66	9.68
	9.25	9.25
Crane	4.73	5.25
		4.23
	3.86	4.21
		3.50
Jack-up	2.77	2.77
	2.72	2.72
	2.68	2.68

This table presents the natural periods of a jack-up model with low natural period (20 meter water depth). The suspended mass in the crane equals to 115 tons

6.4.1. Earthquake input signal

The analysis of the specific case start with analysing the input signal for the model. The time trace of the earthquake for this specific case is given in Figure 6.7. It can be seen that the earthquake describes a stochastic signal. The total time trace can be subdivided in multiple time period as different acceleration signals can be distinguished over time.

The first period captures the moment before 50 seconds. During this period, the first shocks will reach the structure. These shocks describe a high frequent, mediate amplitude wave. They travel faster through the Earth than other waves to arrive at the structure first. Therefore, they are referred to as primary waves. These primary waves are compressional waves that are part of the body waves that travel through the interior of the Earth

The second period captures the moment between 50 and 90 seconds. During this period, the largest amplitudes of shocks arrive at the structure. These shocks describe high frequent, large amplitude waves. These waves are referred to as secondary waves as they arrive at the structure after the primary waves. These secondary waves are shear waves and are also part of the body waves that travel through the interior of the Earth.

The third period captures the moment between 90 and 110 second. During this period, low frequent, mediate amplitude waves arrive at the structure. As these waves travel along the Earth's surface they are referred to as surface waves, or more specific Rayleigh waves. These waves describe a clear oscillation in the time trace as their frequency is much lower than the prior waves.

The fourth period captures the moment after 110 second. During this period, no significant ground motions occur anymore.

It is found that the response of the structure remains limited during first period in which the compression waves arrive at the structure. As this thesis investigates the mitigation of the response of the crane, this first period can be designated as irrelevant and is therefore not presented in the next figures.

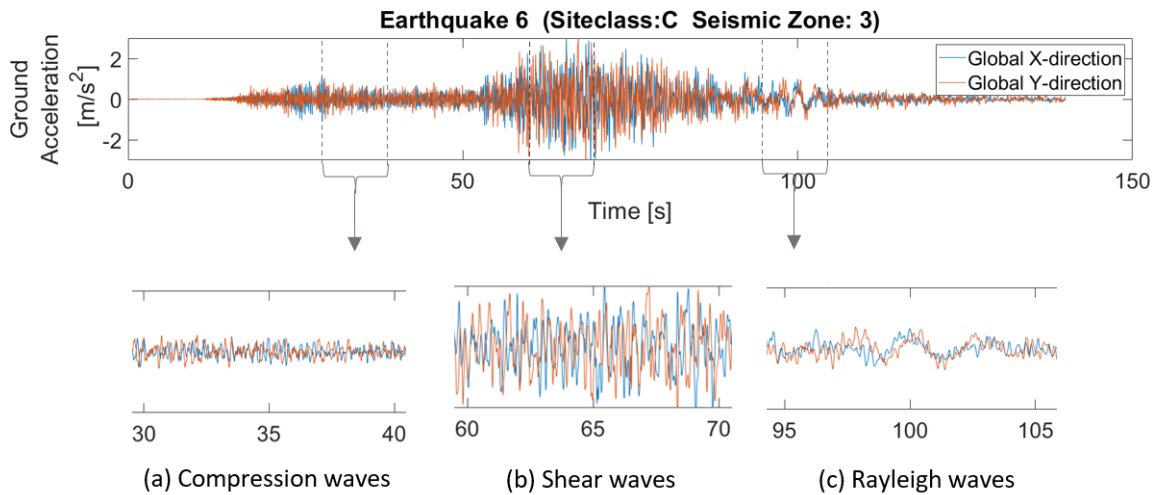


Figure 6.7: Diffentiation of mutiple ground vibrations.

6.4.2. Acceleration of the base of the pedestal

The accelerations that enter the crane via the pedestal describe the response of the jack-up. This response is highly related to the prior described ground motions. During the first period, with the compression waves, a stochastic response with a low amplitude is recorded in the pedestal. This tells us that legs of the jack-up filters out most of the ground motions. As this is not interesting for this thesis this part is excluded from the graph.

The shear waves during the second period cause a stochastic like response with large amplitude of the pedestal. A slight harmonic signal can be distinguished that describes some harmonic motions of the jack-up. This harmonic signal becomes clearer with the advancement over time and is probably caused by the frequency response of the natural period of the jack-up.

The low frequent Rayleigh waves during the third period result in an increasing amplitude of this oscillating response. This is probably caused by the fact that these Rayleigh wave have a frequency that is close to the natural frequency of the jack-up. These large amplitude oscillations mean that the jack-up is moving back and forth harmonically. During the fourth period, the amplitude of the oscillations decreases with time. This implies a decay of the motion response of the jack-up. Moreover, as no difference between the model with and the model without dynamic absorber can be distinguished, it is assumed that the dynamic absorber does not influence the motion of the jack-up for this case.

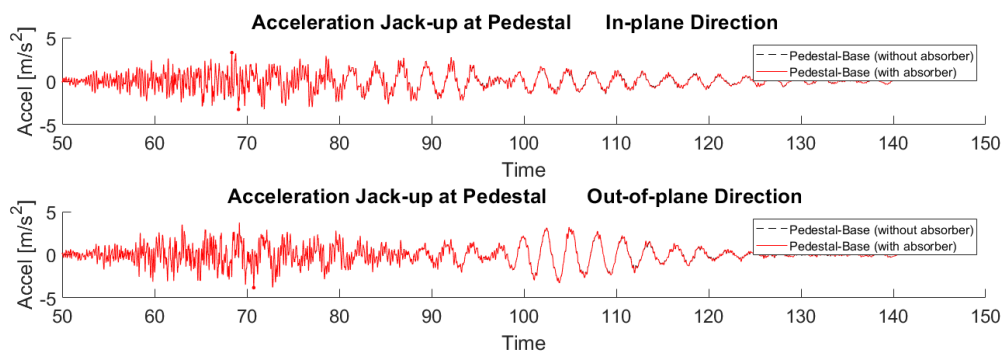


Figure 6.8: Accelerations in the pedestal

6.4.3. Forces in the boom hinge

The forces in the boom hinge describe a similar transition through time as the acceleration of the jack-up. This is a logical consequence as these accelerations are directly transferred to the boom hinge. However, the forces in the boom hinge are also closely related to the displacements of the jib that can be seen in Figure 6.9.

During the shear wave period, a signal with traits of stochastic and harmonic vibrations can be distinguished. The graph shows that forces in the boom hinge remain acceptable compared to the forces that occur during the Rayleigh waves period. Next to that, no significant differences can be found between the two models. This implies that the dynamic absorber has little to no effect on the forces in the boom hinge during this period.

During the Rayleigh wave period, a proper harmonic signal with large force amplitudes occurs. Comparing the two models clearly shows that extreme forces that occur in the boom hinge due to the Rayleigh waves are mitigated with a factor up to 31.5% by the dynamic absorber.

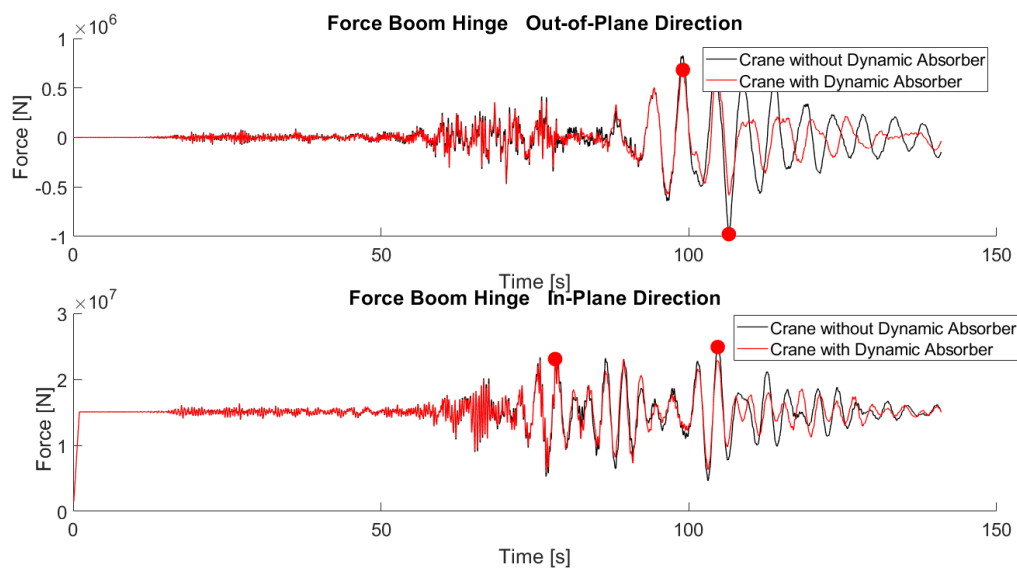


Figure 6.9: Forces in the boom hinge

6.4.4. Displacement of the jib vs the pedestal

The displacement graph of the jib displays a harmonic response over the complete time trace. During the shear wave period, a vibration period of 2.7 seconds is found. As this vibration period is very close to the natural period of the jack-up, this indicates that the displacement of the jib is mainly governed by the motion of the jack-up. This can be substantiated with the jib vs pedestal graph. In this graph can be seen that the crane and the jack-up are in counter phase with each other during this shear wave period.

Furthermore, it can be noted that the amplitude of the response is small compared to amplitudes that are recorded during the Rayleigh wave period. For this Rayleigh wave period, the vibration period becomes approximately 4.2 seconds and is therefore more in line with the natural frequency of the crane. During this period the influence of the dynamic absorber becomes clearly visible.

6.4.5. Displacement of the jib vs the dynamic absorber

The motion of the dynamic absorber is compared to the motion of the jib to investigate why the forces and displacements clearly decrease for the Rayleigh wave period and beyond.

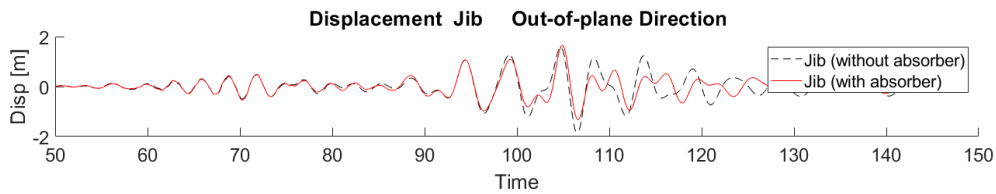


Figure 6.10: Jib displacements

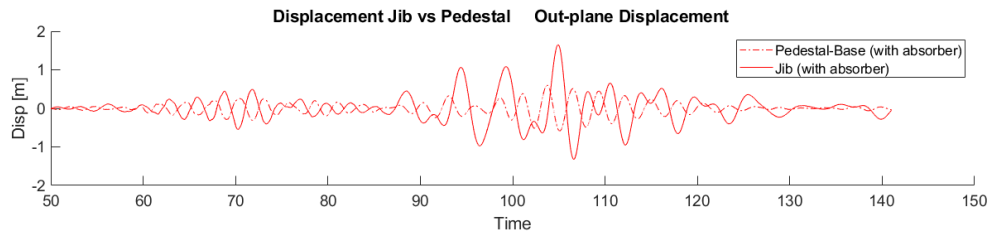


Figure 6.11: Jib vs Pedestal displacements

It is found that the displacement of the dynamic absorber increases drastically as the crane starts to move in its natural frequency. This natural frequency occurs during the Rayleigh wave period. As the dynamic absorber is tuned to this natural frequency and as larger jib displacements occur during this period, more kinetic energy is being transferred from the crane to the dynamic absorber. This kinetic energy is absorbed by motion of the absorber that is relative to the crane. In this way, the dynamic absorber ensures optimal mitigation of the response of the crane.

Next to that, as the jib induces the motion of the dynamic absorber, it is a logical consequence that the absorber starts to move out of phase with the crane. This out of phase motion is not clearly visible for shear waves period. After this period the out of phase motion becomes more visible. The largest time varying *force difference* that can be distinguished from Figure 6.9 occurs around 107 seconds. This mitigating effect can be assigned to the extreme out of phase motion around the 105th second in Figure 6.12

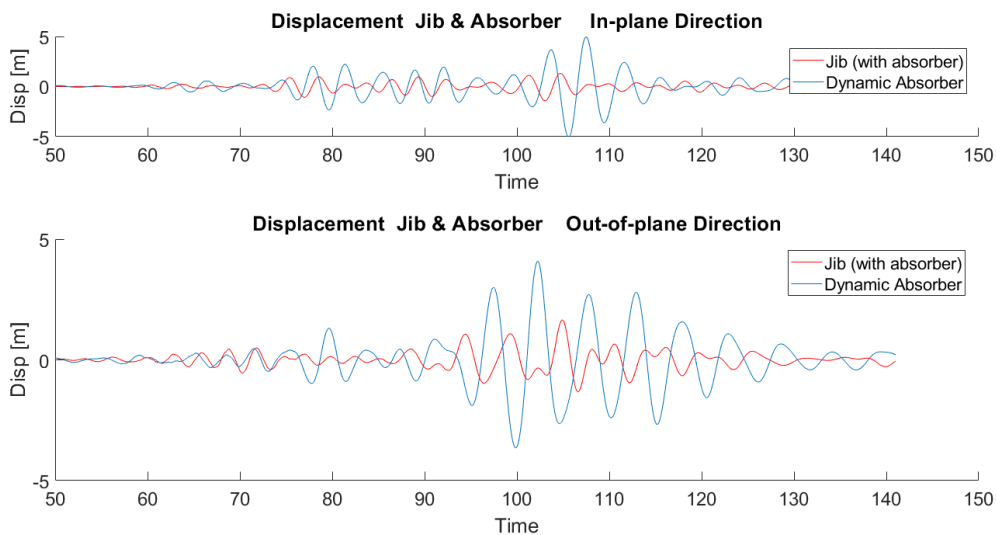


Figure 6.12: Jib vs Dynamic absorber

6.5 Conclusion: Implementation of the dynamic absorber in the crane

In this chapter we have studied the influence of a dynamic absorber on the dynamic response of a crane on a jack-up that is subjected to seismic activity. We studied the influence by comparing the maximum forces that occurred in the boom hinge of a crane model with a dynamic absorber to that of a similar crane model without dynamic absorber. Further more, as it was stated by experts of GustoMSC that the out-of-plane force in the boom hinge has a higher likelihood to cause failure than the in-plane force, we have use the out-of-plane force as main indicator for the outcome of this investigation.

Our findings were that in the vast majority of simulated cases(88%) the dynamic absorber reduces the dynamic response of the crane to seismic activity. As the other 12% of cases only occurred in cases with low risk(relative low force amplitude) and that an overall average mitigation was found of approximately 10%(reduction), we conclude that this measure is a beneficial application to reduce the response of the crane. Since human lives and large economic burdens are at stake during seismic events, a dynamic absorber that reduces these risks can be seen as highly necessary. Moreover, a reduction of a large amplitude force by a dynamic absorber results in a large decrease of the risk since they reduce drastically with the amplitude of the force that acts on the boom hinge.

Next to the general findings, we have discovered that the highest two third of the 12% of worsening cases was caused by cases with a low suspended mass weight. This can be explained by the fact a smaller suspended mass results in an increased eigen period of the crane. This leads to an increased effective mass that participates in the motion of the crane which can be dampened. Since there is more effective mass to dampen, the dynamic absorber can yield larger effect. This effect was clearly visible for the in-plane direction, Figure 6.6.

Another interesting finding is that the dynamic absorber is especially effective in mitigating the dynamic response of the crane near the end of earthquakes. This can be explained by the fact that near the end of an earthquake, the dominant seismic activity consists of Rayleigh waves. These Rayleigh waves have an eigen period that is relatively close to the eigen period of the jack-up structure and crane. Therefore, these Rayleigh waves induce a clear harmonic oscillation of the jack-up structure that is translated to the crane. Since dynamic absorbers are especially effective in mitigating the harmonic oscillations of structures, the dynamic absorber achieves its largest mitigating effects near the end of the earthquake.

Furthermore, our findings show that dynamic absorbers are very suitable for mitigating the response of a crane that is subjected to more common operational conditions, such as waves and wind. As these induce rather harmonic vibrations and as a dynamic absorber highly effective in dampening harmonic motions, a large mitigation can be obtained under these environmental conditions.

Finally, based on the research that is performed in this thesis, we conclude that the dynamic absorber is the best mitigation measure that can be applied on a wind turbine installation crane on a jack-up to counter its dynamic response to seismic events

We conclude that the dynamic absorber is an effective mitigation measure that can be implemented to reduce the dynamic response of the crane to seismic activity.



Conclusions and recommendations

In this thesis, we have studied the dynamic response of a wind turbine installation crane on a jack-up that is subjected to seismic activity by performing seismic time history analysis. Our main objective is to determine the best solution to mitigate the dynamic response of such a crane in case of a seismic event.

The final conclusion of this thesis is that the dynamic absorber is the best solution to mitigate the dynamic response of a wind turbine installation crane on a jack-up that is subjected to seismic activity. The sub-conclusions of the various steps that we have taken to arrive at this conclusion are presented below and are followed by recommendations for further research.

7.1 Conclusions

First, in order to design an adequate model for this research, we have studied the influence of the dynamic response of the crane on the dynamic response of the jack-up. We studied this influence by comparing the maximum lateral motion response of a jack-up model in which a static crane mass is incorporated in the hull mass of the jack-up to a jack-up model with an integrated dynamic crane model.

Our findings were that for the vast majority of simulated cases (78%) the integration of the dynamic crane model led to worse motion responses of the jack-up. Next to that, the maximum motion differences were found up to 0.24 meter (this is equal to 43% of the amplitude of the displacement). Based on these findings we concluded that using the jack-up motions as input for our investigation into the crane dynamics is not valid. Therefore, we used the integrated model during the rest of our research.

Second, we studied existing mitigation measures based on literature[12] and in-field experts. The mitigation measures that were considered during this study are: Ductility through structural configuration, direct damping apparatus, base isolation systems, dynamic absorbers and active control devices.

Based on arguments of both the literature and in-field experts we have found that the base isolation system and the dynamic absorber offer the most promising prospects in reducing the dynamic response of a crane that is subjected to seismic activity. The other measures were considered to be less promising since they can not be retrofitted, offer a low potential of damping in case of this crane or need a complex system that carries more support, maintenance and risks.

Third, to test their implementation for feasibility, we studied how the two most promising mitigation measures could be implemented on the crane of a jack-up. While base isolation systems are widely applied on land-based

structures, in this research, we were not able to implement a base isolation system at the base of the crane in such a way that it would mitigate the dynamic response of the crane.

The main issue with the base isolation system is the fact that the crane tips over due to a static and dynamic overturning moment that pulls the bottom and top side of the base isolation system apart. We have countered this issue by: implementing pre-tension; putting the aft bearing on top of the crane part; encasing the crane part on both the top and bottom side; or a combination of these three. However, this resulted in either cases with high slip-threshold that could not be exceeded by the lateral forces on the bearings, or in cases in which large peak forces occurred in the boom hinge or unacceptable offsets induced even higher overturning moments. We attempted to counter the issues in the latter case by applying a horizontal spring to the bearing. Unfortunately, we still found that high offsets occurred or that the response of the crane did not decrease. Since we did not succeed in finding a mitigative implementation of this base isolation system while keeping the offset rather acceptable, we concluded that this mitigation measure is not feasible for a wind turbine installation crane due to its overturning moment.

For the dynamic absorber, we did find a feasible implementation method. Based on literature, we have implemented the dynamic absorber in the tip of the boom as this is an anti-node location (where the largest amount of kinetic energy is present) of the most dominant eigen mode. Next to that, we have defined the mass of the dynamic absorber as 5% of the equivalent mass of the dominant eigen mode of the crane since the literature suggested that this is an economic optimum in practice. Additionally, we have tuned the natural frequency of the dynamic absorber to the natural frequency of the crane by calculating the stiffness between dynamic absorber and tip of the crane. These calculations were based on a crane model with a one degree of freedom spring-mass system. After determining the location, mass and stiffnesses, we have implemented the dynamic absorber as a rigid mass that is connected to the tip of the crane by an elastic and a viscous element. Subsequently, we have investigated the dynamic response of the crane with this dynamic absorber for a random test case and found that the dynamic absorber indeed affects and mitigates the response of the crane.

Based on these findings, we concluded that only the dynamic absorber is a feasible solution and continued with the further investigation of this measure for multiple configurations.

Fourth, to further investigate the performance of the dynamic absorber, we compared the response of a crane with dynamic absorber to that of a similar benchmark crane without dynamic absorber in a Monte Carlo simulation experiment. We studied the influence by comparing the maximum forces that occurred in the boom hinge of these crane models. Since in-field experts indicated that the out-of-plane forces in the boom hinge have a higher likelihood of causing failures than the in-plane forces, we took the out-of-plane forces as the main indicator for the dynamic response of the crane.

Our findings were that for the vast majority of simulated cases (88%) the dynamic absorber reduces the dynamic response of the crane to seismic activity. Since the other 12% of cases only occurred in cases with relatively low risks (i.e. a relative low force amplitude) and that an overall average mitigation was estimated at approximately 10%, we concluded that implementing this measure on a crane is beneficial to reduce the risks that are associated with earthquakes.

In this study, we did not investigate the tuning of the mass and stiffness of the dynamic absorber in more depth. Nonetheless, we found a reduction of the dynamic response of the crane for this (probably suboptimal) implementation of the dynamic absorber. Therefore, we expect this mitigation measure to be able to reduce the dynamic response of the crane even more when implemented with further optimized mass and stiffness.

Next to these more general findings, we discovered that the highest two-thirds of the 12% of cases in which the dynamic response of the crane increased, was caused by cases with a low suspended mass weight. We assume that this is caused by the lower equivalent mass of the crane that is associated with the higher natural period of these cases. As in these cases the dynamic absorber can influence more mass, any negative influence will lead to a larger amplitude of negative influence for the low weight cases.

Another interesting finding was that the dynamic absorber is especially effective in mitigating the dynamic response of the crane near the end of earthquakes. We found that the large harmonic crane motions and forces in these phase are mitigated up to 31,5%, Section 6.4.3. In this phase, the jack-up develops a clear harmonic oscillation with an amplitude similar to that of its prior vibrations. This is the result of the Rayleigh waves of the earthquake. As the crane comes into resonance with these clear harmonic oscillations of the jack-up, it develops more extreme amplitudes than during the prior vibrations of the earthquake. Since dynamic absorbers are particularly effective in mitigating these harmonic oscillations, we see that the dynamic absorber achieves its largest mitigating effects near the end of the earthquake.

The finding that the dynamic absorber is especially effective in the case of harmonic Rayleigh waves is highly relevant. The reason for this is that it supports the idea that a dynamic absorber might also be suitable to mitigate the response of cranes that are subjected to more common operational conditions that are also of a harmonic nature. Examples of such operation conditions are wind and waves.

Finally, based on the research performed in this thesis, we conclude that the dynamic absorber is the best mitigation measure that can be applied on a wind turbine installation crane on a jack-up to counter its dynamic response to seismic events.

7.2 Recommendations

In this final section, we provide some recommendations for future research based on our findings and experiences.

Our main recommendation is to look further into the details of the cause of the dynamic response of the crane to seismic activity since we expect that the largest share of the dynamic response of the crane may be related to vertical ground motions instead of horizontal that we have been focusing on. In a later stage of our research we were surprised to find that for a jack-up standing on taller legs and therefore having smaller horizontal accelerations, the tip of the crane reaches extremely high amplitudes of accelerations. We assume that the high vertical stiffness of the jack-up causes a transfer of the vertical ground motions to the base of the crane without much dampening. This vertical acceleration of the base of the crane might induce the high dynamic response of the tip of the crane in both the in-plane and out-of plane direction that we observe. Therefore, to mitigate the earthquake response of the crane, a vertical base isolator may even be more effective than a dynamic absorber and yield better results.

Next to that, we recommend to look further into the details of a dynamic absorber in cases with more common operational conditions such as waves and wind. The reason for this is that based on the literature and our own findings we also expect the dynamic absorber to be effective in these particular conditions. This is related to our before mentioned finding that the dynamic absorber is especially effective in mitigating the dynamic response of the crane near the end of earthquakes since these are of a more harmonic nature.

Additionally, we recommend to investigate which particular type of dynamic absorber can achieve the most optimal mitigation results for a crane since we know that some types of dynamic absorbers can induce more viscous damping than the one we have used. An example of such a dynamic absorber is a tuned liquid damper

with sloshing gates.

Furthermore, we recommend to study a variation of the mass and stiffnesses of the dynamic absorber as we expect that this may lead to better performance of the dynamic absorber. In our investigation, we idealized and simplified the crane to a mass-spring system but as the crane possesses of multiple dominant vibration modes this is not entirely correct. Next to that, we only used four average dynamic absorbers to achieve a somewhat optimal dynamic absorber for all cases.

As a final recommendation, we recommend GustoMSC to further investigate the dynamics of the jack-up model in relation to the way the crane model is implemented (namely using a fixed hull mass distribution versus integrated dynamic crane model). We found that our implementation of an integrated crane model negatively affected the dynamics of the jack-up model as compared to a jack-up model with a fixed hull mass distribution. In this further investigation, we recommend to change the way the weight of the suspended mass is implemented in the fixed hull mass distribution. In our current implementation we did not take into account that the suspended mass is decoupled from the jack-up structure while it is effectively decoupled in reality. We suggest to take this into account in further investigations by neglecting the weight of the suspended mass in the two degrees in the horizontal plane.

Bibliography

- [1] Arash Hemmati; Erkan Oterkus; Nigel Barltrop. Fragility reduction of offshore wind turbines using tuned liquid column dampers. Technical Report 127, Department of Naval Architecture, Ocean and Marine Engineering, University of, 2017.
- [2] Richard T Barrett. *Fastener Design Manual*, page 16. NASA, 1990.
- [3] T.J.P. Blankenstein. Mitigative measures for jackups subjected to earthquakes. Master's thesis, Delft University of Technology, 2020.
- [4] Michael H.scott; Gregory L. Fenves. Krylov subspace accelerated newton algorithm: Application to dynamic progressive collapse simulation of frames. *Journal of Structural Engineering*, 2010. doi: 10.1061/(ASCE)ST.1943-541X.0000143.
- [5] International Organisation for Standardization. 19901-2: Petroleum and natural gas industries - specific requirements for offshore structures - part 2: Seismic design procedures and criteria., 2015. URL <https://www.iso.org/standard/61142.html>.
- [6] International Organisation for Standardization. 19905-1: Petroleum and natural gas industries — site-specific assessment of mobile offshore units — part 1: Jack-ups, 2016. URL <https://www.iso.org/standard/68135.html>.
- [7] International Organisation for Standardization. 19902: Petroleum and natural gas industries — fixed steel offshore structures, 2017. URL <https://www.iso.org/standard/27507.html>.
- [8] International Organisation for Standardization; InfraTerra inc. Iso/tc 67/sc 7: N 994 revised seismic hazard maps, 2018.
- [9] GustoMSC. Future proof wind turbine installation, 2021. URL <https://www.gustomsc.com/design/wind-installation/ng-20000x>.
- [10] R.J.M. Pijpers; H.M.Slot. Friction coefficients for steel to steel contact surfaces in air and seawater. *Journal of Physics: Conference Series*, 1669, 2020. doi: 10.1088/1742-6596/1669/1/012002.
- [11] Hans M. Hilber; Thomas J. R. Hughes; and Robert L. Taylor. Improved numerical dissipation for time integration algorithms in structural dynamics. *Earthquake Engineering & Structural Dynamics*, 5(3):283–292, 1977. doi: 10.1002/eqe.4290050306.
- [12] Junbo Jia. *Modern Earthquake Engineering Offshore and Land-based Structures*. Springer, 2017. ISBN 978-3-642-31853-5.
- [13] J Linthorst. Seismic analysis of cranes on jackup-ups. Master's thesis, Delft University of Technology, 2019.
- [14] Minjie Zhu; Berkeley University of California. The open system for earthquake engineering simulation, 2021. URL <https://openseespydoc.readthedocs.io/en/latest/index.html>.
- [15] Technical University of Denmark. The global wind atlas., 2021. URL <https://globalwindatlas.info/>.

-
- [16] S.B.Latooij. Seismic response of jack-ups; an improved procedure using time history analysis. Master's thesis, Delft University of Technology, 2018.
- [17] Prof.S.P. Timoshenko. On the transverse vibrations of bars of uniform crosssection. *The London, Edinburgh, and Dublin Philosophical Magazine and Journal of Science*, 43(253):125–131, 1992. doi: 10.1080/14786442208633855.



Close-up maps

Taiwan Strait

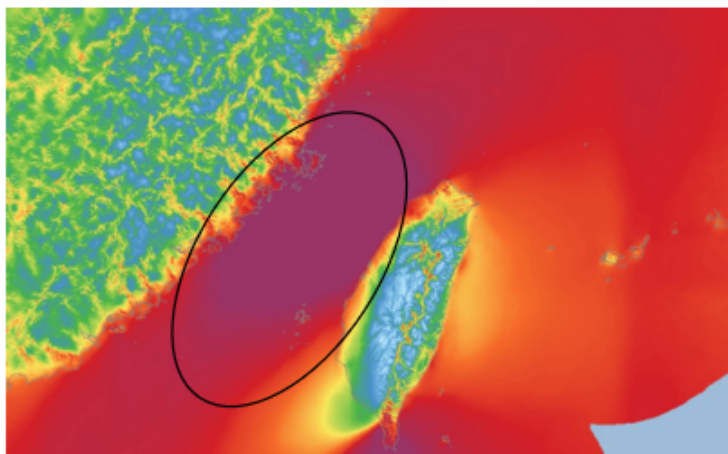
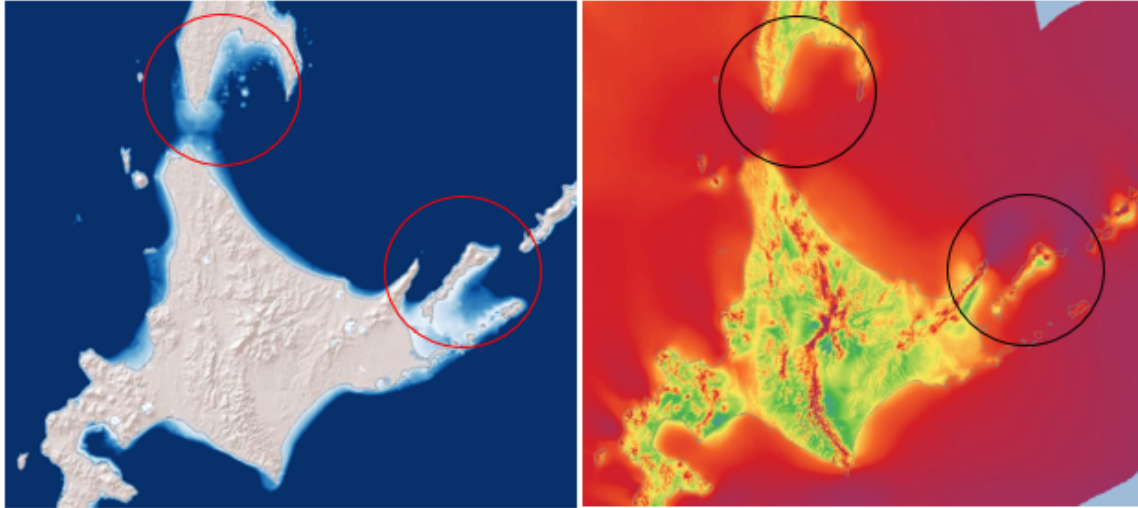


Figure A.1: Close up maps of the possible locations for wind turbine installation.

Possible locations for bottom founded offshore wind farms

The Northside of Japan



0-70 meter waterdiepte

mean wind speed 0-10 m/s

The southside of Japan

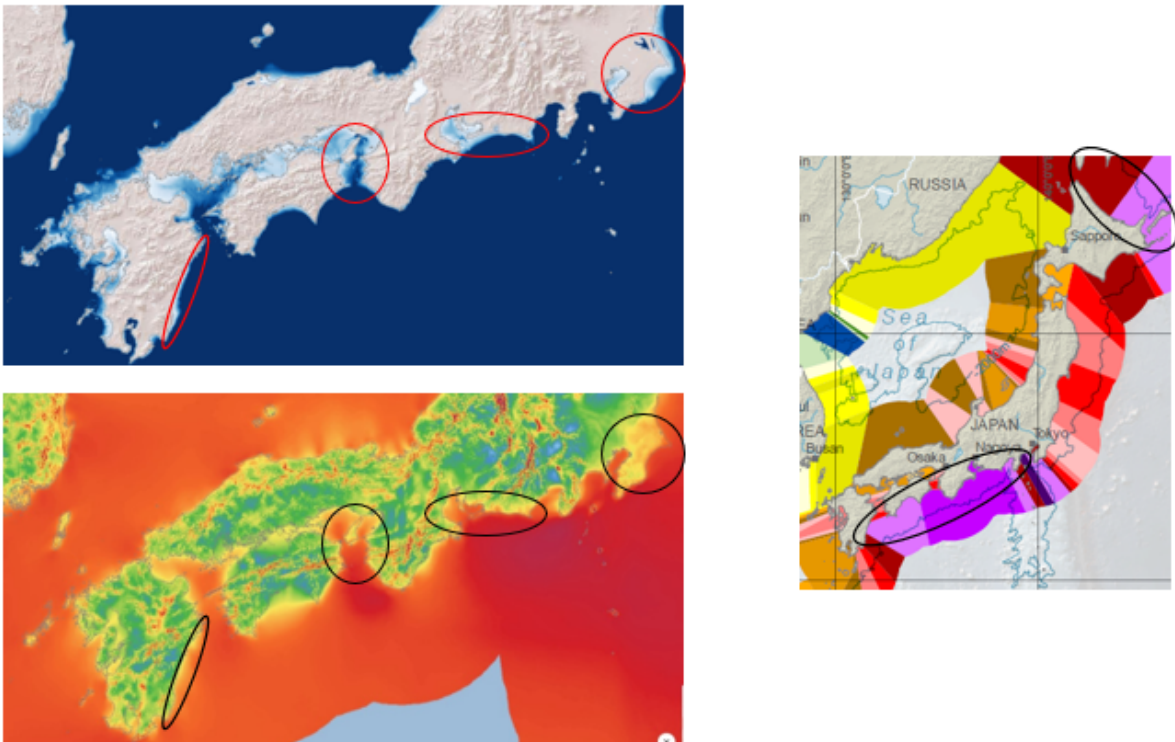


Figure A.2: Close up maps of the possible locations for wind turbine installation .

B

Variable distributions

This appendix shows the distributions of the variables that we have varied in our study to the influence of the integrated crane on the motion of the jack-up.

A motion of the jack-up model with the crane integrated on the jack-up is compared to the motion of the jack-up in which the crane mass is implemented as hull mass distribution over the hull nodes of the jack-up. This comparison is further explained in chapter Chapter 4.

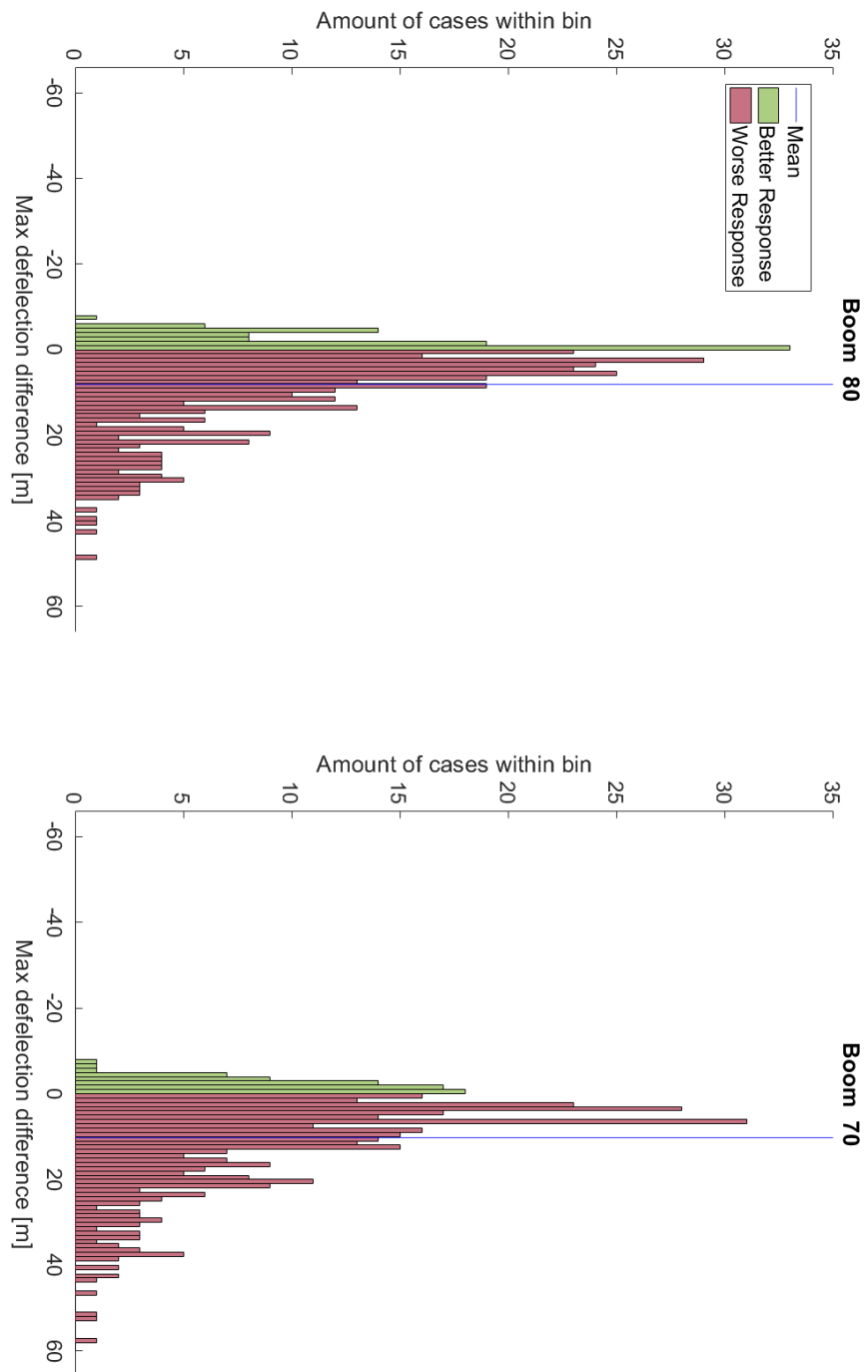


Figure B.1: Variable distributions of the max of longitudinal, transverse and torsional direction.(Differences have been compared for the center point of the a jack-up.

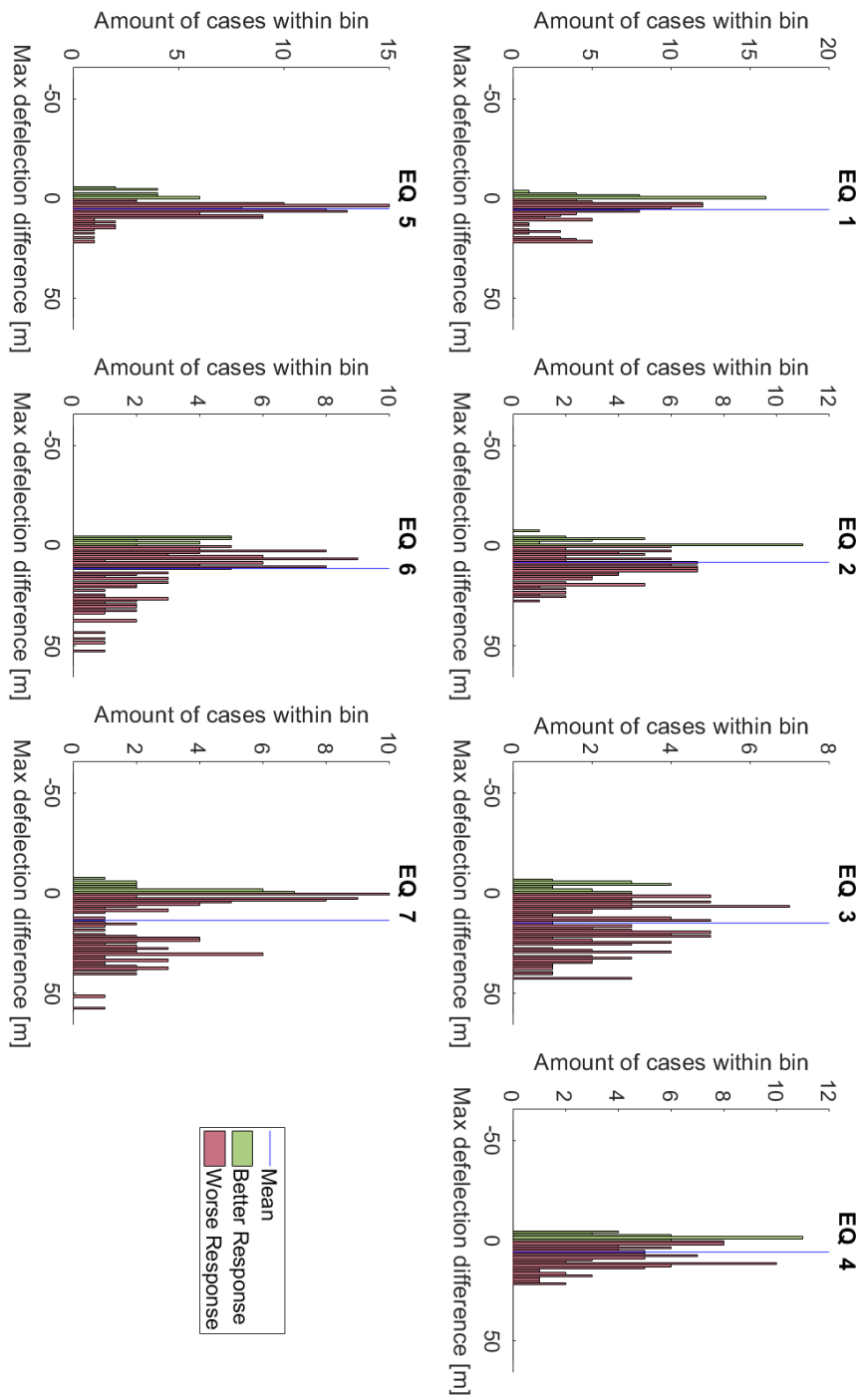


Figure B.2: Variable distributions of the max of longitudinal, transverse and torsional direction.(Differences have been compared for the center point of the a jack-up.

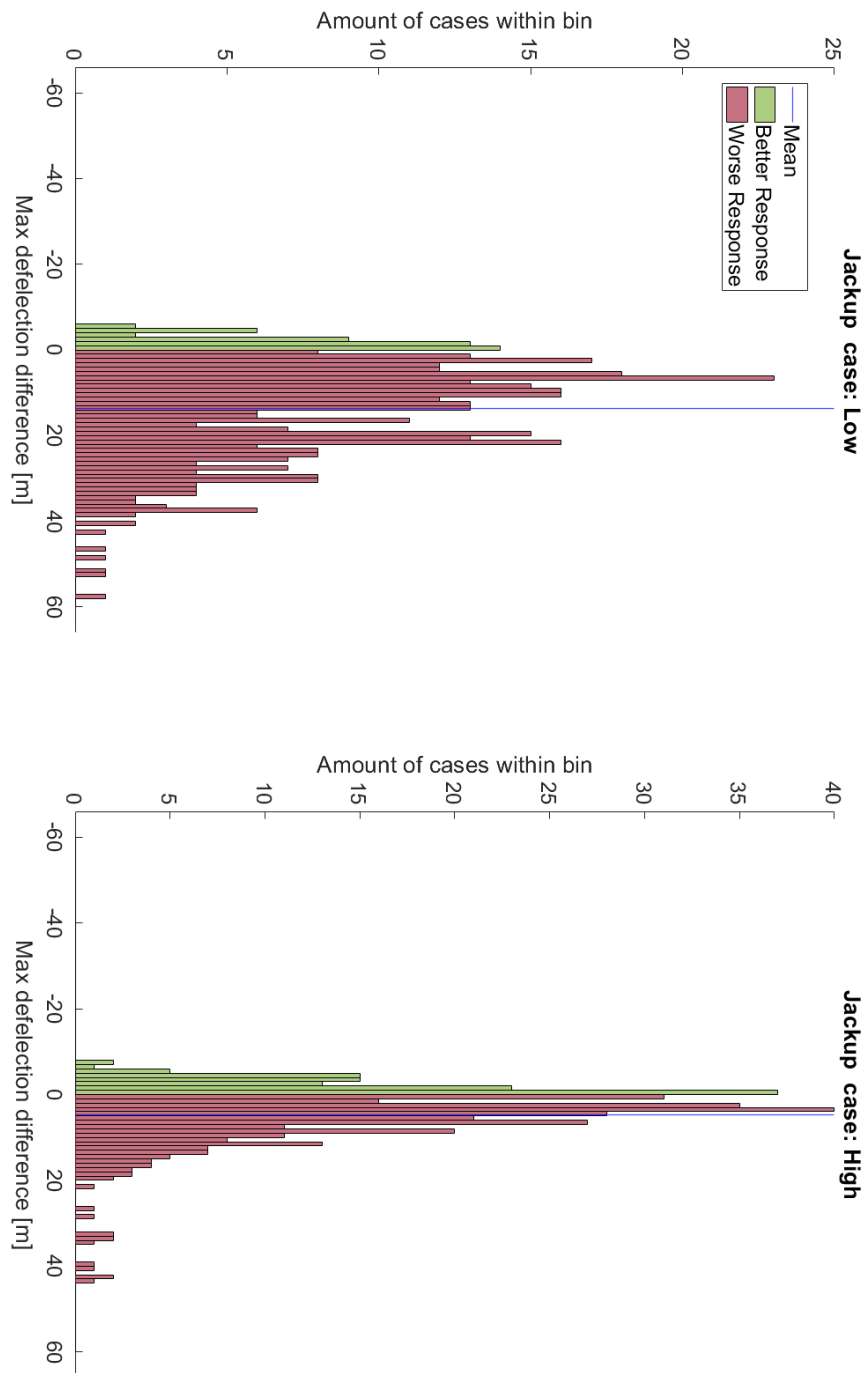


Figure B.3: Variable distributions of the max of longitudinal, transverse and torsional direction.(Differences have been compared for the center point of the a jack-up.

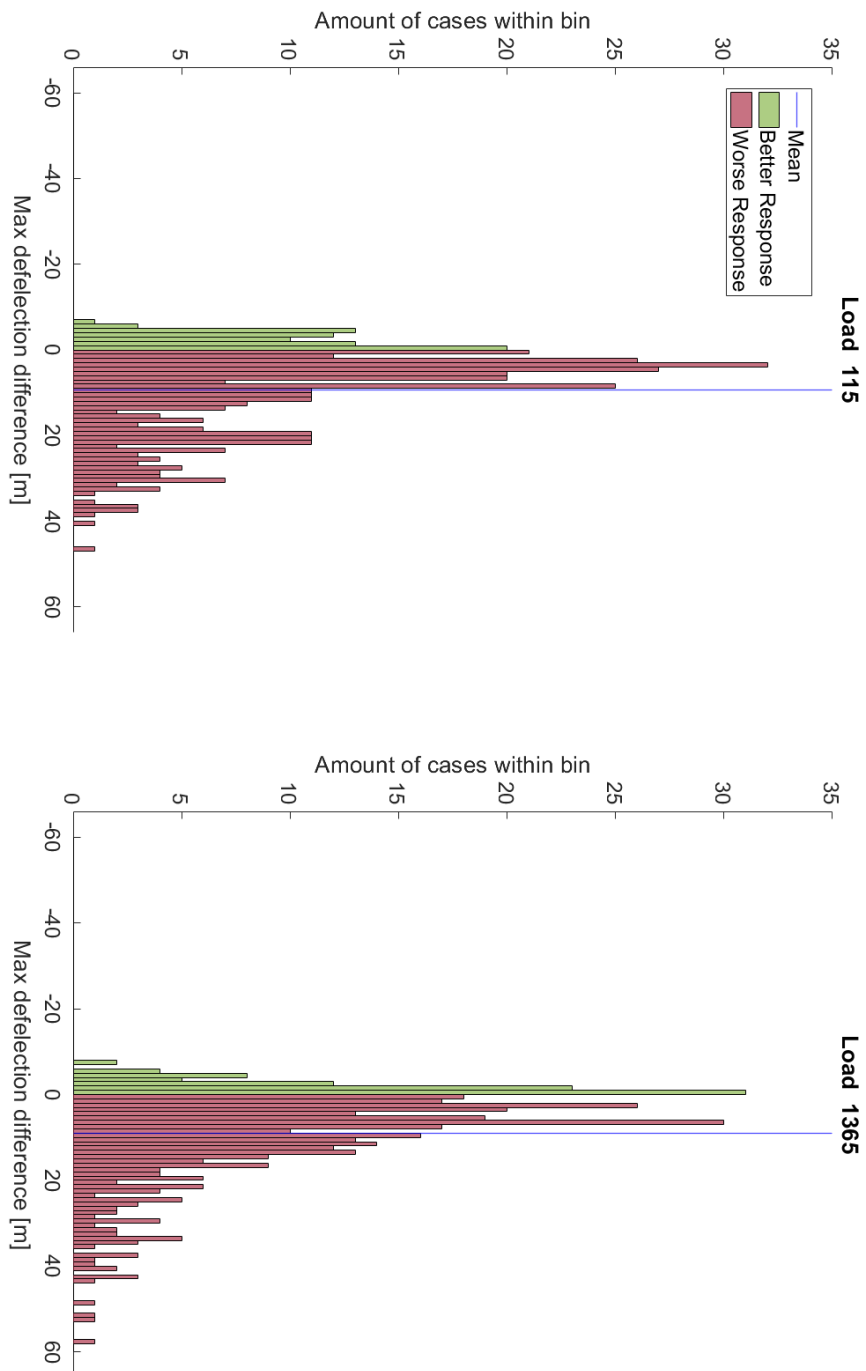


Figure B.4: Variable distributions of the max of longitudinal, transverse and torsional direction.(Differences have been compared for the center point of the jack-up.

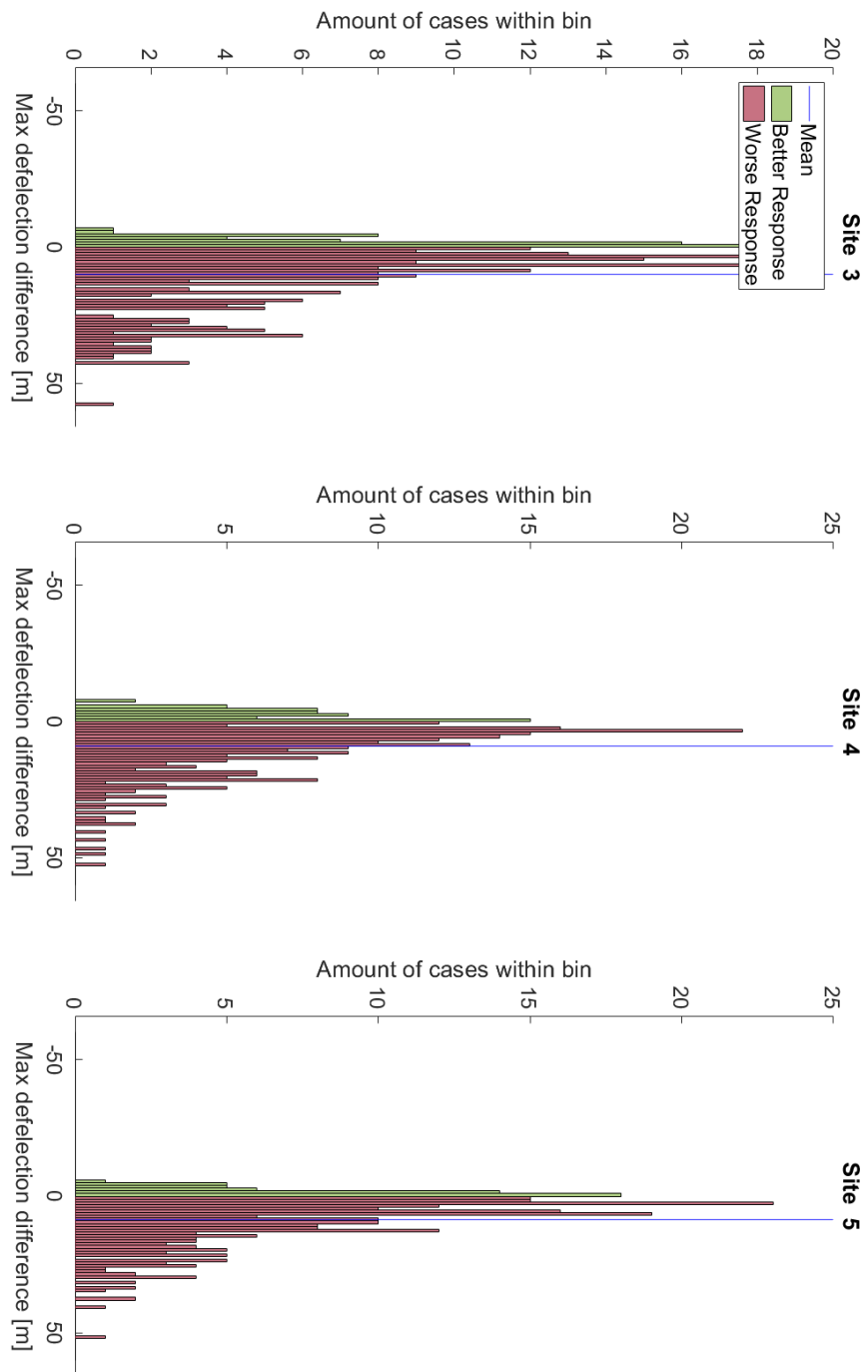


Figure B.5: Variable distributions of the max of longitudinal, transverse and torsional direction.(Differences have been compared for the center point of the a jack-up.

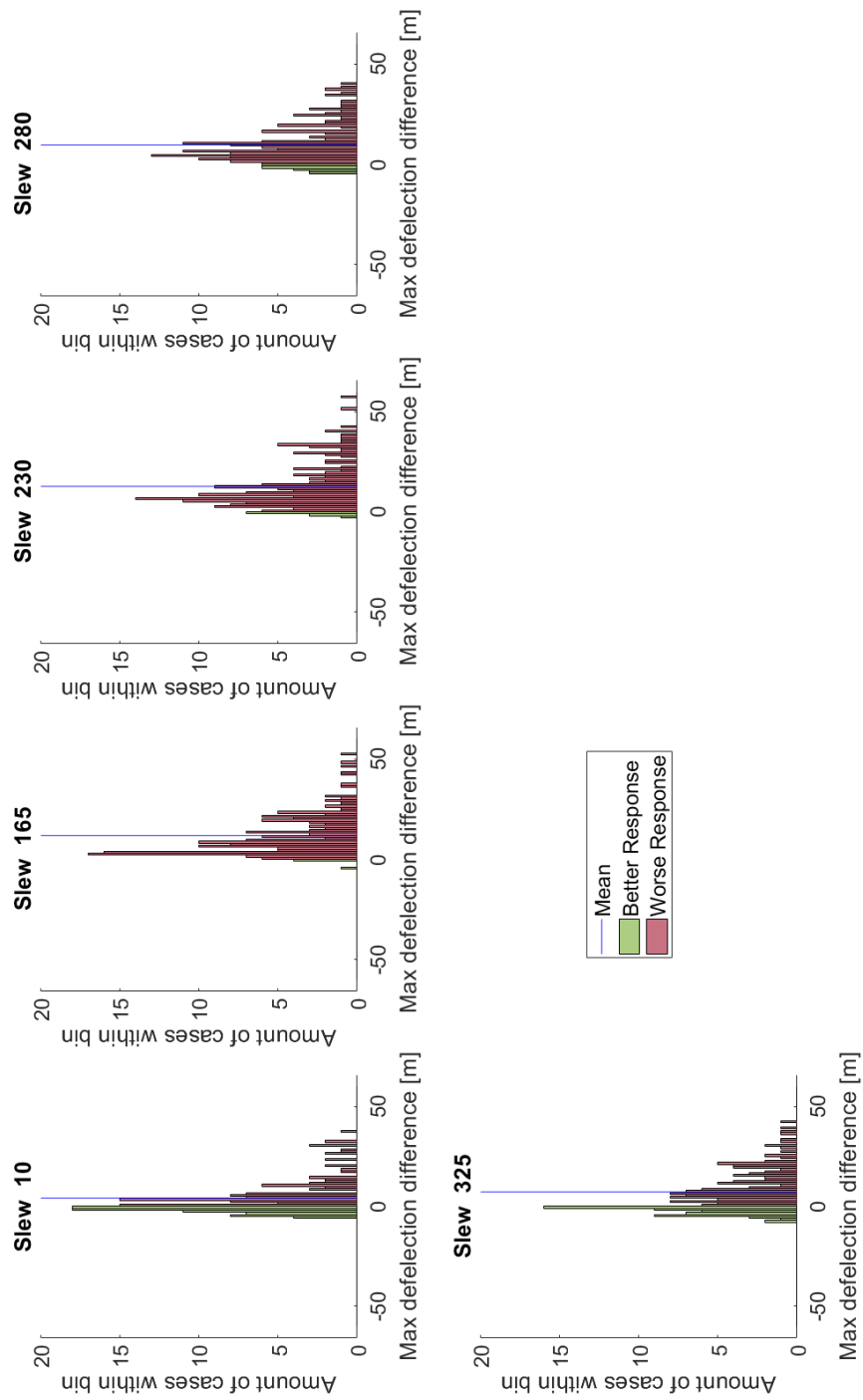


Figure B.6: Variable distributions of the max of longitudinal, transverse and torsional direction.(Differences have been compared for the center point of the a jack-up.



How the OpenSees model is build:

Generate equations of motions by building the model:

Model Builder:

1. Define the number of dimensions
2. Define number of Degrees of Freedom at the nodes
3. Define Nodes by their coordinates and their nodal mass
4. Define Constraints (Boundary conditions)
5. (Possibility to define materials or material behavior)
6. Define Geometric Transformation:
 - P-Delta effect (transforming beam element stiffness and resisting force from local to global-coordinate system, considering second order P-Delta effects).
7. Define elements by two adjacent nodes and element properties (no mass)
 - Elastic Timoshenko beam elements (E,I,A,G)
 - Zero length elements with elastic uniaxial materials (K or C)
 - Zero length elements with viscous uniaxial materials (K)
 - Flat Slider Bearing Element(K) with a friction model (μ) for lateral forces
 - Single Friction Pendulum Bearing Element(K) with a friction model (μ) for lateral forces
8. Perform an Eigen analysis to determine the eigenvalues and eigenvectors
9. Define a Linear Time series which defines the time via the load pattern
10. Define a Load Pattern
 - Plain pattern Gravitational Forcing on each node
 - Uniform Excitation Environment is given an acceleration, forcing on the boundaries

The Matrix Equation for **Opensees** is now created:

$$\mathbf{F}_I(\ddot{\mathbf{x}}) + \mathbf{F}_R(\dot{\mathbf{x}}, \mathbf{x}) = \mathbf{F}_E$$

Where \mathbf{F}_I is the acceleration-dependent inertial force vector, \mathbf{F}_R is the velocity (damping) and displacement-dependent (stiffness) resisting-force vector. $\mathbf{P}(t)$ is the external applied-force vector. The acceleration, velocity and displacement vectors are all time-dependent.

Analysis of the model

1. Define how to handle boundary conditions, enforcing the constraints.
 - Plain (Gravity)
 - Transformation method (Transient)
2. Define how DOF are numbered (with Reverse Cuthill McKee algorithm (RCM))
3. Define the analysis model (Creates the System of Equations (SOE))
 - Static (Gravity) solves $\mathbf{KU}=\mathbf{R}$
 - Transient (Transient) solves the time dependent analysis
4. Define convergence test at the end of an iteration step (Energy increment)
5. Define algorithm to solve the non-linear equations
 - Modified Newton-Rapson method to advance to the next step (tangent stiffness matrix is not updated each step)
 - Krylov-Newton uses modified Newton method with Krylov subspace acceleration to advance to the next step. (needed for Friction boundaries)

Figure C.1: Explanation to build the jack-up model part 1

6. Define Integrator which determines:
 - i. The predictive step for time t+dt
 - ii. The tangent matrix, residual vector at any iteration
Residual vector: $\mathbf{R}(\ddot{x}\dot{x}x) = \mathbf{F}_E - \mathbf{F}_I(\ddot{x}) - \mathbf{F}_R(\dot{x}, x)$
 - iii. The corrective step based on the displacement increment dU
 - Load Control(Gravity)
 - Hilbert-Hughes-Taylor Method (HHT) (Transient) allows for energy dissipation and second order accuracy
7. Assign damping to all nodes and elements using Rayleigh damping
8. Define how to store and solve the system of equation during the analysis
 - BandGeneral SOE uses an un-symmetric banded system of equations which will be solved using the Lapack('Linear Algebra Package') solver

Figure C.2: Explanation to build the jack-up model part 2